

**PARTS LIST**

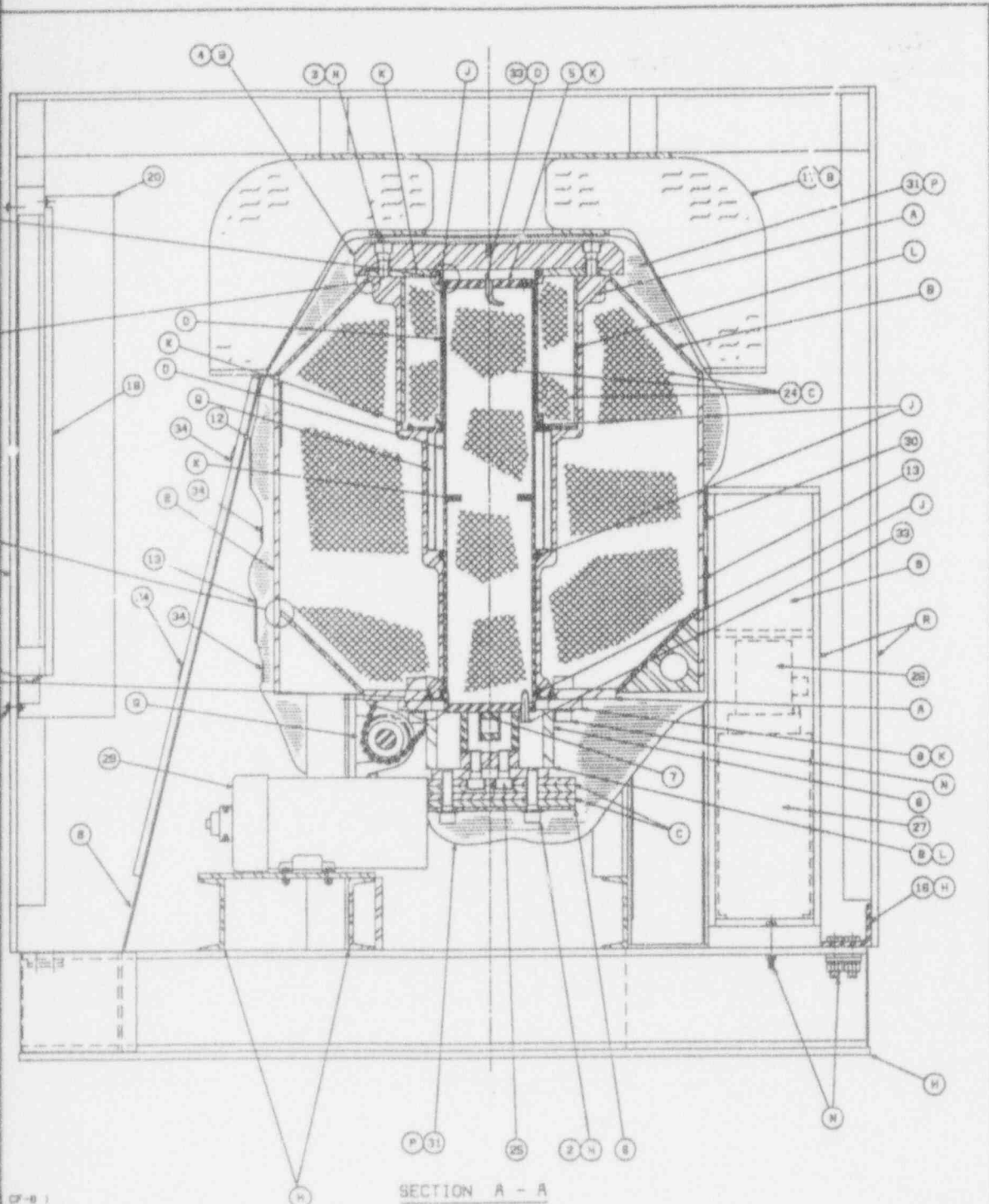
1. SHIELD COLLAR ( END USE ONLY )
2. 3/4-10 UNC x 5.50 in. LONG SOCKET HEAD CAP SCREWS (4)
3. 3/4-10 UNC x 2.50 in. LONG SOCKET HEAD CAP SCREWS (4)
4. SHIPPING COVER 1.75" THK.
5. SHIELDING DRAWER
6. DRAWER BOTTOM BRACKET
7. DRAWER SUPPORT BAR
8. SHIPPING BRACKET ASSEMBLY
9. PACKING MATERIAL
10. HOIST SLING ( 3/4" DIA. WIRE ROPE )
11. LIFTING EYELET
12. RADIATION CAUTION PLATE - AECL-RCC SPEC DG0006 (3)
13. AECL IDENTIFICATION PLATE - AECL-RCC SPEC DG0007 (3)
14. CATEGORY LABEL - AECL-RCC SPEC DG0102 (2)
15. 1/2-13 UNC x 9.00 in. LONG SQUARE HEAD BOLTS (3)
16. SHIPPING BRACKET (2) WITH 5/8-11 x 1.25" LONG HEX HEAD SCREWS (8)
17. CRUSH SHIELD ASSEMBLY
18. LOWER BACK COVER
19. #10 WOOD SCREWS
20. PLATFORM
21. 1/4-20 x 1.00 LONG HEX HEAD CAP SCREW (4)
22. 1/4 WSH. WASHER FLAT (4)
23. 1/4-20 HEX NUT (4)
24. LEAD SHIELDING
25. 3/4-10 x 2.00 LONG HEX HEAD CAP SCREW (4)
26. SHIELDING PLUG ( END USE ONLY )
27. TOP DRAWER ( END USE ONLY )
28. 1.50 - 6 THREADED ROD x 8" LONG (2)
29. ELECTRIC MOTOR 220Y 3 PHASE AKA) V-BELT DRIVE SYSTEM
30. RADIATION CAUTION PLATE WITH SPECIFIED CONTENT (1) AECL-RCC SPEC DG0006 (1)
31. THERMAL BLANKET
32. MAIN ENCASUREMENT 3/8" THICK
33. DRAIN TUBE
34. 0.5 inch. STANDARD PACKING STRAPS

**MATERIALS**

- A. STAINLESS STEEL CASTING ( ASTM A 206-74 )
- B. HRS PLATE ASTM A36
- C. LEAD COMMON ASTM B29-55
- D. STAINLESS STEEL TUBE TYPE 304 ASTM A-268
- E. CHAIN #448 AMERICAN STANDARD No 50 STAINLESS
- H. STRUCTURAL STEEL ASTM A-36
- J. GRAPHITE BEARING GR 9828 (4)
- K. STAINLESS STEEL PLATE GRADE 304 ASTM A-242
- L. STAINLESS STEEL PIPE TYPE 304 ASTM A-312
- N. SAE J-429 GRADE 8 ALLOY STEEL
- P. KAOHOL CERAMIC FIBER BLANKET ( 0.5 in. THK. ( 4 mil ) AND STEEL WIRE MESH ( 1 in. gr. )
- Q. STAINLESS STEEL SOURCE RACK 8.8 in DIA. WITH STAINLESS STEEL WELDED CAPSULES CO
- R. 1/2 in. THK. PLYWOOD CRATE STIFFENED W/

**NOTES**

- 1) CONFORMS TO I.A.E.A. TYPE B(U) REQUIRED
- 2) GROSS HEIGHT 9700 lbs ( 4400 kg )
- 3) PROJECTED FLOOR LOADING 531 lbs/sq ft
- 4) CAPACITY UP TO 28,000 CI Co-60
- 5) AECB CERTIFICATE CON/2013/B(U)
- 6) UBOOT CERTIFICATE USA/6125/B(U)
- 7) WELDING PERFORMED IN ACCORDANCE WITH CS
- 8) MANUFACTURED IN ACCORDANCE WITH NORDIC
- 9) ASSEMBLED IN ACCORDANCE WITH NORDIC



SECTION A - A

SHOWING POSITION OF ELECTRIC MOTOR | SCALE 1/4" = 1"

CF-81

TEEL

1lb/sq ft 1. POLYETHYLENE SHEET

ON 1 x 9.3 in | 21 on |  
IN COBALT 60  
4" LUMBER

age/sq on 1

BOARD 555  
TICAL SPECIFICATION (N/PR 0010 J0300  
ATION 08 0078 J0300

REV.	DESCRIPTION	DATE	BY	APP'D.	DATE	CHECKED	DATE
A	DRIP TRAY, S.S., 48" x 36"						
B	D.C.S., 48" x 36"						

		<b>MORRISON</b> INTERNATIONAL, INC. 10000 W. 10th Ave., Denver, CO 80202	
TITLE: <b>ORINACELL 220</b> <b>ACTIVE SHIPPING PACKAGE</b> IMPROVISED DESIGN		DRAWING NO.: <b>CB0001-001</b>	
REVISIONS: <b>AS NOTED</b>		SHEET: <b>1 OF 1</b>	

ANSTEC  
APERTURE  
CARD

Also Available on  
Aperture Card

9403170262-01

### Damage to the Shipping Cover

The shipping cover geometry is shown in Figure 2.7.1.2-i)-F6. It is secured to the main body of the GC-220 using four 3/4-10 UNC screws with a tensile strength of 180,000 psi. (See Table 2.3-T1.)

As shown in Figure 2.7.1.2-i)-F6, the shipping cover is mounted over a register on the inner head plug. The radial clearance between the register and the cover is .006 in at face A and 0.014 in at face B. This is less than the 0.063 clearance at face C and the 0.047 inch clearance at face D. Therefore, any load passed through the shipping cover is transmitted directly to the main body through the register before the bolts are loaded.

In the 15.5° side drop, lateral forces are transmitted to the shipping cover as the crush shield deforms and are relieved as the main body rotates toward the impact plane. It is extremely conservatively assumed that the crush plane proceeds directly through to the shipping cover, even though Figure 2.7.1.2-i)-F7 shows that it will hit the main body before it hits the cover.

For this orientation, the forces on the cover plate are shown in Figure 2.7.1.2-i)-F8. Appendix 2.10-G shows the expected inertial load on the unit to be 57 g's.

Noting that the main body of the GC-220 weighs 8500 lb and resolving forces yields:

$$F_x = 8500(57)\cos 15.5 = 466,900 \text{ lb}$$

$$F_y = 8500(57)\sin 15.5 = 129,500 \text{ lb}$$

Assuming a conservative coefficient of dynamic friction equal to 0.3 yields a friction force equal to  $(0.3)(129,500) = 38,800$  lb. The net shearing force on the shipping cover is 428,100 lb.

The shear area for the cover is shown in Figure 2.7.1.2-i)-F9. It is assumed to be equal to the projected area of 40% of the circumference of the register. From Figure 2.7.1.2-i)-F9, this area is found to be equal to 23.8 in<sup>2</sup>. Thus, the shear stress is:

$$\tau = F/A = 428,100/23.8 = 18,000 \text{ psi}$$

The shipping cover is Type A-36 mild steel. It has a minimum tensile strength of 58,000 psi. (See Table 2.3-T1) It's shear strength is taken to be  $0.82(58,000) = 47,560$  psi. As this exceeds the applied stress, the shipping cover will not fail in shear.

By inspection, the shear area of the inner head plug exceeds the shear area of the shipping cover. Therefore, failure of the cover will occur before the inner head plug fails.



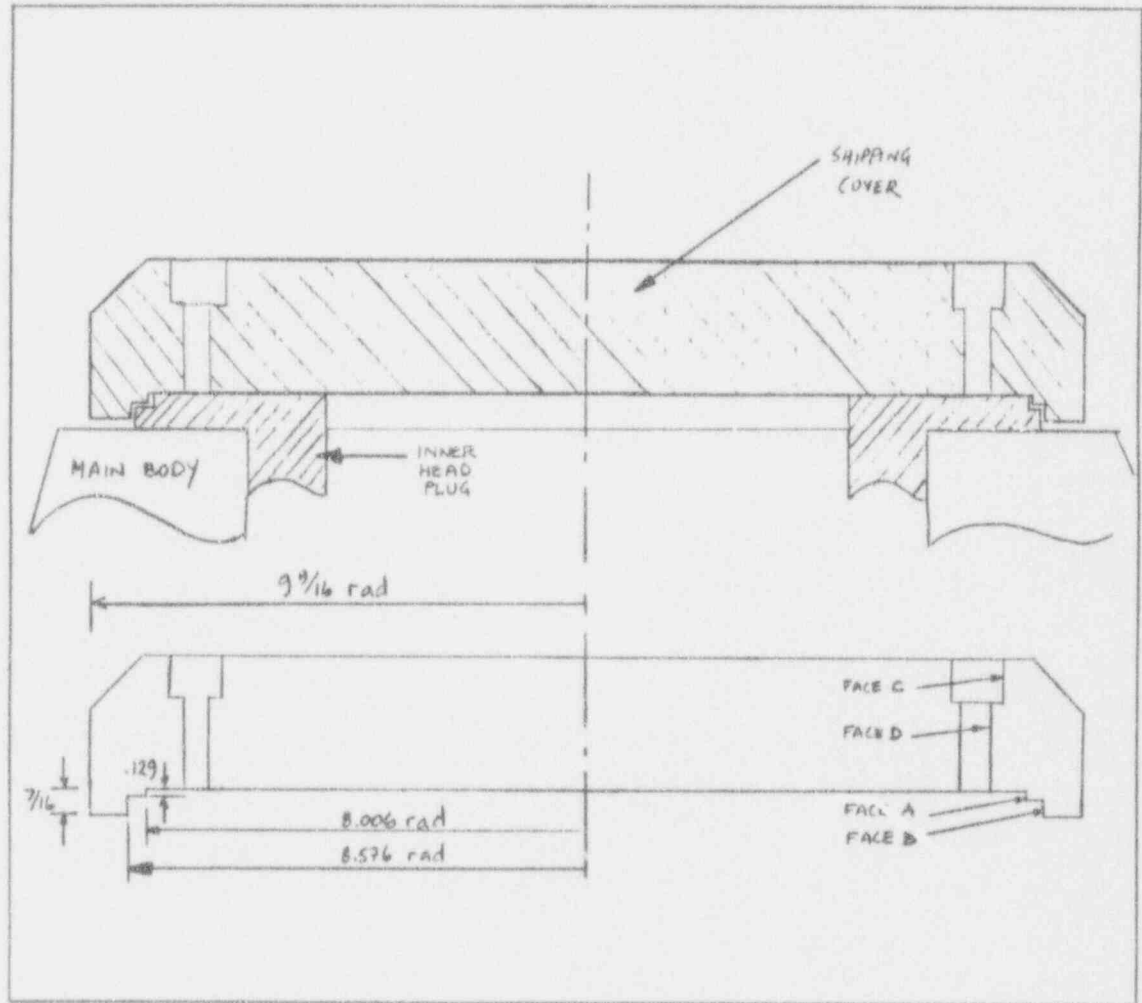


Figure 2.7.1.2-i)-F6 Shipping Cover Geometry

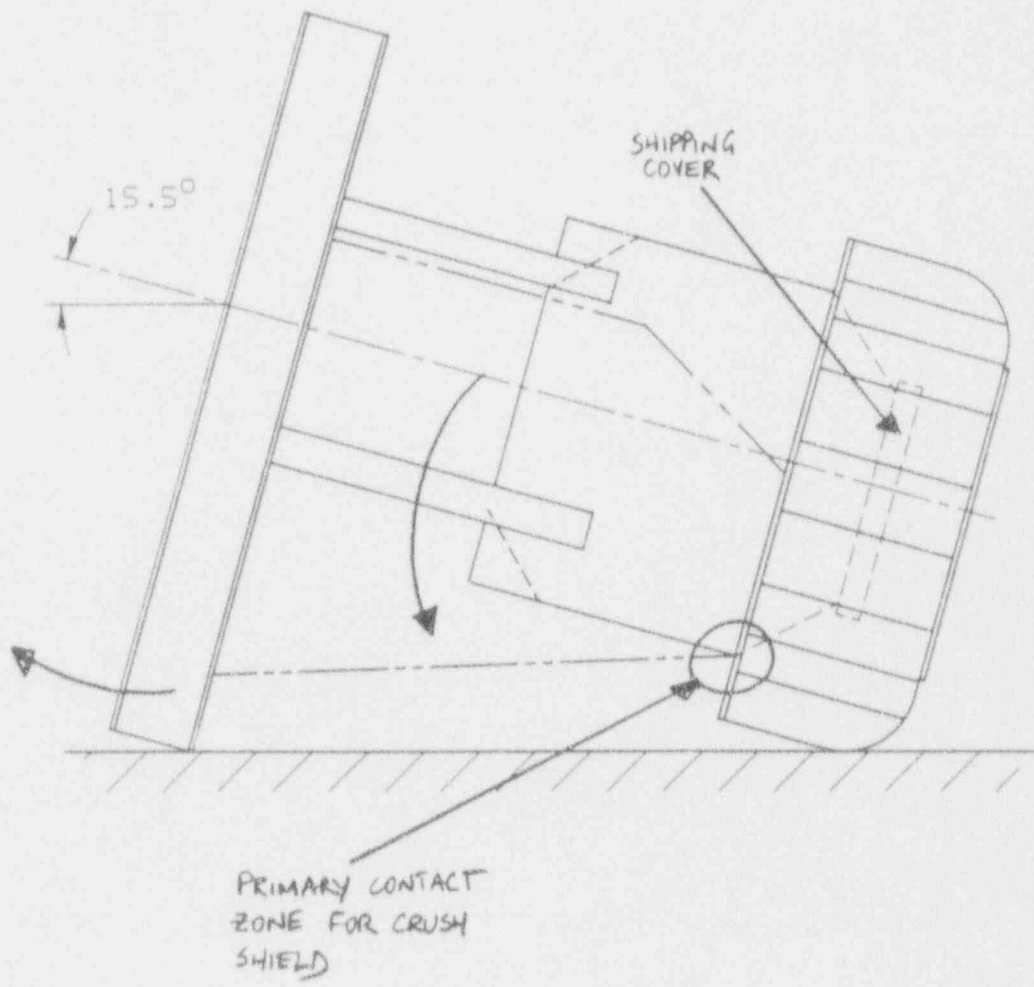
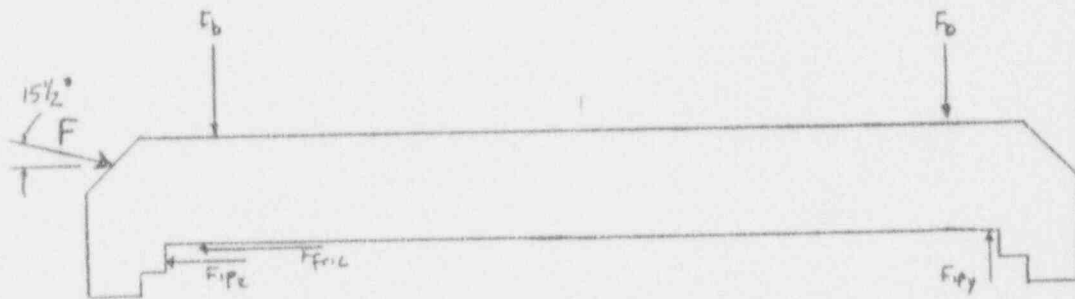
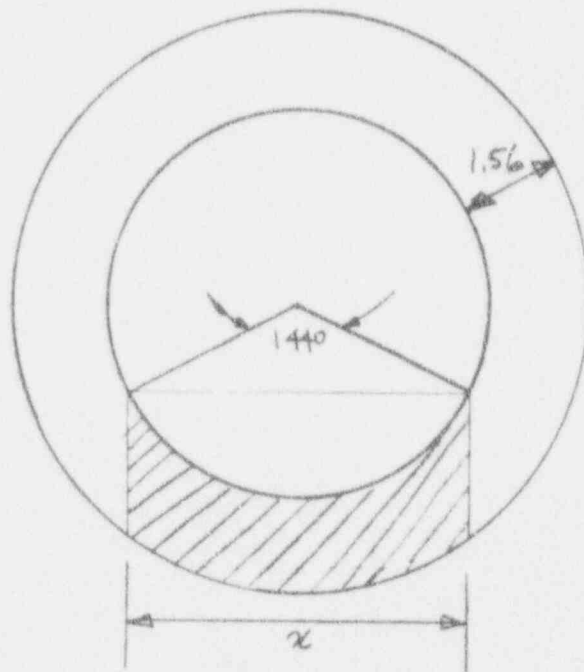


Figure 2.7.1.2-i)-F7. Front Side/Back Side Drop Orientation



- $F$  = force due to impact (57 g's)
- $F_{fric}$  = force due to friction
- $F_{ip}$  = reaction force due to inner head plug
- $F_b$  = bolt preload

Figure 2.7.1.2-i)-F8 Forces Acting on the Shipping Cover



$$x = 2R \cos 72 = 2(8.006) \sin 72 = 15.2''$$

$$A_{\text{shear}} \approx 15.2 (1.56) = 23.8 \text{ in}^2$$

Figure 2.7.1.2-i)-F9 Shear Area of the Shipping Cover

### Damage to the Crush Shield Connection

Forces on the crush shield have been previously resolved into axial and radial components  $F_x = 466,900$  lb and  $F_y = 129,500$  lb.  $F_y$  tends to push the crush shield toward the main body and, as such, prevents the crush shield from slipping during the drop.  $F_x$  tends to force the crush shield inward and attempts to cause the 1 1/2 inch threaded rods to fail in double shear.

The 466,900 lb load is assumed to be evenly split between the two threaded rods. Each threaded rod has a stressed area of 1.4 square inches and is loaded in double shear. Therefore, the shear stress on the rod is:

$$\tau = 233,450/2*1.4 = 83,400 \text{ psi}$$

The rods are ASTM A-183 Class B7 with a minimum tensile strength of 125,000 psi. Their shear strength is assumed to 82 % of this value or 102,500 psi. As this value exceeds the applied stress the rod will not fail in double shear and the crush shield will remain attached.



### Damage to the Shipping Cover

In the 0° side drop orientation shown in Figure 2.7.1.2-ii)-F1, the shipping cover is not directly loaded. Forces are transmitted radially through the crush shield to the main body of the unit and to the fasteners. Forces passed to the shipping cover are small in comparison with the forces resulting from the 15.5° and 48° drop orientations. Therefore, they are not considered further.

### Damage to the Crush Shield Connection

The high peak inertial load expected in a side drop may cause the shear failure of the 1.5 inch diameter threaded rods. However, this failure is of little consequence as the crush shield is not required for the successful completion of a subsequent fire test.

The detailed geometry of the top of the package is shown in Figure 2.7.1.2-ii)-F6. The 16 gauge stainless steel cone is connected to the shipping cover using four 3/8 inch diameter screws. It is not connected to the crush shield. It's function is to protect the kaowool insulation in case the crush shield is detached. This enables the unit to survive this drop orientation with little significant damage to the kaowool.

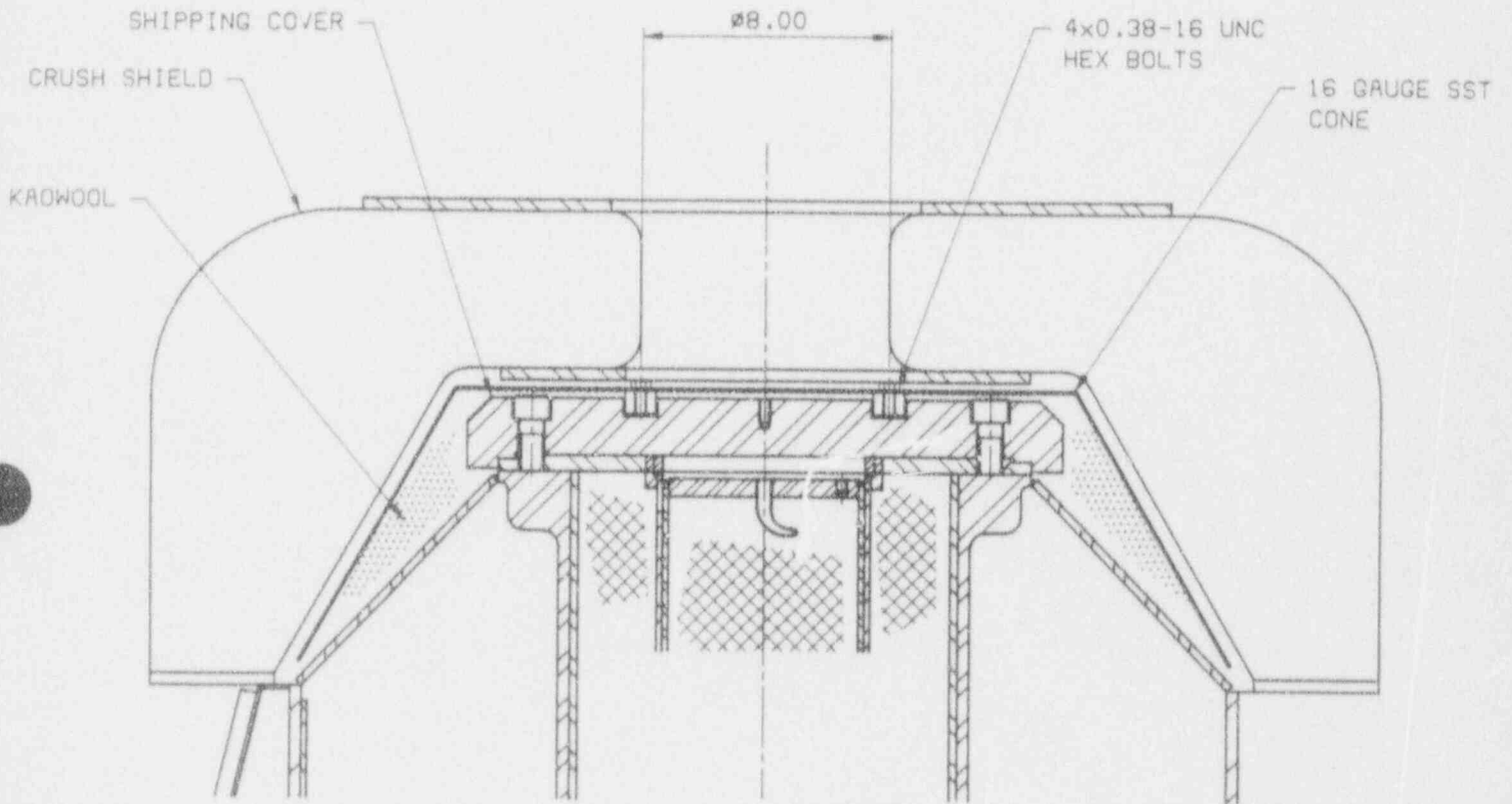


Figure 2.7.1.2-ii)-F6 Crush Shield Geometry

### Damage to the Shipping Cover

The shipping cover geometry is shown in Figure 2.7.1.3-i)-F5. It is secured to the main body of the GC-220 using 4 3/4-10 UNC screws. Each screw has a tensile strength of 180,000 psi. (See Table 2.3-T1.)

As shown in Figure 2.7.1.3-i)-F5, the shipping cover is mounted over a register on the inner head plug. The radial clearance between the register and the cover is .006 in at face A and 0.014 in at face B. This is less than the 0.063 clearance at face C and the 0.047 inch clearance at face D. Therefore, any load passed through the shipping cover is transmitted directly to the main body through the register before the bolts are loaded.

In the top corner drop, lateral forces are transmitted to the shipping cover as the crush shield deforms. For a 48° drop involving the skids, the forces on the cover plate are shown in Figure 2.7.1.3-i)-F6.

Appendix 2.10-G shows an expected inertial loading of 55 g's on the unit. In practice, these forces are transmitted to the main body of the container via the crush shield rings and fasteners. However, for the purposes of this analysis, it is conservatively assumed that the entire inertial load is transmitted directly through to the shipping cover as shown in Figure 2.7.1.3-i)-F6.

Noting that the main body of the GC-220 weighs 8500 lb and resolving forces yields:

$$F_x = 8500(55)\cos 48 = 312,800 \text{ lb}$$

$$F_y = 8500(55)\sin 48 = 347,400 \text{ lb}$$

Assuming a conservative coefficient of dynamic friction equal to 0.3 yields a friction force equal to  $(0.3)(347,400) = 104,200$  lb. Thus, the net shearing force on the shipping cover is 208,600 lb.

The shear area for the shipping cover was previously calculated to be 23.8 in<sup>2</sup>. (See section 2.7.1.2-i).) Thus, the shear stress on the cover is:

$$\tau = 208,600/23.8 = 8,740 \text{ psi}$$

The shipping cover is Type A-36 mild steel. It has a minimum tensile strength of 58,000 psi. (See Table 2.3-T1) It's shear strength is taken to be  $0.82(58,000) = 47,560$  psi. As this exceeds the applied stress, the shipping cover will not fail in shear.

By inspection, the shear area of the inner head plug exceeds the shear area of the shipping cover. Therefore, failure of the cover will occur before the inner head plug fails.

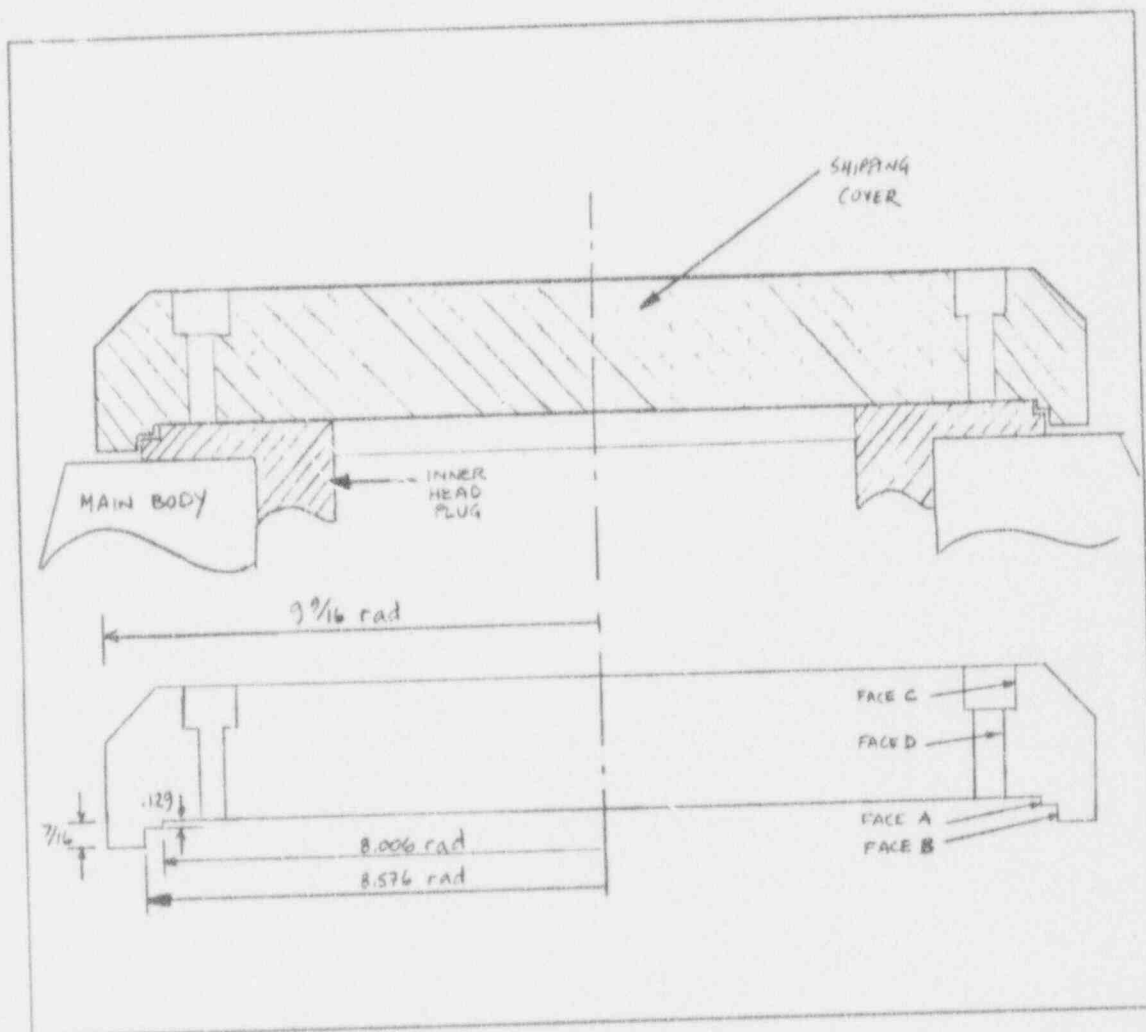
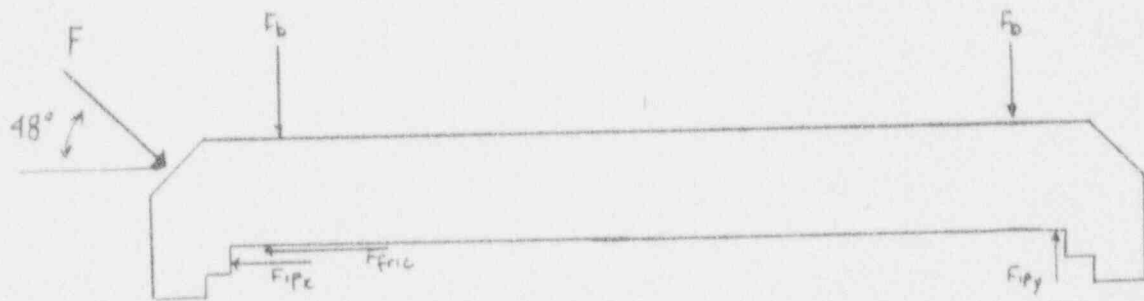


Figure 2.7.1.3-i)-F5. Shipping Cover Geometry



- $F$  = force due to impact
- $F_{fric}$  = force due to friction
- $F_{ip}$  = reaction force due to inner head plug
- $F_b$  = bolt preload

Figure 2.7.1.3-i)-F6. Forces Acting on the Shipping Cover



### Damage to the Crush Shield Connection

Forces on the crush shield have been previously resolved into axial and radial components  $F_x = 312,800$  lb and  $F_y = 347,400$  lb.  $F_y$  tends to push the crush shield toward the main body and, as such, prevents the crush shield from slipping during the drop.  $F_x$  tends to force the crush shield inward and attempts to cause the 1 1/2 inch threaded rods to fail in double shear.

The 312,800 lb load is assumed to be evenly split between the two threaded rods. Each threaded rod has a stressed area of 1.4 square inches and is loaded in double shear. Therefore, the shear stress on the rod is:

$$\tau = 156,400/2*1.4 = 55,900 \text{ psi}$$

The rods are ASTM A-183 Class B7 with a minimum tensile strength of 125,000 psi. Their shear strength is assumed to be 82 % of this value or 102,500 psi. As this value exceeds the applied stress, the rod will not fail in double shear and the crush shield will remain attached.

APPENDIX 2.10-G

Technical Report TR-9403-GC220



THE IMPACT ANALYSIS OF  
THE IMPACT LIMITER FOR THE GC-220

THE USE OF RECTANGULAR FIN DATA  
TO REPRESENT THE PERFORMANCE OF CURVED FINS

A Report for NORDION INTERNATIONAL

by

Whitman Wright

of

Pierre-Pont Engineering

December, 1993

CONTENTS

1.	Summary .....	1.1
2.	Introduction .....	
2.1	The Task .....	2.1
2.2	Configuration of the Transport Package .....	2.1
2.3	Loading Angles to be Investigated .....	2.1
2.4	Basis of Analysis .....	2.1
2.5	Mode of Deformation of Fins Loaded in Plane of Fin Direction .....	2.1
2.6	Sloping Fins .....	2.2
2.7	Energy to be Absorbed .....	2.2
3.	In-plane and Lateral Buckling Analysis of Fins Laterally Restrained at Point of Loading .....	
3.1	Introduction .....	3.1
3.2	Individual Finite Element Computer Runs .....	3.2
3.3	Summary of Buckling Loads .....	3.5
3.4	Summary of Maximum Deflections .....	3.6
3.5	Summary of Equivalent Elastic Energy Absorptions .....	3.6
3.6	Comments on the Finite Element Investigation .....	3.6
4.	Overall Analysis of Fins Laterally Restrained at Point of Loading .....	
4.1	General Rules .....	4.1
4.2	A Preliminary Overview of Plastic Hinge Action .....	4.1
4.3	Comparison with the Davis Data .....	4.2
4.4	Sloping Fins .....	4.4
5.	Overall Analysis of Fins without Lateral Restraint at Point of Loading .....	5.1
5.1	Introduction .....	5.1
5.2	The Effect of Slope on the Energy Absorbed by the Plastic Hinges .....	5.1
6.	Overall Behaviour of the Impact Limiter .....	6.1
7.	Impact Limiter with Loading Zero Degrees from Central Axis .....	
7.1	Energy Absorbed by the Fins in Direct Crushing and Plastic Hinge Action .....	7.1
7.2	Estimation of the Crushing Loads .....	7.1
8.	Impact Limiter with Loading 10 Degrees from Central Axis .....	
8.1	Introduction .....	8.1
8.2	Energy Absorbed by the Fins in Direct Crushing and Plastic Hinge Action .....	8.1
8.3	Total Energy Absorbed by the Impact Limiter .....	8.3
8.4	Estimation of the Crushing Loads .....	8.3
9.	Impact Limiter with Loading 42 Degrees from Central Axis .....	
9.1	Introduction .....	9.1
9.2	Energy Absorbed by the Fins in Direct Crushing and Plastic Hinge Action .....	9.1
9.3	Total Energy Absorbed by the Impact Limiter .....	9.4
9.4	Estimation of the Crushing Loads .....	9.4
10.	Impact Limiter with Loading 74.5 Degrees from Central Axis .....	
10.1	Introduction .....	10.1
10.2	Energy Absorbed by the Fins in Direct Crushing and Plastic Hinge Action .....	10.1
10.3	Total Energy Absorbed by the Impact Limiter .....	10.2
10.4	Estimation of the Crushing Loads .....	10.2



11.	Summary of Design Rules .....	11.1
12.	Symbols and Conventions .....	12.1
A.	Appendix A - Input Data for Finite Element Studies of Fins .....	A.1
B.	Appendix B - The Evans Report .....	
B.1	Introduction.....	B.1
B.2	The Experimental Data from the Evans Report .....	B.2
B.3	Working Formulas .....	B.3

SECTION 1 - SUMMARY

Energy from 30 Foot Drop

The total energy to be absorbed by the transport package = 3,060,000 in.lbs.

Crush Distances and Energies Absorbed by the Impact Limiter

Drop Angle From Central Axis (degrees)	Crush Distance (approx) (inches)	Energy Absorbed by Impact Limiter (in.lbs)	Percentage of Total Drop Energy
0 (90)	7.8	3,060,000	100
10 (80)	5.9 (average)	2,259,000	74
42 (48)	10.0	2,218,000	72
74.5 (15.5)	5.5	1,558,000	51

Crushing Forces on the Impact Limiter (g's)

Drop Angle From Central Axis (degrees)	Forces		
	To Produce Fin Buckling	Average	At Crushing of Exterior Plates
0 (90)	122	50	Not relevant
10 (80)	92	45	Not relevant
42 (48)	21	26	55
74.5 (15.5)	13	33	57

## SECTION 2 - INTRODUCTION

### 2.1 THE TASK

With respect to Figure 2.3-F1 of the SAR (same as Figure 6 of Irvine Ref.(2)) and Figure 2.3-F2 of SAR (same as Figure 5 of Irvine Ref.(2)), answer the following question:

"Justify the use of rectangular fin data to represent the performance of the curved fins on the Model GC-220 package crush shield."

The output shall consist of the following:

- (1) A stand-alone report describing the structural analysis prepared & approved by a competent structural engineer/consultant.
- (2) Using 6 inch fin height as reference, produce 4 new curves (figures) that superimpose on the existing figures [ [Absorbed Energy/ Plastic Moment] parameter versus [(Deformation/ Original Height) x 100%] parameter ] for the following range of variables:
  - 1) zero (0°) & ten (10°) fin loading angle.
  - 2) top corner and side drop orientations of the package.
  - 3.1) Zero (0%) to 45% maximum crush range as defined by Davis, Irvine &
  - 3.2) the fin crush "extrapolated" range as defined by
$$45\% \leq \delta_{FIN\ CRUSH} \leq \text{max. crush as defined by the fin "bottoming out".}$$

### 2.2 CONFIGURATION OF THE TRANSPORT PACKAGE

See Figs. 2.1 and 2.2.

### 2.3 LOADING ANGLES TO BE INVESTIGATED

See Fig. 2.3.

### 2.4 BASIS OF ANALYSIS

- (1) Title 10, Code of Federal Regulations, Nuclear Regulatory Commission, Part 71, Packaging and Transportation of Radioactive Material.
- (2) "Destructive Tests Related to Development of LMFBR Fuel Shipping Casks", A.R. Irvine, et al, IAEA-SM-147/21, 1971.
- (3) "Energy Absorbtion Capabilities of Plastically Deformed Struts", F.C. Davis, Structural Analysis of Shipping Casks, ORNL, TM-1312, Vol. 9, U.S. Atomic Energy Commission 1971.
- (4) "Experimental Study of the Stress-Strain Properties of Cask Materials Under Specified Impact Conditions", J.H. Evans, ORNL Engineering, ORNL, Oak Ridge, Tennessee 37830.

### 2.5 MODE OF DEFORMATION OF FINS LOADED IN PLANE OF FIN DIRECTION

The behaviour of fins directly load at zero slope angle appears to be broadly composed of the following stages:

- (1) An initial interval of direct compression, with stress increasing with the strain. The extent of this interval depends upon the thickness-height ratio of the affected fin, also upon the end restraint conditions of the fin.

- (2) A stage intermediate between (1) above and (3) below.
- (3) A stage where the fin buckles sideways and forms one or more plastic hinges. The number of plastic hinges formed depend upon the end restraint conditions. The energy absorbed is a product of plastic hinge moment per unit length, plastic hinge length and plastic hinge angle of rotation. The plastic hinge moment per unit length depends upon the stress level of the material, which in turn is affected by strain rate and strain hardening. With three plastic hinges in the member, the maximum possible hinge rotation is about 6.3 radians, giving an energy absorption capacity of  $6.3 M_p$ , where:

$$M_p = \text{plastic moment capacity} = (b t^2/4)F_y. \quad [2.1]$$

In Fig. 5.1 of the Davis report, energy absorption capacities as high as  $22 M_p L$  were shown. We believe that the divergence in the results can be attributed to the following factors:

- (1) Direct shortening before the formation of plastic hinges.
- (2) Increased material strengths as a result of high strain rate and high strain.
- (3) Some degree of "inertial support" resisting the tendency of the fins to snap sideways under very rapid loading.

## 2.6 SLOPING FINs

From the shape of the buckled fins as shown in Fig. 5.9 of the Davis report, it would appear that the zero degree slope fins received substantial lateral support at their top edges. This is not surprising because of a combination of the following effects:

- (1) A substantial degree of friction between the edge of the fin and the descending hammer, probably augmented by local crushing of the contact surface as yield stresses are exceeded.
- (2) The inertia of the hammer, which cannot easily be displaced sideways in the brief time available. If the fin were free to displace sideways, a structural buckling end restraint K factor of 2.0 would be appropriate. Under the actual conditions encountered, a structural buckling end restraint factor K of 0.8 would seem to be more appropriate in this case. It is possible that the detail shape of the outside edge of the 8 inch fin was such that the fin could slip sideways under the impact. This would greatly reduce the end restraint conditions and hence the energy absorption capacity of that fin.

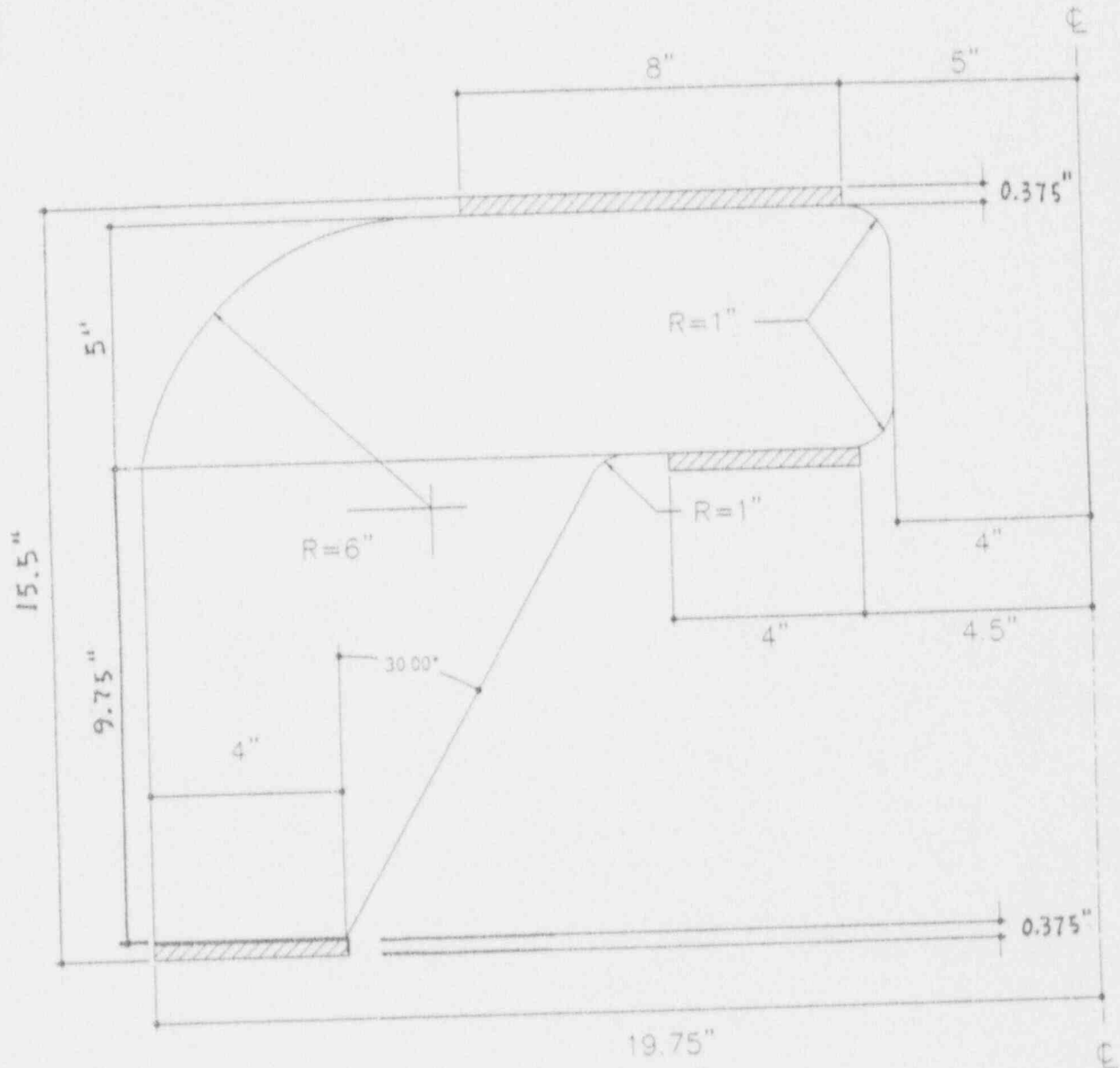
## 2.7 ENERGY TO BE ABSORBED

Weight of transfer unit = 8,500 lbs.

Drop distance = 360 inches.

Energy to be absorbed =  $W s$ .

=  $8,500 \times 360 = 3,060,000$  in.lbs.



0.375 THICK

Figure 2.1 Details of Impact Limiter  
(Part 1)

2.F1



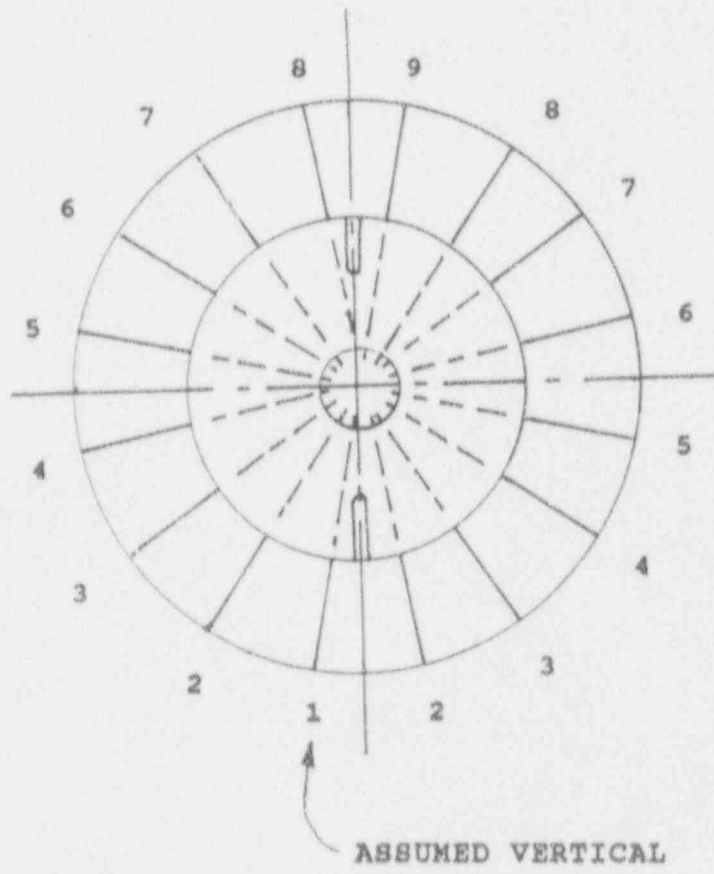


Figure 2.2 Details of Impact Limiter  
(Part 2)

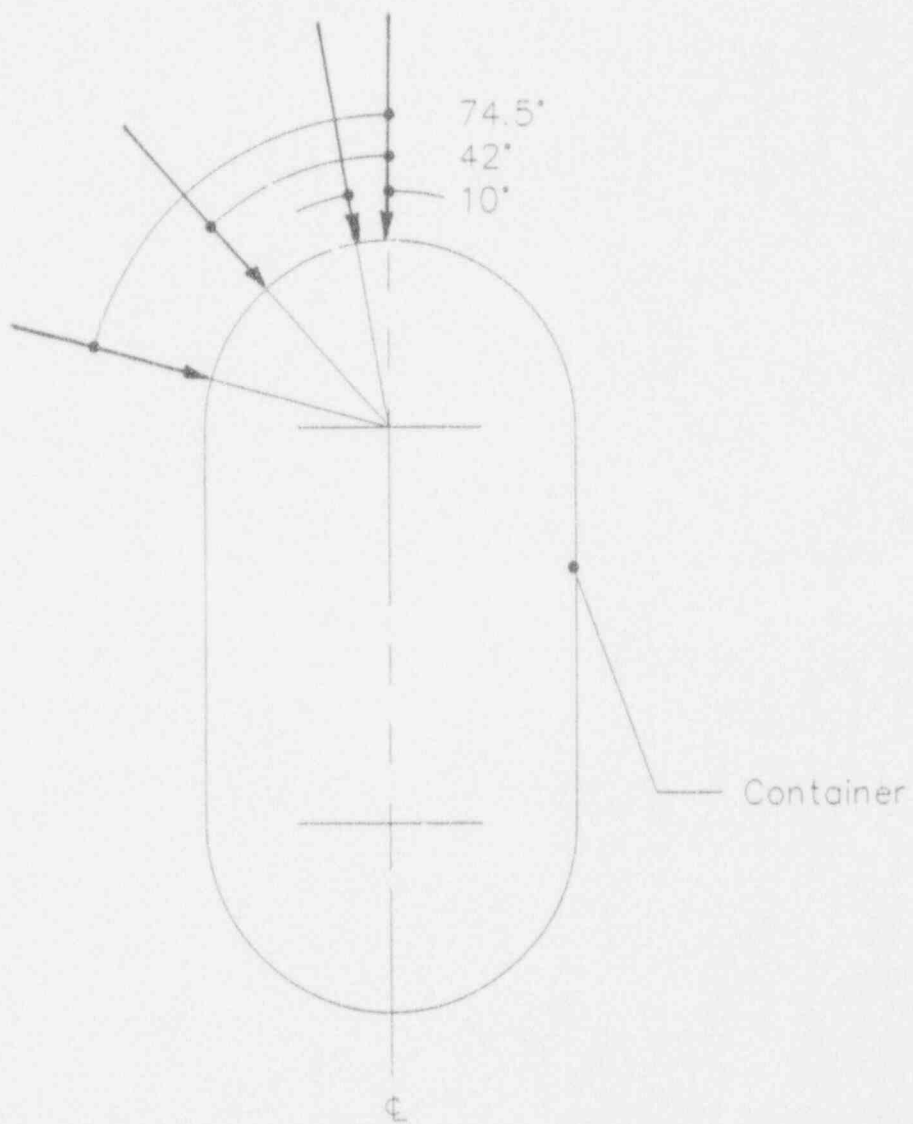


Figure 2.3 Load Angles Investigated in This Report

SECTION 3 - IN PLANE AND LATERAL BUCKLING ANALYSIS OF FINS  
LATERALLY RESTRAINED AT POINT OF LOADING

3.1 INTRODUCTION

3.1.1 Purpose of the Investigation

In the curve for the six inch high one-half inch thick fin shown in Fig. 5.1 of the Davis report (Fig. 4.3 of this report), a substantial fraction of the energy absorbed is due to plastic direct shortening of the fin before any substantial lateral buckling takes place. A careful study is required to determine how much energy will be absorbed by the GC-220 fins by direct crushing. For these reasons, a finite element investigation was carried out for the GC-220 fins. This work is described directly below.

3.1.2 Symbols and Conventions

Symbols and conventions are given in Section 12 of this report.

3.1.3 Finite Element Investigation

The in-plane and lateral buckling analysis of the fins is investigated with the aid of the linear elastic and buckling modules of the finite element program COSMOS/M Version 1.70, using the COSMOS/M SHELL4 element. The load angles used (measured from the central axis of rotation of the impact limiter) were 0°, 10°, 46°, and 74.5°. A smooth interpolation curve was passed through these points, permitting an interpolation of the results to other drop angles.

3.1.4 The Secant Modulus of Elasticity

If one starts with the Evans formula:

$$F_{ed} = 73,000 + 345,000 e,$$

the secant modulus of elasticity becomes:

$$E_s = 345,000 / (1 - 73,000 / F_{ed})$$

The secant modulus of elasticity is illustrated in Fig. 3.1. If one uses the secant modulus of elasticity in the finite element model and succeeds, by a number of trial runs, in approximating a match between the stress level and the secant modulus of elasticity for each element, one has then succeeded in approximately satisfying the strength of materials requirement that both equilibrium and compatibility be satisfied throughout the finite element model.

The Von Mises stress (taken as 57% of the uniaxial stress) is considered to be the best indicator of the stress state of a finite element.

### 3.1.5 Relationships Among Von Mises Stress, Uniaxial Normal Stress and Secant Modulus of Elasticity

Von Mises Range (psi)	Normal Stress for $E_s$ (psi)	$E_s$ (psi)
41,610	91,250	1,725,000
62,415	127,750	805,000
83,220	164,250	621,000
104,025	200,750	542,143
124,830	237,250	498,333
145,635	273,750	470,455
166,440	310,250	451,154
187,245	346,750	437,000
208,050	383,250	426,176
228,855		

### 3.2 INDIVIDUAL FINITE ELEMENT COMPUTER RUNS

The finite element model used for the fins is shown in Figs. 3.2 and 3.3. Because the material was expected to undergo very substantial inelastic action, the loads were applied seven times in succession, as illustrated in Fig. 3.8. In general terms, the steps carried out for each such load application (run) were as follows:

- (1) Except for Run No. 1, for which all the elements are assigned a modulus of elasticity of 29,000,000 psi, decide upon the Von Mises stress levels to be considered as boundaries between different groups of elements. Each such element group, where the stresses exceed a selected minimum value, is assigned a new reduced modulus of elasticity.

In the earlier runs, the stress levels taken to indicate the onset of yielding are considerably higher than the actual yield stresses. In the later runs, these stresses are gradually reduced to the actual dynamic yield stresses. The reduced modulus of elasticity corresponding to a particular stress level is also gradually reduced with successive runs, with the secant modulus of elasticity (Fig. 3.1) as the lower limit.

- (2) Determine the element numbers of the individual elements to be included in each element group (classified by stress level).
- (3) Assign the appropriate reduced modulus of elasticity to each such group of more highly stressed elements.
- (4) Establish the elastic buckling strength of the finite element model constructed in Step 4.
- (5) Apply the elastic buckling loads established in Step 4 to the finite element model (now treated as a non-buckling plate subject to in-plane loads).

The individual runs are described in more detail, as follows:

Run No. 1:

$E = 29,000,000$  psi throughout

- (1) Find the buckling loads.
- (2) Apply the buckling load to find the in-plane stresses.

The actual stress of interest is the Von Mises stress which, for a specimen subject to uniaxial stress is 57% of the yield stress. For ductile material, the Von Mises stress is considered to be the best indicator of the onset or degree of yielding. Using the following formula from Evans:

$$F_{ed} = 73,000 + 345,000 e$$

the Von Mises stress at the onset of yield should be  $0.57 \times 73,000 = 41,610$  psi.

Run No. 2:

Using the Von Mises stresses from Run No. 1:

Run No. 1 Von Mises Stress (psi)	Run No. 2 $E_s$ (psi)
0	29,000,000
100,000	25,777,000
150,000	21,091,000
200,000	17,846,000
250,000	15,467,000
300,000	

The specified elements associated with each value of  $E_s$  are listed in Appendix A.

- (1) Find the buckling loads
- (2) Apply the buckling loads to find the in-plane Von Mises Stresses.

Run No. 3:

The new values of  $E$  given below are obtained as follows:

- (1) Select a normal stress  $F_{ed}$  corresponding to the Von Mises stress.
- (2) Compute the corresponding value of  $E_s$ .
- (3) Multiply by 3.

This obviously gives a much higher value of  $E$  than the true value. However, this is necessary at this stage to avoid overshoot in the iteration process.

Using the Von Mises stresses from Run No. 2:

Run No. 2 Von Mises Stress (psi)	Run No. 3 $E_s$ (psi)
0	29,000,000
70,000	11,838,000
105,000	2,643,000
175,000	1,902,000
210,000	1,630,000
245,000	1,487,000
280,000	

- (1) Find the buckling loads.
- (2) Apply the buckling loads to find the in-plane Von Mises stresses.

For Run No. 3, two alternatives were considered, as follows:

- (a) Lateral restraint in the X-Y plane at the applied loads perpendicular to the applied loads.
- (b) The absence of such restraint.

The lateral restraint just referred to would result from the inertia of the cask as the impact limiter underwent crushing, and would not be considered to be present if the ratio of the lateral restraining force to the applied force exceeded the tangent of the angle of friction (which is taken as 20 degrees).

Run No. 4:

In this case the uniaxial normal stresses corresponding to the average Von Mises stresses obtained in Run 2 (not Run 3) were computed. Then the corresponding secant modulae were computed and multiplied by two (again to avoid overshoot)

Run No. 2 Von Mises Stress (psi)	Run No. 4 $E_s$ (psi)
0	29,000,000
80,000	3,450,000
120,000	1,610,000
160,000	1,242,000
200,000	1,084,000
240,000	

- (1) Find the buckling loads.
- (2) Apply the greater of the buckling loads or 70 percent of the loads used in

Run No. 2, to find the in-plane Von Mises stresses.

Run No. 5

In this case the normal stresses corresponding to the average Von Mises stresses obtained in Run 4 were computed and multiplied by 1.5 (to avoid overshoot).

Run No. 4 Von Mises Stress (psi)	Run No. 5 $E_s$ (psi)
0	
60,000	2,587,500
90,000	1,207,500
120,000	931,500
150,000	813,215
180,000	747,500

Run No. 6

Run No. 5 Von Mises Stress (psi)	Run No. 6 $E_s$ (psi)
0	
50,000	1,725,000
75,000	805,000
100,000	621,000
150,000	542,143
200,000	498,333

Run No. 7

Run No. 6 Von Mises Stress (psi)	Run No. 7 $E_s$ (psi)
0	
41,610	1,725,000
62,415	805,000
83,220	621,000
104,025	542,143
124,830	498,333



3.3 SUMMARY OF BUCKLING LOADS  
(Thousands of Pounds)

Run No.	Load Cases			
	1	2	3	4
1	269.6	165.5	125.9	134.0
2	223.3	159.3	122.9	131.3
3	46.1	65.0	73.1	65.4
3a (1)	46.2	75.2	72.6	(2)
4	34.1	56.5	78.4	52.3
5	37.5	59.7	51.4 (3)	72.3
6	40.9	65.6	101.4 (4)	72.8
7	50.3	80.4	(5)	49.6
Average (6)	42.9	68.6	76.4	64.9

Notes:

(1) 3a - with special lateral restraint

Lateral restraint reaction:

Case:

1 44,000 lbs

2 51,000 lbs

3 34,000 lbs

Do not assume lateral restraint further.

(2) Not applicable. Loads already laterally restrained.

(3) Model too flexible.

(4) Model too stiff.

(5) Not run because it was not believed that another run would provide any more useful data in this case.

(6) Average of Runs No. (5), (6) and (7), except for Load Case 3, which is the average of Runs No. (5) and (6).

The initial buckled shapes of the fins for the final computer runs are shown in Figs. 3.4 to 3.7.

3.4 SUMMARY OF MAXIMUM DEFLECTIONS  
(Inches)

Run No.	Load Cases			
	1	2	3	4
5	0.275	0.136	0.126	0.008
6	0.216	0.128	0.186	0.008
7	0.009	0.009	(1)	0.008

Notes

(1) Not run.

3.5 SUMMARY OF EQUIVALENT ELASTIC ENERGY ABSORPTION  
(Thousands of Inch Pounds)

Run No.	Load Cases			
	1 (74.5°)	2 (42°)	3 (10°)	4 (0°)
5	14.3	4.5	3.6	2.4
6	7.7	3.4	8.6	2.4
7	2.2	3.7		1.9
Average (1)	8.1	3.7	6.1	2.2

Notes:

(1) Average of Runs No. (5), (6) and (7), except for Case 3, which is the average of Runs No. (5) and (6).

3.6 COMMENTS ON THE FINITE ELEMENT INVESTIGATION

3.6.1 Strain Energy Absorbed by Direct Crushing

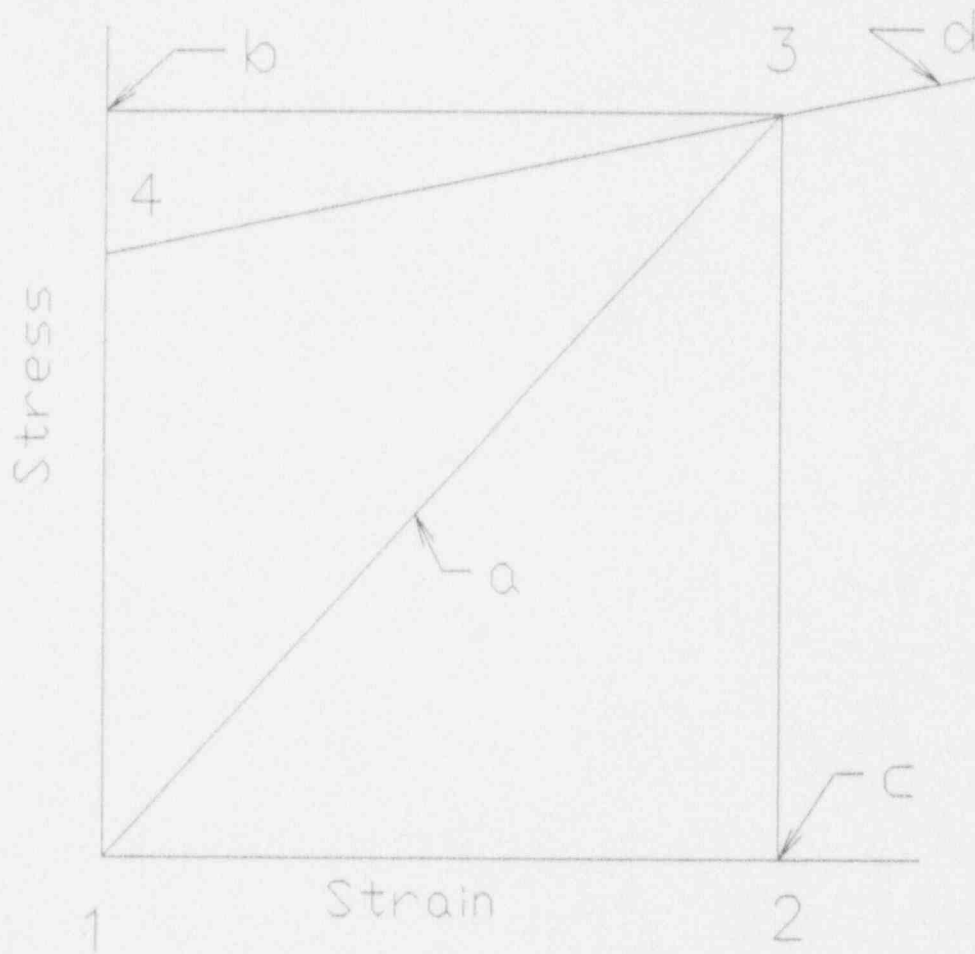
The results of the finite element investigation of the inelastic structural stability and energy absorption capabilities are rather conclusive, in spite of the variations between the different finite element runs. They show that, unlike the six inch high half inch thick fin of Davis Fig. 5.1, the ability of the GC-200 fins to absorb energy due to direct crushing is rather low.

3.6.2 Location of Plastic Hinges

The buckled shapes of the fins in the finite element studies provide a good indication of where the plastic hinges will start to form, once the affected fins start to buckle. Once a plastic hinge starts to form, it will have a strong tendency to remain in the same location as the collapse proceeds.

It should be noted that the actual strain energy absorbed by direct crushing will be much higher than the elastic strain energy, and in fact will be almost double the elastic strain energy. We will assume that the strain energy absorbed equals 1.6 times the elastic strain energy. In this investigation, we will use 1.6 times the "average" strain energies given in Subsection 3.5 (an approximation to

area 1-2-3-4 divided by area 1-2-3 in Fig. 3.1). We realize that the procedure is approximate. However, the direct crushing energy values are small compared to the total energies involved.

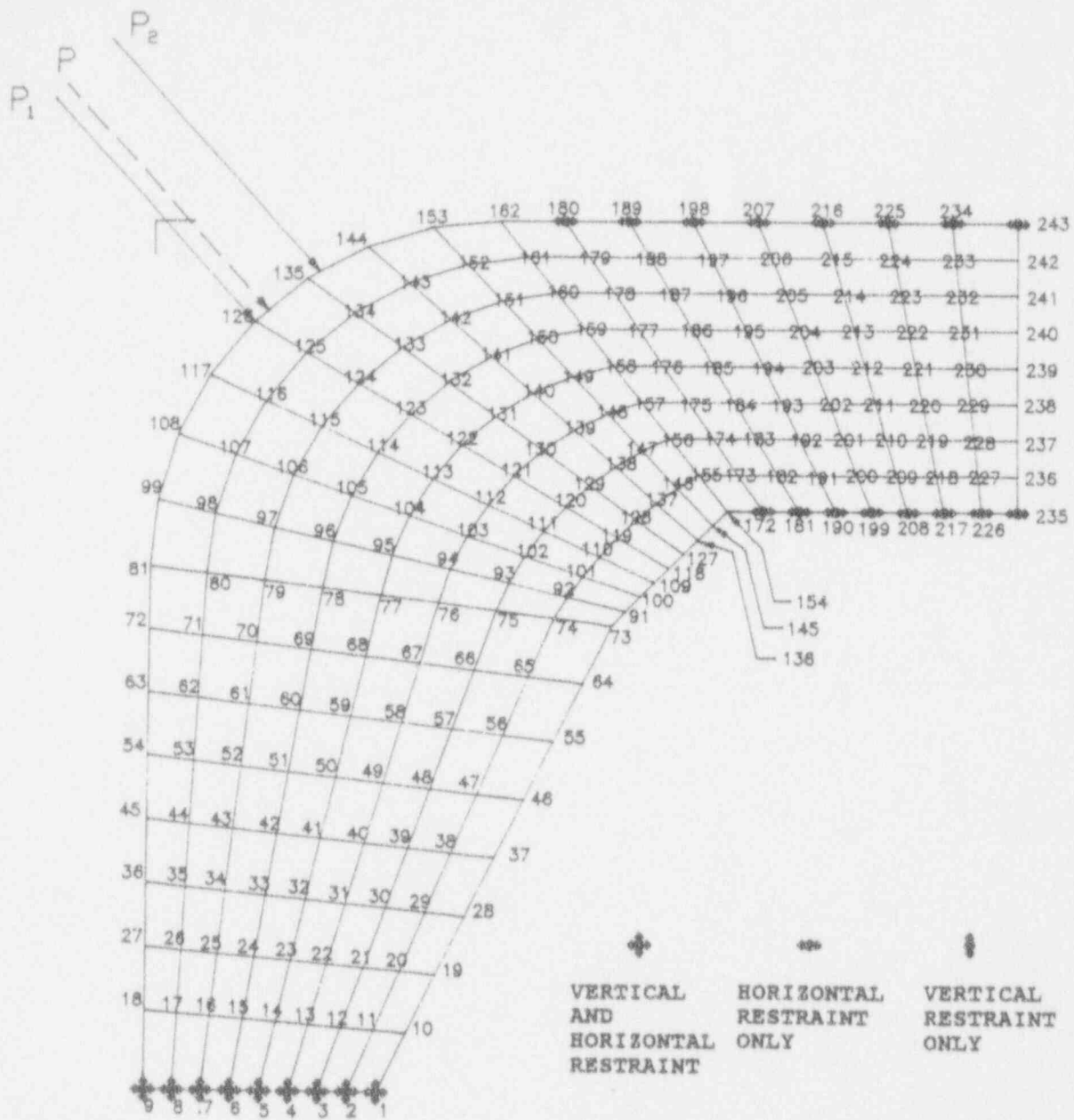


For stress level B and strain level C, the secant modulus of elasticity is the slope of line a, thus:

$$E_s = b/c$$

The tangent modulus elasticity for the same stress and strain is the slope of the line d.

Figure 3.1 Secant and Tangent Modulae of Elasticity



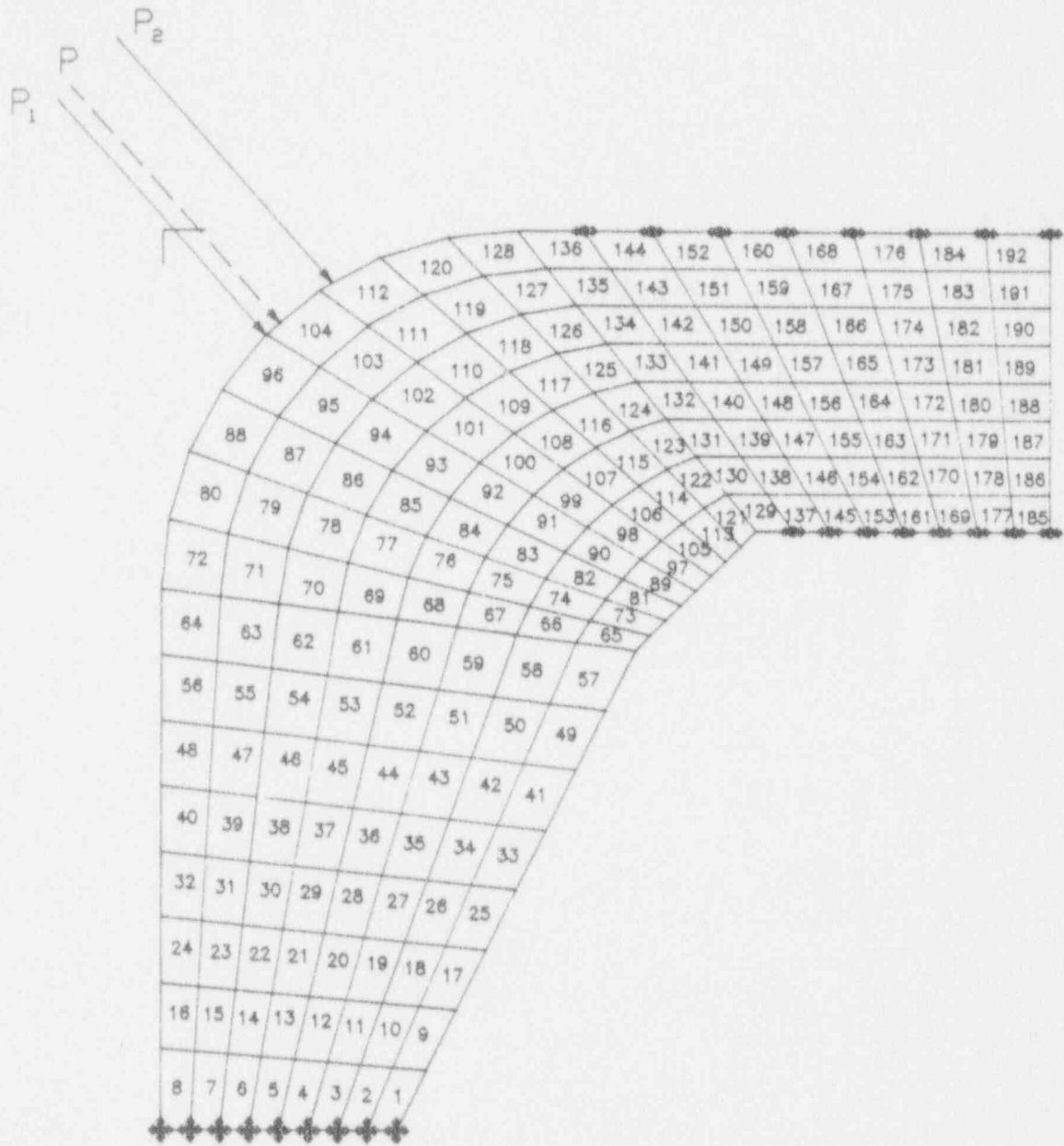
Loading No. 2

42 degrees from vertical  
 (48 degrees from horizontal)

All nodes shown as restrained are also restrained against deflection perpendicular to the paper and against rotation about the horizontal axis parallel to the paper.

The nodes nearest to the load application (in this load case 125 and 135) are also restrained against deflection perpendicular to the paper

Figure 3.2 Node Numbers and Restraints of Finite Element Model of Fin



Loading No. 2  
 42 degrees from vertical

Figure 3.3 Element Numbers of Finite Element Model of Fin

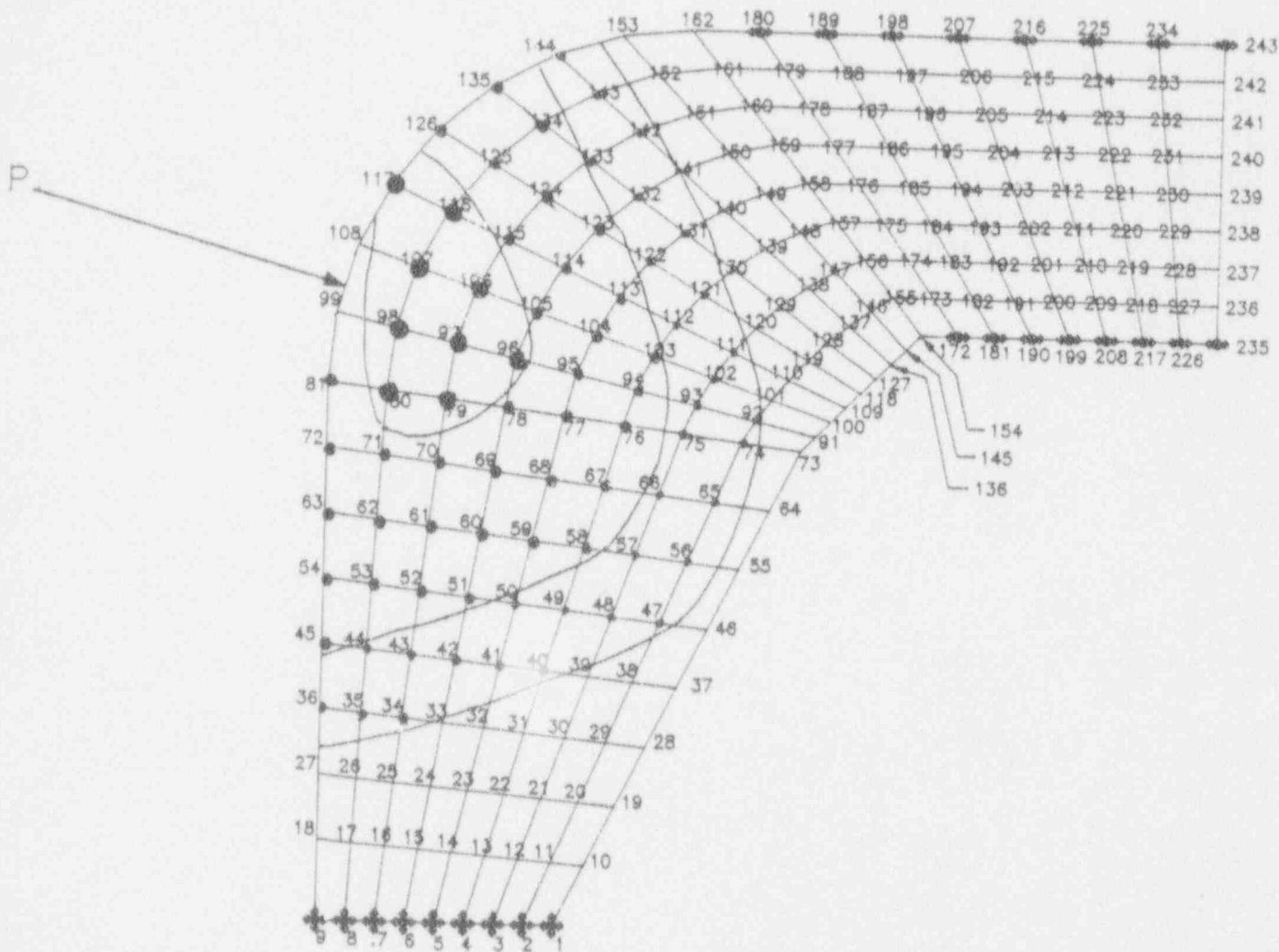


Figure 3.4 Initial Buckled Shape of Vertical Fin  
 Loaded at 74.5 Degrees from the Central Axis  
 of the Transport Package  
 (Loading No. 1)



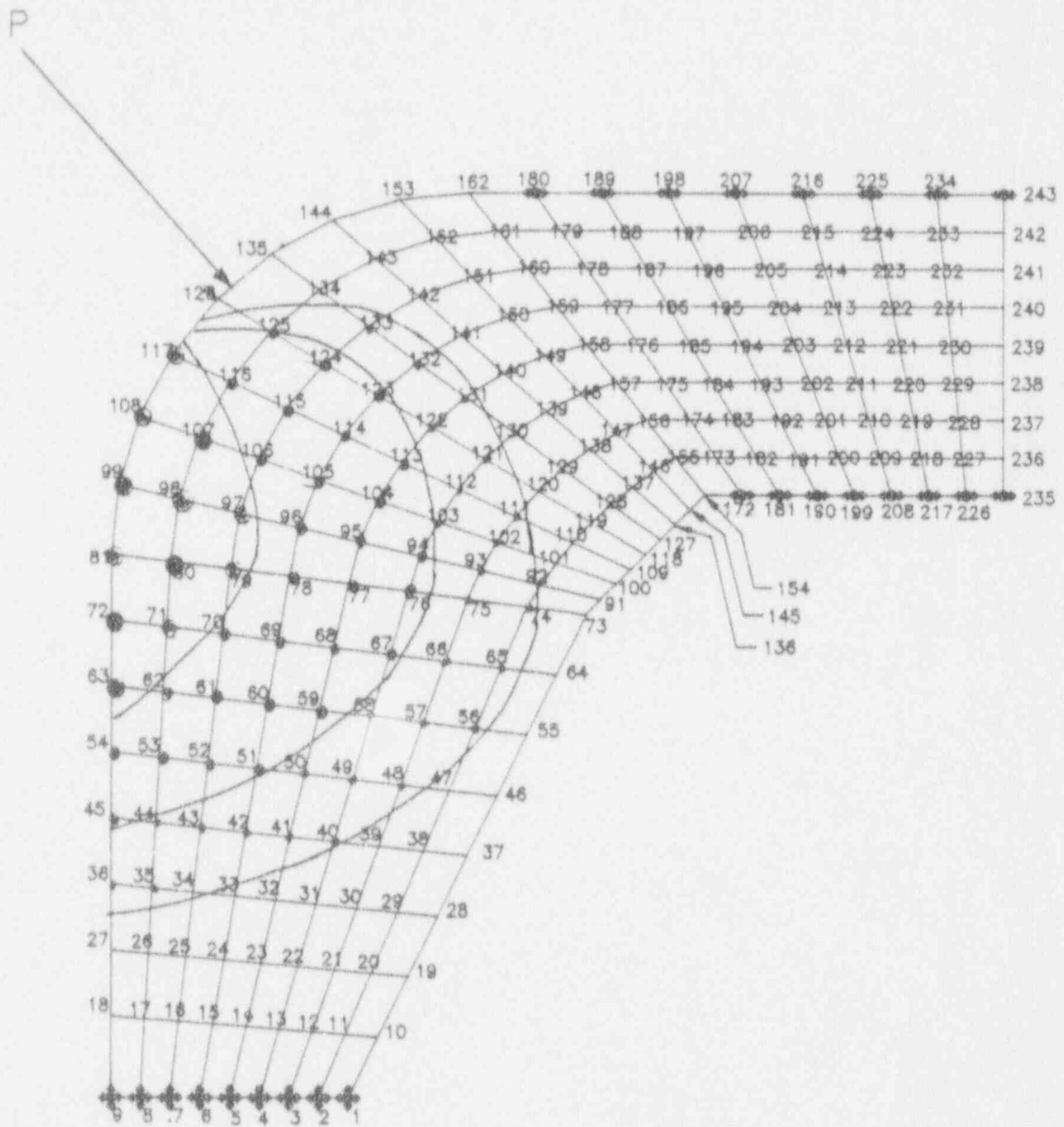


Figure 3.5 Initial Buckled Shape of Vertical Fin  
 Loaded at 42 Degrees from the Central Axis  
 of the Transport Package  
 (Loading No. 2)

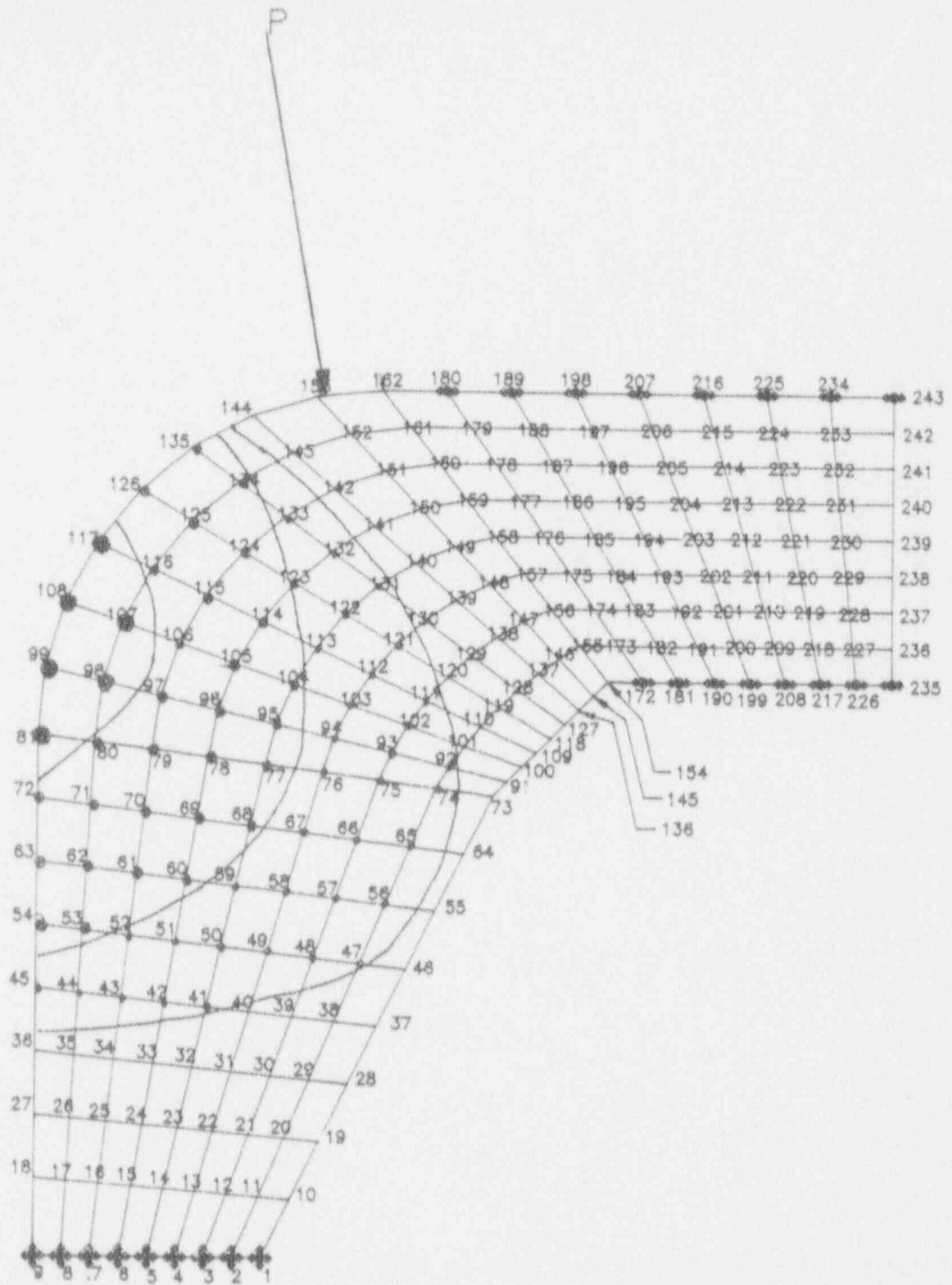


Figure 3.6 Initial Buckled Shape of Vertical Fin  
 Loaded at 10 Degrees from the Central Axis  
 of the Transport Package  
 (Loading No. 3)

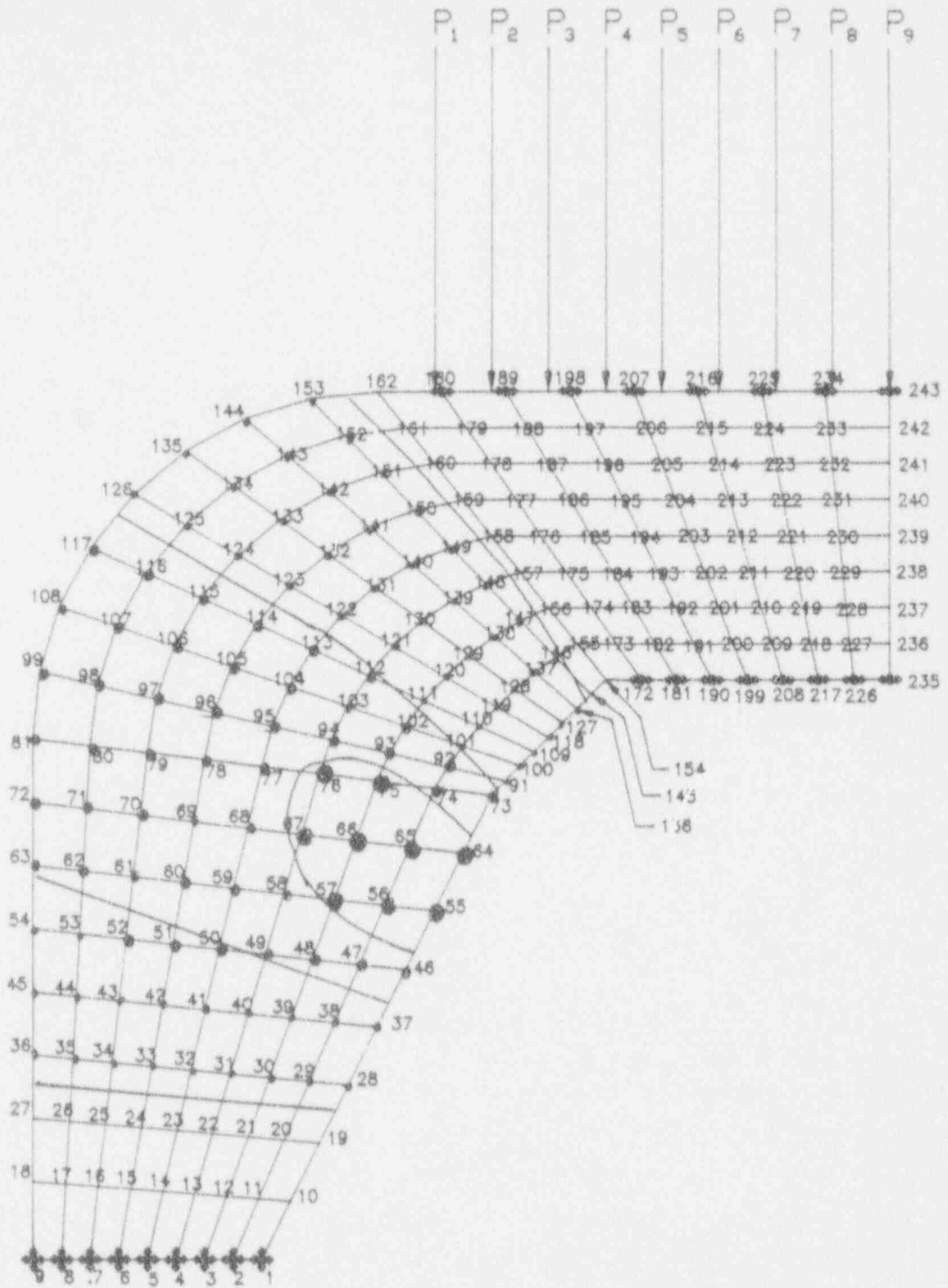


Figure 3.7 Initial Buckled Shape of Vertical Fin  
 Loaded at Zero Degrees from the Central Axis  
 of the Transport Package  
 (Loading No. 4)

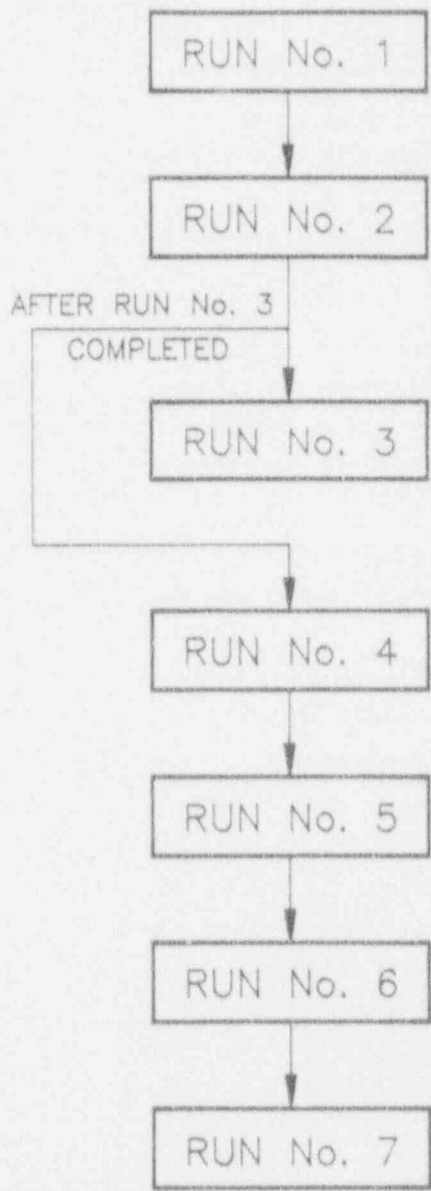


Figure 3.8 Organization of Computer Runs to Establish Buckling Loads and Energy Absorbtion in Direct Crushing

SECTION 4 - OVERALL ANALYSIS OF FINS LATERALLY RESTRAINED  
AT POINT OF LOADING

4.1 GENERAL RULES

- (1) The typical region of formation of plastic hinges for the GC-220 are as shown in Fig. 4.1. Because of the X-direction restraint provided by the upper horizontal plates, the direction of movement will not be the same as the direction of the load, but, especially after plastic hinge formation, will be almost entirely downward, as shown in fig. 4.1.
- (2) The plastic hinges are all shown parallel, and the central hinge is shown half way between the other two hinges. This condition will only be approximated in the actual situation. However, any departure from the situation will cause additional distortions of the fin and the attached plates that will not be included in the analysis. Such distortions will cause energy absorptions that will not be considered.

To summarize, the assumption of parallel hinges and the central hinge halfway from the others is the simplest assumption for analysis purposes. To the extent that this condition is departed from, it will cause energy absorbing distortions to take place that will largely compensate for any error in assuming parallel hinges.

- (3) The plastic moment of resistance supplied by a plastic hinge at the beginning of plastic hinge action is as follows:

$$M_{pe} = 73,000 b t^2/4 = 18,250 b t^2 \text{ inch.lbs.} \quad [4.1]$$

For 3/8" thick fins:

$$M_{pe} = 18,250 \times 0.375^2 b \text{ inch.lbs.} = 2,566.4 \text{ inch.lbs/inch fin width.}$$

It will be seen from Section 4.2 that this formula is very conservative for large plastic hinge action and that a modified formula (Eq. 4.4) should be used in such a situation.

- (4) Referring to Fig. 4.2, the vertical in-plane displacement causing plastic hinge action = crush distance minus the vertical movement due to direct in-plane shortening, = d.
- (5) The action height of the plastic hinge of a vertical fin, h', is illustrated in Figs. 4.1 and 4.2. The angle is obtained thus:

$$d = h'(1 - \cos r)$$

$$1 - \cos r = d/h' \quad [4.2]$$

$$\cos r = 1 - d/h' = 1 - e'$$

$$\text{where } e' = (e_0 - e_b)/(1 - e_b)$$

- (6) The total plastic hinge rotation = 4 r. For many of the plastic hinges of the GC-220, the width of all the plastic hinges can be taken as the width of the central hinge. For the cases where this does not apply, each plastic hinge length will be dealt with explicitly.

4.2 A PRELIMINARY OVERVIEW OF PLASTIC HINGE ACTION

In order to be able to make a preliminary estimate of the plastic hinge energy absorption, a preliminary analysis will be presented here. The height of action of the plastic hinge will be conservatively assumed to equal 9.75 inches (see

Fig. 2.2).

The average width of hinge will be assumed to equal  $4.0 + (9.75/2) \tan 30^\circ = 6.81$  inches.

For fins  $3/8$  inch thick:

$$M_{pe} = 2,566.4 \times 6.81 = 17,477 \text{ in.lbs.}$$

The value of  $Kh/t$  then =  $0.8 \times 6.0 / 0.5 = 9.6$

The maximum possible hinge rotation =  $2 \pi$ .

#### 4.3 COMPARISON WITH THE DAVIS DATA

Consider the behaviour of a fin of zero degree slope, 0.5 inches thick and 6 inches high. Assume a lateral buckling K value of 0.8. Referring to Section 11(5) of this report, the buckling strain is estimated at 0.10.

The energy absorbed in direct crushing per unit volume =  $73,000 e + 172,500 e^2$

Values of e	Values of U (in.lbs)		$M_p/M_{po}$
	per Unit Volume	Per Inch Width	
0.02	1,529	4,587	2.45
0.04	3,196	9,588	5.11
0.06	5,001	15,003	8.00
0.08	6,944	20,832	11.11

For plastic hinge formation, the height of plastic hinge action =  $h(1 - e_b) - t = 6.0(1 - 0.08) - 0.5 = 5.02$  inches.

$$M_p \text{ per inch width} = 73,000 t^2/4 = 18,250 t^2 = 18,250 \times 0.5^2 = 4,562.5 \text{ in.lbs.}$$

$$M_p \text{ for 3 plastic hinges} = 3 \times 4,562.5 = 13687.5 \text{ in.lbs/inch width.}$$

$$\cos r = 1 - (e - e_b)h/h' = 1 - (e - 0.08) \times 6.00/5.02 = 1 - (e - 0.08) \times 1.195 = 1.0956 - 1.195 e.$$

Values of e	Cos r	r(rads)	Values of U		$M_p/M_{po}$
			$U_h$	$U_{total}$	
0.10	0.976	0.220	3,011	23,843	12.72
0.12	0.952	0.311	4,257	25,789	13.38
0.14	0.928	0.382	5,229	26,051	13.90
0.16	0.904	0.442	6,050	26,882	14.34
0.18	0.881	0.493	6,750	27,582	14.71
0.20	0.857	0.541	7,405	28,237	15.06
0.25	0.797	0.649	8,883	29,715	15.85
0.30	0.737	0.742	10,156	30,988	16.53
0.35	0.677	0.827	11,320	32,152	17.15
0.40	0.618	0.905	12,387	33,219	17.72
0.50	0.498	1.050	14,372	35,204	18.78
0.60	0.379	1.182	16,179	37,011	19.74
0.70	0.164	1.406	19,245	40,077	21.37
0.80	0.140	1.430	19,573	40,405	21.54
0.90	0.020	1.551	21,229	42,061	22.43
1.00	0.000	1.571	21,503	42,335	22.58

When the above results are plotted for the six inch high fin as Curve No. 1 on Davis Fig. 5.1 (Fig. 4.3 of this report), the following can be observed:

- (1) The results in the direct crushing area are definitely unconservative, probably as the result of unavoidable initial eccentricity. A better formula would be:

$$U_b = 50,000 e + 70,000 e^2 \quad [4.3]$$

This formula is plotted in Fig. 4.4 for the 3.5 inch high and 6.0 inch high fins, using an  $e_o$  of 0.30 for the 3.5 inch fin and 0.10 for the 6.0 inch fin. Curve 2 applies to the 3.5 inch fin. The curve for the 6.0 inch high fin is indistinguishable from the Davis curve.

- (2) The results in the plastic hinge area are definitely conservative, probably because of the neglect of strain hardening in the formula used. A better formula for  $M_p$  would be:

$$M_{pe} = (73,000 b t^2/4)(1 + e') \quad [4.4]$$

where  $e'$  is the fin shortening ratio is due to plastic hinge action

$$e' = (e - e_b) h/h' \quad [4.5]$$

$$U_h = M_p r,$$

where  $r$  = the total hinge rotation in radians.

These formulas will be used for the calculations of energy absorption in the plastic hinges.

The curve for the six inch high one-half inch thick fin is replotted as Curve No. 3 on the Davis Fig. 5.1 in Fig. 4.3 of this report, using formulas 4.1, 4.2, 4.3 and 4.4. The formula curve can be seen to be slightly more conservative than the Davis curve in the shortening ratio intervals from 0.15 to 0.55.

#### 4.4 SLOPING FINNS

##### The Angle Between the Load and the Plane of the Fin

As the drop angle approaches the central axis of the transfer package (vertical in Fig. 2.3), the angle between the direction of the load and the plane of the fin is reduced. Referring to Fig. 4.4, it can be seen that the relationships is as follows:

$$c = a \cos b$$

where  $c$  = angle between direction of load and plane of fin.

$a$  = slope angle of fin measured from the fin in a vertical plane at time of drop.

$b$  = angle of drop from the horizontal.

Example: Consider the 22.5 degree fin at a drop angle of 42 degrees from the centroidal axis.

$$a = 22.5 \cos(90^\circ - 42^\circ) = 22.5 \cos 48^\circ = 22.5 \times 0.669 = 15.06^\circ.$$

##### Rotation of Plastic Hinges

Referring to Fig. 4.5, note that the applied load is assumed to be constrained to move in a vertical direction. The angle  $a$  is the angle between the line of



action of the load and the plane of the fin. The following relationships then apply:

Referring again to Fig. 4.5:

$$h = h_f \cos a$$

$$g = h_f \sin a$$

$$h_b = h_f(1 - e_b)$$

$$a' = \text{asin}(g/h_b)$$

$$h' = h_b \cos a$$

$$d_b = h - h'$$

$$d_h = d - d_b$$

$$h'' = h - d$$

$$a'' = \text{atan}(g/h'')$$

$$m = h'' \sec a''$$

$$e' = 1 - m/h_b$$

$$\cos r = r + a'' - a$$

where  $e_b$  = fin shortening ratio in the direction of the fin, at buckling strain,

$a$  = initial slope of the fin,

$r'$  = rotation of the plastic hinge at the base of the fin,

and the other terms are illustrated in Fig. 4.5 or defined in Section 12.

In the case where  $e_b$  is negligible:

$$h' = h_f \cos a$$

$$g = h_f \sin a$$

$$h'' = h' - d$$

$$\tan a'' = g/h''$$

$$m = h'' \sec a''$$

$$e' = 1 - m/h_f$$

$$\cos r = 1 - m/h_f$$

$$r' = r + a'' - a$$

In computing the effect of strain hardening on  $M_p$ , the difference between  $r$  and  $r'$  is conservatively neglected.

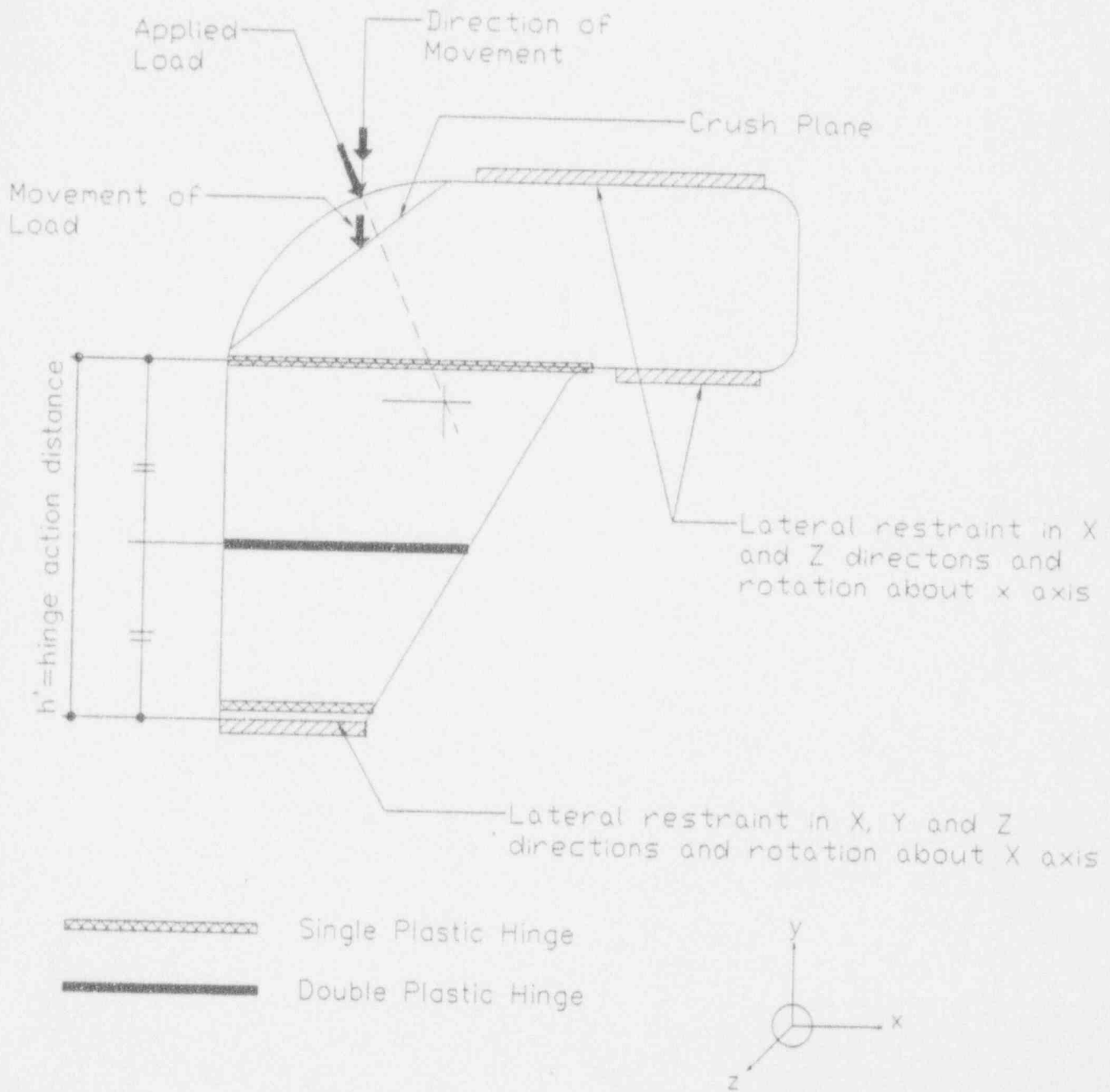
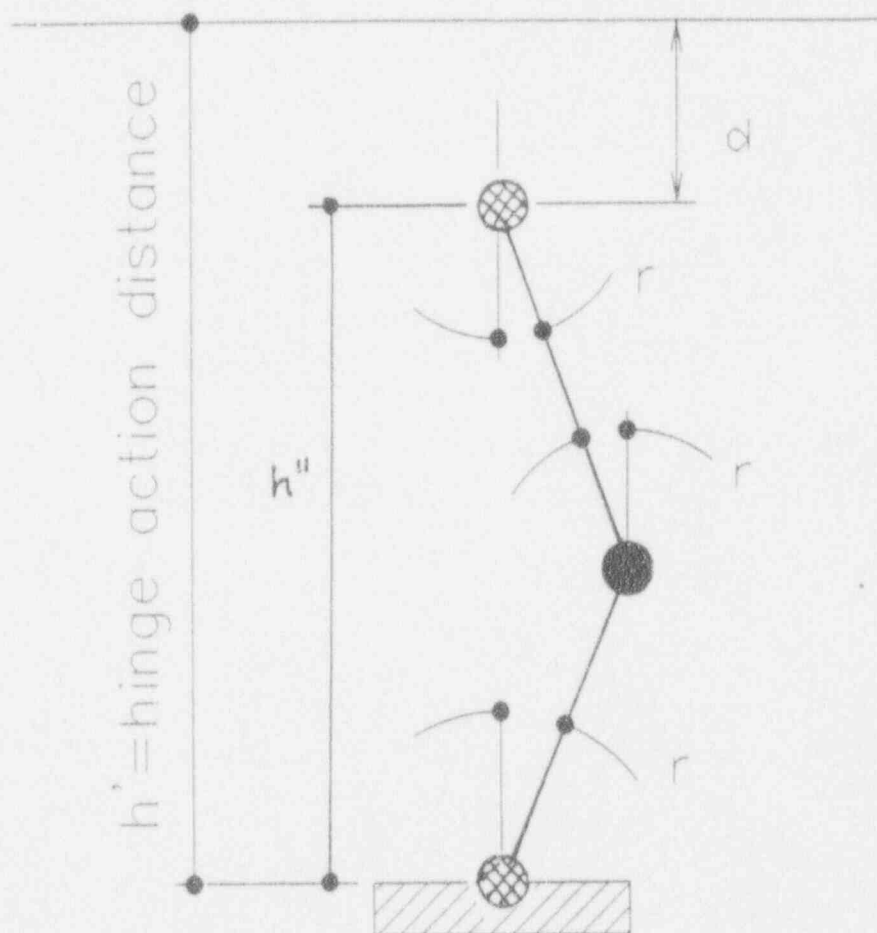


Figure 4.1 The General Characteristics of a Plastic Hinge for the GC-220



-  Single Plastic Hinge
-  Double Plastic Hinge

Figure 4.2 Plastic Hinge Action-Height, Shortening and Plastic Hinge Rotation

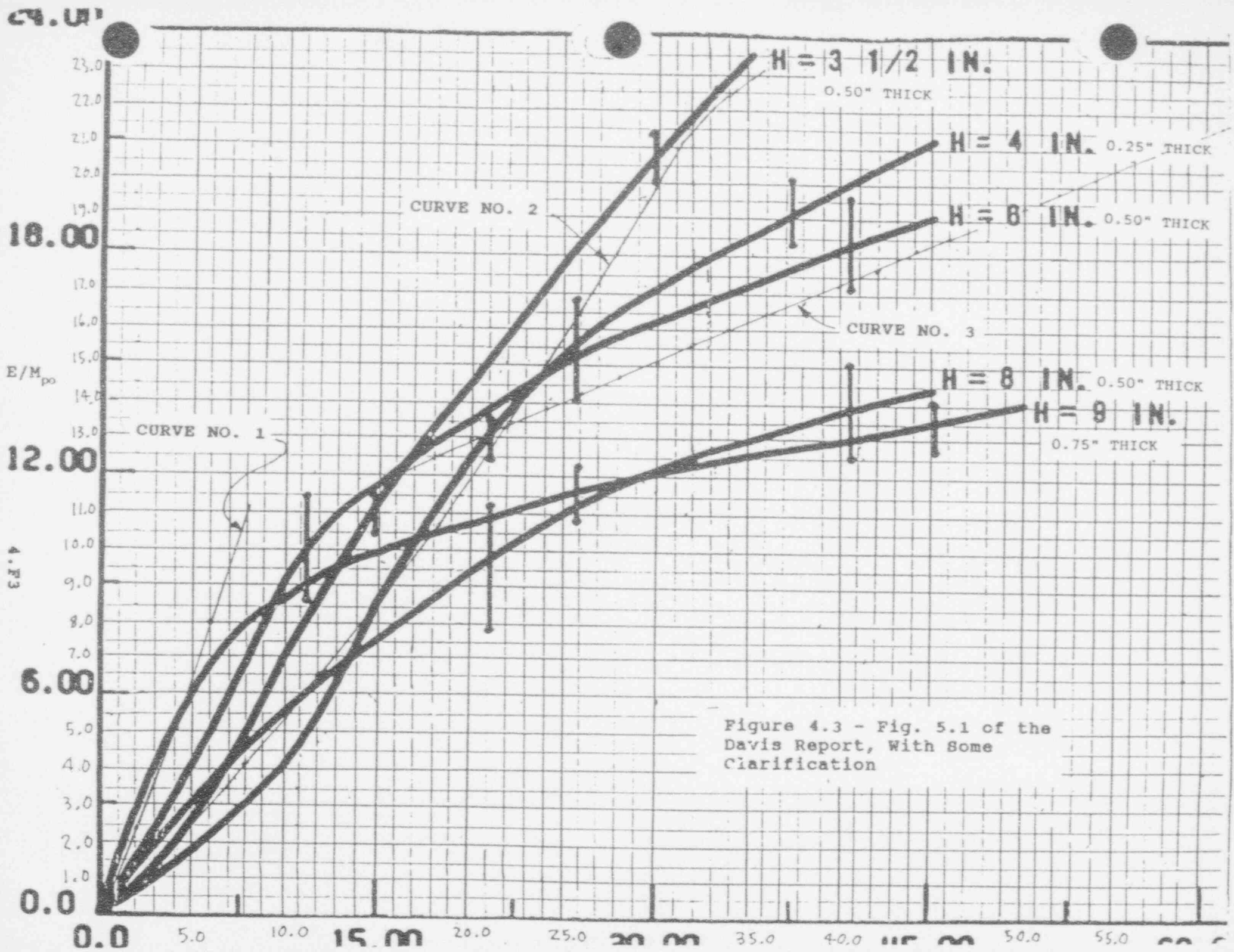
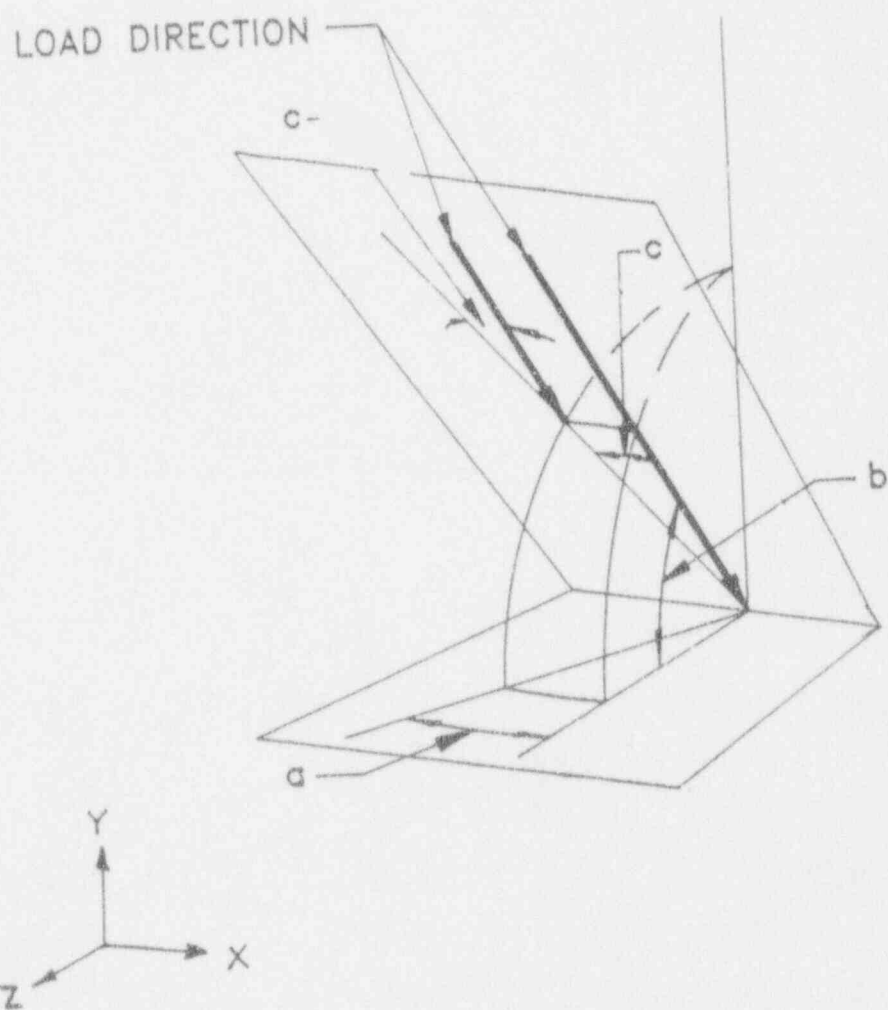


Figure 4.3 - Fig. 5.1 of the Davis Report, With Some Clarification



Angle between direction of fin and direction  
of load =  $c = a \cos b$

Fig. 4.4 Computation of Load Angle on Fin

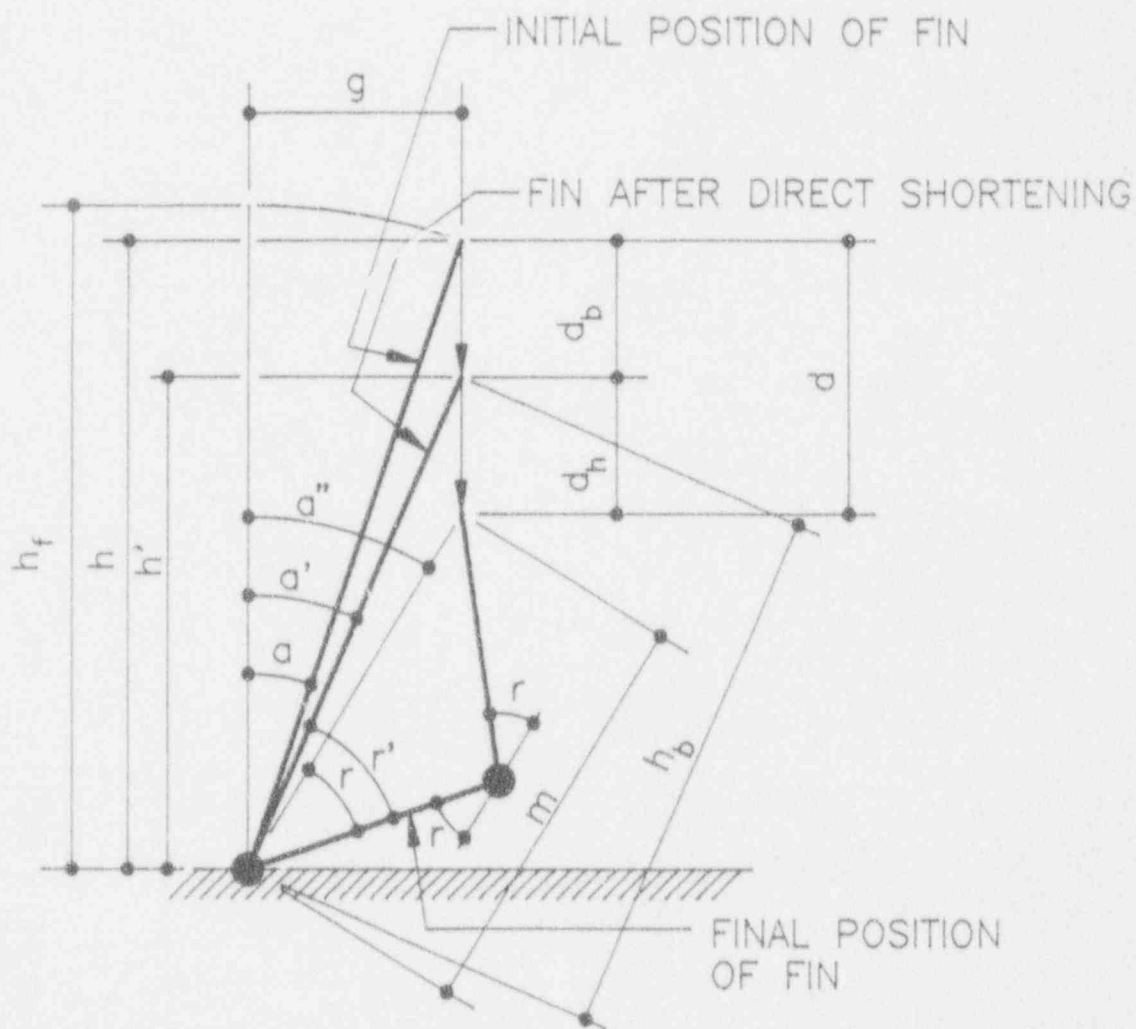


Fig. 4.5 Plastic Hinges in a Sloping Fin with Lateral Restraint at the Top

SECTION 5 - OVERALL ANALYSIS OF FINS WITHOUT LATERAL  
RESTRAINT AT POINT OF LOADING

5.1 INTRODUCTION

If the angle of load is more than 20 degrees out of the plane of the fin, no out-of-plane lateral restraint should be assumed at the point of loading, except where that lateral restraint is provided by the impact limiter itself. This has the following implications for such cases:

- (1) No direct compressive plastic shortening should be assumed.
- (2) In many cases, the number of plastic hinges will be reduced from one double hinge plus one single hinge to only one single hinge. Whether this rule applies must be decided for each case on an individual basis.

5.2 THE EFFECT OF SLOPE ON THE ENERGY ABSORBED BY THE PLASTIC HINGES

Referring to Fig. 5.1:

$$h' = h \cos a$$

$$h'' = h' - d$$

$$\cos (a + r) = h''/h_f$$

$$r = a + r - a$$

$$e' = 1 - \cos r$$



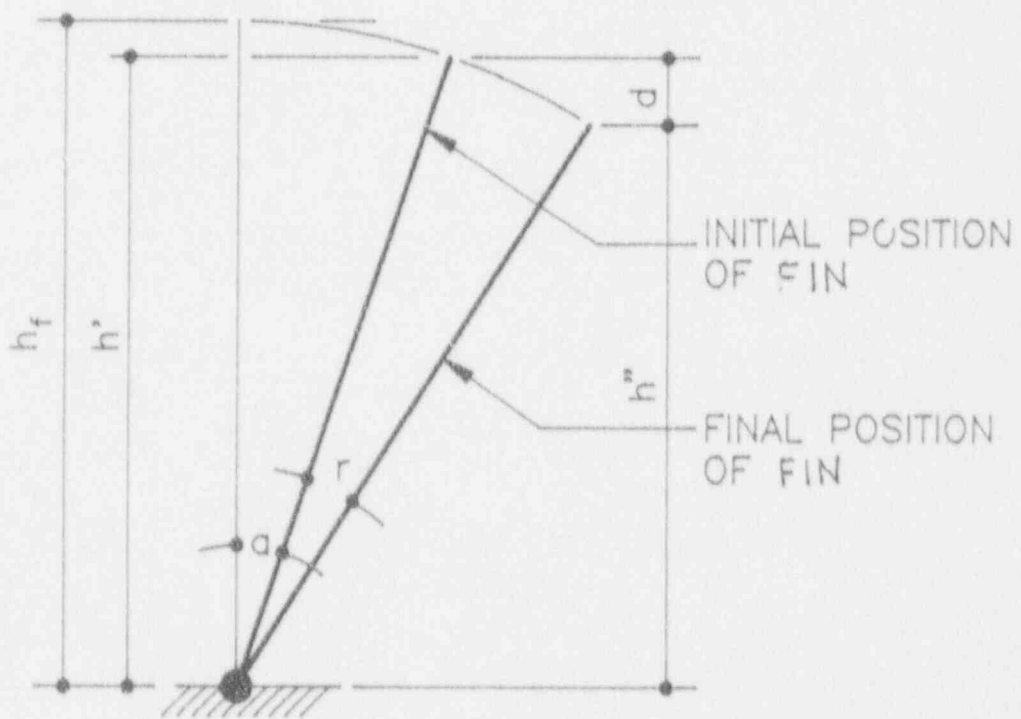


Figure 5.1 Plastic Hinge in a Sloping Fin with No Lateral Restraint at the Top

## SECTION 6 - OVERALL BEHAVIOUR OF THE IMPACT LIMITER

For large fin deflections, the overall action of the impact limiter modifies and complicates the behaviour of the individual fins. This aspect of the behaviour of the impact limiter is considered in this section.

In considering the action of individual fins, it was assumed that the lateral restraint provided by the two upper horizontal plates of Fig. 2.2 is in the horizontal plane only. In actual practice for large deflections the action is more like that illustrated in Fig. 6.1.

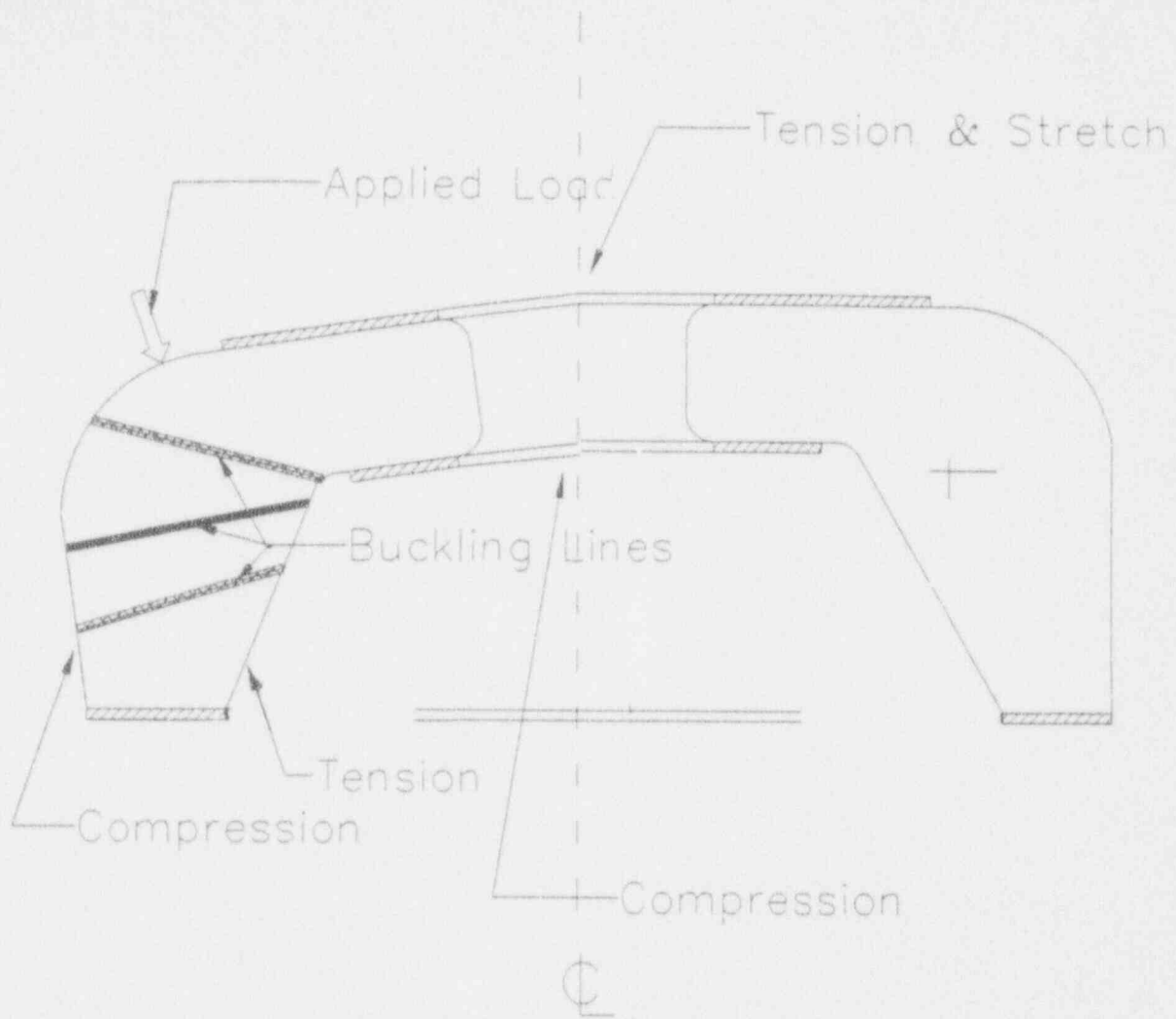


Figure 6.1 Effect of Large Deflections on Overall Action of Impact Limiter

## SECTION 7 - IMPACT LIMITER WITH LOADING ZERO DEGREE. FROM CENTRAL AXIS

### 7.1 ENERGY ABSORBED BY THE FINS IN DIRECT CRUSHING AND PLASTIC HINGE ACTION

The assumed method and location of plastic hinge formation will be as shown in Figs. 4.1 and 4.2.

From formulas 4.4 and 4.5

$$M_{pe} = (73,000 b t^2/4)(1 + e')$$

$$U_h \text{ per fin} = M_{pe} r$$

In the case of a totally collapsed fin,  $e' = 1.0$ .

$$\text{Here } M_{pe} = (73,000 \times 6.81 \times 0.375^2/4)(1 + 1.0) = 34,954 \text{ in.lbs.}$$

There will be a single plastic hinge top and bottom plus a double plastic hinge at mid-height.

$$\text{Total } r = 2 \pi, \text{ giving } U_h \text{ per fin} = 34,954 \times 6.28 = 219,622 \text{ in.lbs.}$$

For an end drop and full plastic collapse, the total energy absorbed by all 16 fins would be:

$$\text{Total } U_h = 219,622 \times 16 = 3,513,953 \text{ in.lbs.}$$

This is more than 100% of the total impact energy, even neglecting the small amount of energy absorbed in direct shortening. The assumed crush distance to absorb this amount of energy = 9.0 inches. The actual crush distance would be very approximately  $9.0 \times 3,060,000/3,513,953 = 7.8$  inches.

### 7.2 ESTIMATION OF THE CRUSHING LOADS

#### The Load to Produce Fin Buckling

Sixteen fins participate equally in direct buckling. From Paragraph 3.3, the estimated force =  $16 \times 64,900 = 1,038,400 \text{ lbs} = 1,038,400/8,500 = 122 \text{ g's.}$

#### The Average Load to Absorb the Drop Energy

$$\text{The average load} = 3,060,000/7.8 = 390,439 \text{ lbs} = 390,439/8,500 = 50 \text{ g's.}$$

## SECTION 8 - IMPACT LIMITER WITH LOADING 10 DEGREES FROM CENTRAL AXIS

### 8.1 INTRODUCTION

It is assumed that the fins undergo direct buckling in the same manner as for zero degree loading (Section 8 and Figs. 4.1 and 4.2). In all cases, the angle between the direction of the load and the plane of the fin will be less than 20°. For each fin there will be a single plastic hinge top and bottom plus a double plastic hinge at mid-height.

However, in this case, only one of the fins will undergo full collapse before bottoming out of the cask. The distances of movement of the different fins are given in Fig. 8.1.

### 8.2 ENERGY ABSORBED BY THE FINS IN DIRECT CRUSHING AND PLASTIC HINGE ACTION

One Zero Degree Fin (Fin No. 1) - Direct Crushing

Ref. Sect. 3.5.

$$1.6 \times 6,100 = 9,760 \text{ in.lbs.}$$

One Zero Degree Fin (Fin No. 1) - Plastic Hinges

$$e' = 1.0$$

$$U_h = 2,566.4 \times 6.81 \times 2 \pi \times 2.0 = 219,560 \text{ in.lbs}$$

Two 22.5 Degree Fins (Fin No. 2) - Direct Crushing

$$2 \times 1.6 \times 2,200 = 7,046 \text{ in.lbs}$$

Two 22.5 Degree Fins (Fin No. 2) - Plastic Hinges

Referring to Figs. 4.2 and 8.1:

$$e' = 9.1/9.8 = 0.93$$

$$\cos r = 1 - d/h = 1 - 0.93 = 0.07$$

$$r = 85.9 \text{ degrees} = 1.50 \text{ radians}$$

$$U_h = 2 \times 2,566.4 \times 6.81 \times 1.93 \times 4 \times 1.50 = 404,652 \text{ in.lbs}$$

Two 45 Degree Fins (Fin No. 3) - Direct Crushing

$$2 \times 1.6 \times 2,200 = 7,046 \text{ in.lbs}$$

Two 45 Degree Fins (Fin No. 3) - Plastic Hinges

$$e' = 8.7/9.8 = 0.89$$

$$\cos r = 1 - 0.89 = 0.11$$

$$r = 83.6 \text{ degrees} = 1.46 \text{ radians}$$

$$U_h = 2 \times 2,566.4 \times 6.81 \times 1.89 \times 4 \times 1.46 = 385,698 \text{ in.lbs}$$

Two 67.5 Degree Fins (Fin No. 4) - Direct Crushing

$$2 \times 1.6 \times 2,200 = 7,046 \text{ in.lbs}$$

Two 67.5 Degree Fins (Fin No. 4) - Plastic Hinges

$$e' = 7.4/9.8 = 0.76$$

$$\cos r = 1 - 0.76 = 0.24$$

$$r = 75.8 \text{ degrees} = 1.32 \text{ radians}$$

$$U_h = 2 \times 2,566.4 \times 6.81 \times 1.76 \times 4 \times 1.32 = 324,727 \text{ in.lbs}$$

Two 90 Degree Fins (Fin No. 5) - Direct Crushing

$$2 \times 1.6 \times 2,200 = 7,046 \text{ in.lbs}$$

Two 90 Degree Fins (Fin No. 5) - Plastic Hinges

$$e' = 5.9/9.8 = 0.60$$

$$\cos r = 1 - 0.60 = 0.40$$

$$r = 66.5 \text{ degrees} = 1.16 \text{ radians}$$

$$U_h = 2 \times 2,566.4 \times 6.81 \times 1.60 \times 4 \times 1.16 = 259,424 \text{ in.lbs}$$

Two 112.5 Degree Fins (Fin No. 6) - Direct Crushing

$$2 \times 1.6 \times 2,200 = 7,046 \text{ in.lbs}$$

Two 112.5 Degree Fins (Fin No. 6) - Plastic Hinges

$$e' = 4.8/9.8 = 0.49$$

$$\cos r = 1 - 0.49 = 0.51$$

$$r = 59.3 \text{ degrees} = 1.035 \text{ radians}$$

$$U_h = 2 \times 2,566.4 \times 6.81 \times 1.49 \times 4 \times 1.035 = 215,555 \text{ in.lbs}$$

Two 135 Degree Fins (Fin No. 7) - Direct Crushing

$$2 \times 1.6 \times 2,200 = 7,046 \text{ in.lbs}$$

Two 135 Degree Fins (Fin No. 7) - Plastic Hinges

$$e' = 3.7/9.8 = 0.38$$

$$\cos r = 1 - 0.38 = 0.620$$

$$r = 51.5 \text{ degrees} = 0.899 \text{ radians}$$

$$U_h = 2 \times 2,566.4 \times 6.81 \times 1.38 \times 4 \times 0.899 = 173,409 \text{ in.lbs}$$

Two 157.5 Degree Fins (Fin No. 8) - Direct Crushing

$$2 \times 1.6 \times 2,200 = 7,046 \text{ in.lbs}$$

Two 157.5 Degree Fins (Fin No. 8) - Plastic Hinges

$$e' = 3.0/9.8 = 0.31$$

$$\cos r = 1 - 0.31 = 0.694$$

$$r = 46.1 \text{ degrees} = 0.804 \text{ radians}$$

$$U_h = 2 \times 2,566.4 \times 6.81 \times 1.13 \times 4 \times 0.804 = 147,218 \text{ in.lbs}$$

One 180 Degree Fin (Fin No. 9) - Direct Crushing

$$1.6 \times 2,200 = 3,520 \text{ in.lbs}$$

One 180 Degree Fin (Fin No. 9) - Plastic Hinges

$$e' = 2.6/9.8 = 0.27$$

$$\cos r = 1 - 0.27 = 0.735$$

$$r = 42.7 \text{ degrees} = 0.745 \text{ radians}$$

$$U_h = 2,566.4 \times 6.81 \times 1.27 \times 4 \times 0.745 = 66,125 \text{ in.lbs}$$

### 8.3 TOTAL ENERGY ABSORBED BY THE IMPACT LIMITER

One zero degree fin - direct crushing =	9,760
One zero degree fin - plastic hinges =	219,560
Two 22.5 degree fins - direct crushing =	7,040
Two 22.5 degree fins - plastic hinges =	404,652
Two 45 degree fins - direct crushing =	7,040
Two 45 degree fins - plastic hinges =	385,698
Two 67.5 degree fins - direct crushing =	7,040
Two 67.5 degree fins - plastic hinges =	324,727
Two 90 degree fins - direct crushing =	7,040
Two 90 degree fins - plastic hinges =	259,424
Two 112.5 degree fins - direct crushing =	7,040
Two 112.5 degree fins - plastic hinges =	215,555
Two 135 degree fins - direct crushing =	7,040
Two 135 degree fins - plastic hinges =	173,409
Two 157.5 degree fins - direct crushing =	7,040
Two 157.5 degree fins - plastic hinges =	147,218
One 180 degree fin - direct crushing =	3,520
One 180 degree fin - plastic hinges =	66,125
Total =	<hr/> 2,258,928 in.lbs

### 8.4 ESTIMATION OF THE CRUSHING LOADS

#### The Load to Produce Fin Buckling

Sixteen fins participate in the buckling, but not all simultaneously with full force. Assume that the maximum load is 75% of what would occur if all the fins buckled simultaneously. The 64,900 lbs for Case 5 (Paragraph 3.3) will be used, rather than the 76,400 lbs for Case 4, because it is believed to be a better average fin buckling load.

The maximum buckling force then =  $0.75 \times 16 \times 64,900 = 778,800$  lbs =  $778,800/8,500 = 45$  g's.

#### The Average Load to Absorb the Drop Energy

The average crush distance is taken to equal 5.9 inches (central fin in Fig. 8.1).

The average force =  $2,258,928/5.9 = 382,869$  lbs =  $382,869/8,500 = 45$  g's.



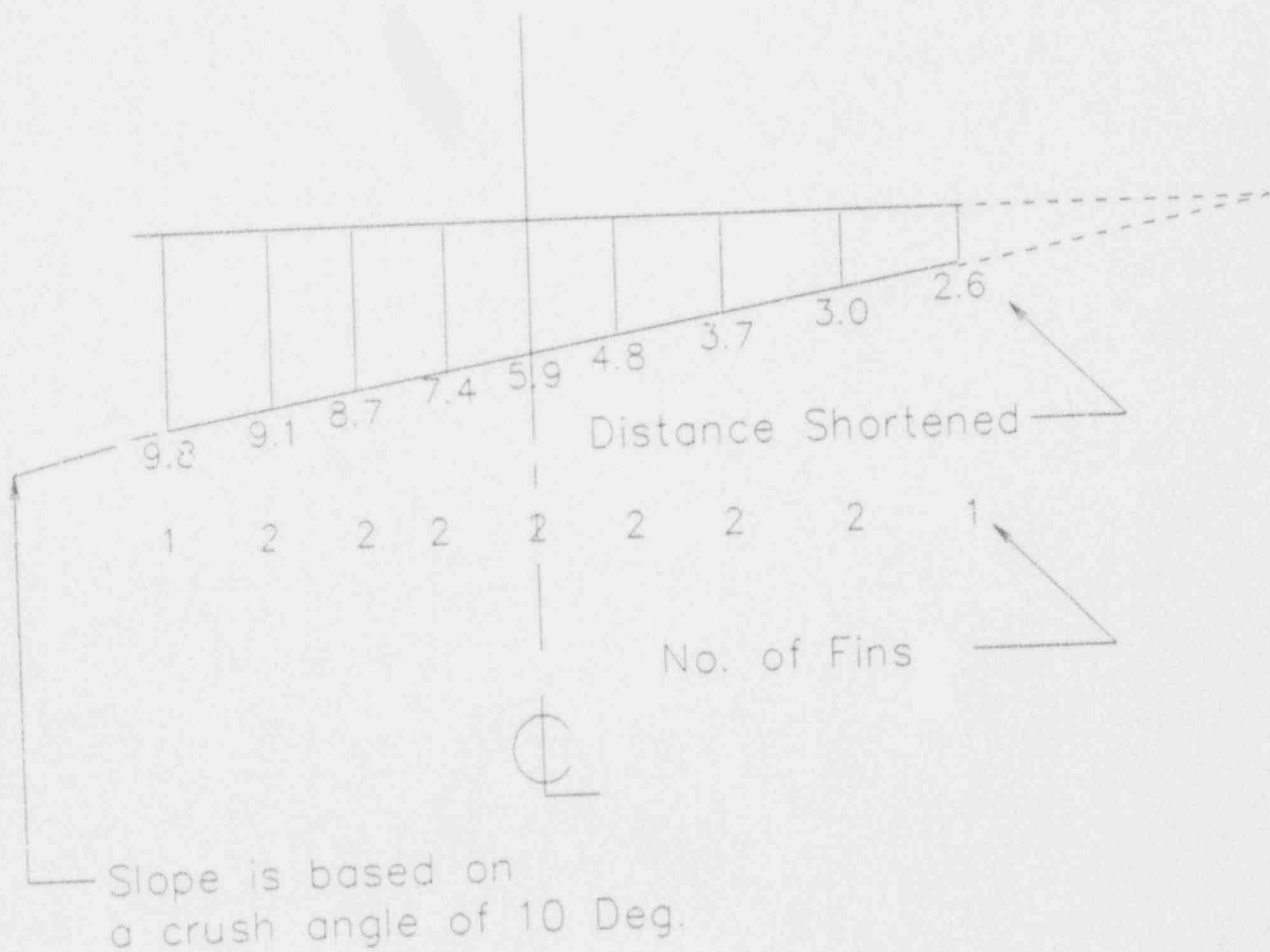


Figure 8.1 Shortening of Individual Fins  
Due to Crushing of Impact Limiter  
(Drop 10 Degrees from Vertical)

## SECTION 9 - IMPACT LIMITER WITH LOADING 42 DEGREES FROM CENTRAL AXIS

### 9.1 INTRODUCTION

The crush distance for direct crushing of the top plate is taken as the distance measured in the direction of load action. To compensate for the slope of the top plate relative to the direction of load, the crushing stress in the top plate and adjacent fin is taken as 35,000 psi.

The possible modes of plastic hinge action are shown in Fig. 9.1. The fins are expected to fail first by Mode 1 and then by Mode 2. As can be seen in Fig. 9.1(c), substantial interference can be expected between Modes 1 and 2, because the formation of Mode 1 will increase the strain energy to be expected in the formation of Mode 2.

In these calculations, the total energy absorption by the plastic hinges will be taken as the sum of the energies for Modes 1 and 2 without any extra allowance for interference. For the sloping fins, the crush distance for the fins will be conservatively be taken as the crush distance as projected in the plane of the zero degree fin. For all the Mode 1 actions, assume two single plastic hinges plus one double plastic hinge.

### 9.2 ENERGY ABSORBED BY THE FINS IN DIRECT CRUSHING AND PLASTIC HINGE ACTION

#### One Zero Degree Slope Fin - Direct Crushing

##### Crushing of Fin

Ref. Sect. 3.5

$$U_b = 1.6 \times 3,700 = 5,920 \text{ in.lbs}$$

##### Crushing of Top Plate

The effective direct crushing area will be similar to that shown for the case of the 74.5 degree fin in Fig. 10.3. However, the effective stresses will be reduced, as discussed in Subsection 9.1.

Crush distance = 2.8 inches.

$$U_b = 35,000 \times 0.375 \times (8.375 + 1.5) \times 2.8 = \underline{179,156 \text{ in.lbs}}$$

$$\text{Total} = 185,076 \text{ in.lbs}$$

#### One Zero Degree Slope Fin - Plastic Hinges

##### Mode 1 Action

Height of fin action = 9.9 inches.

Crush distance = 9.9 inches (Fig. 9.2).

The position of the plastic hinges will be as shown in Fig. 4.1.

$e' = 1.0$

$$U_h = 2,566.4 \times 6.81 \times 2.0 \times 2 \pi = 219,560 \text{ in.lbs}$$

### Mode 2 Action

The position of the plastic hinges will be as shown in Fig. 9.3. Assume one double plastic hinge plus one single hinge.

Height of fin action = 5.0 inches.

Crush distance = 5.0 inches

$e' = 1.0$

$$U_h = 2,566.4 \times (10.0 \times 2 + 15.2) \times 2.0 \times \pi/2 = \underline{283,804 \text{ in.lbs}}$$

$$\text{Total} = 503,364 \text{ in.lbs}$$

### Two 22.5 Degree Slope Fins - Direct Crushing

#### Crushing of Fins

$$U_b = 2 \times 1.6 \times 3,700 = 11,840 \text{ in.lbs}$$

#### Crushing of Top Plate

Crush distance = 0.5 inches

$$U_b = 2 \times 35,000 \times 0.375 \times (3.375 + 1.5) \times 0.5 = \underline{63,984 \text{ in.lbs}}$$

$$\text{Total} = 75,824 \text{ in.lbs}$$

### Two 22.5 Degree Fins - Plastic Hinges

#### Mode 1 Action

Height of fin action = 9.9 inches

Crush distance = 9.2 inches (Fig. 9.2)

$e' = 9.2/9.9 = 0.93$

$\cos r = 1 - 0.93 = 0.07$

$r = 1.00$

$$U_h = 2 \times 2,566.4 \times 1.93 \times 6.81 \times 2 \pi = 423,751 \text{ in.lbs}$$

#### Mode 2 Action

Angle between fin and load

$= 22.5 \cos (90^\circ - 42^\circ) = 15.06^\circ = 0.26 \text{ rads}$

Assume one double plastic hinge plus one single hinge.

Height of fin action = 5.0 inches (Fig. 9.3)

Crush distance = 4.1 inches (Fig. 9.4)

$e_b$  is negligible.

Referring to Section 4.4 and Fig. 4.5:

$h' = h_f \cos a = 5.0 \cos 15.06^\circ = 4.83 \text{ inches}$

$g = h_f \sin a = 5.0 \sin 15.06^\circ = 1.3 \text{ inches}$

$h'' = h' - d = 4.83 - 4.1 = 0.73 \text{ inches}$

$\tan a'' = g/h'' = 1.30/0.73 = 1.78$

$a'' = 60.7^\circ = 1.06 \text{ rads}$

$m = h'' \sec a'' = 0.73 \times 2.04 = 1.50 \text{ inches}$

$e' = 1 - m/h_f = 1 - 1.50/5 = 0.70$

$\cos r = 1 - e' = 1 - 0.7 = 0.30$

$r = 72.5^\circ = 1.28 \text{ radians}$

$r' = r + a'' - a = 1.28 + 1.06 - 0.26 = 2.08 \text{ rads}$

$$U_h = 2 \times 2,566.4 \times (10.0 \times 2 \times 1.28 + 15.2 \times 2.08) \times 1.69 = 493,679 \text{ in.lbs}$$

$$\text{Total} = 917,430 \text{ in.lbs}$$

Two 45 Degree Fins - Direct Crushing

Crushing of Fins

Load angle = 30.1°. See below  $U_b$  = 0 in.lbs

Crushing of Top Plate

Not relevant = 0 in.lbs

Total = 0 in.lbs

Two 45 Degree Fins - Plastic Hinges

Mode 1 Action

Angle between load and plane of fin  
 =  $45 \cos(90^\circ - 42^\circ) = 30.1^\circ$ .  
 Assume one single plastic hinge.  
 Height of fin action = 9.9 inches  
 Crush distance = 7.1 inches (Fig. 9.2)

$$e' = 7.1/9.9 = 0.72$$

$$\cos r = 1 - 0.72 = 0.28$$

$$r = 73.6 \text{ degrees} = 1.284 \text{ radians}$$

$$U_h = 2 \times 2,566.4 \times 6.81 \times 1.72 \times 4 \times 1.284 = 308,784 \text{ in.lbs}$$

Mode 2 Action

Angle between load and plane of fin  
 =  $45 \cos(90^\circ - 42^\circ) = 30.1^\circ = 0.526 \text{ rads.}$   
 Height of fin action = 5.0 inches (Fig. 9.3)  
 Crush distance = 1.67 inches (Fig. 9.5)

Referring to Subsection 5.2 and Fig. 5.1:

$$h' = h \cos a = 5.0 \cos 30.1^\circ = 4.33 \text{ inches.}$$

$$h'' = h' - d = 4.33 - 1.67 = 2.66 \text{ inches.}$$

$$(a + r) = \arccos(h''/h_f) = \arccos(2.66/5.0)$$

$$= 5.79^\circ = 1.00 \text{ rads.}$$

$$r = (a + r) - a = 1.00 - 0.526 = 0.474 \text{ rads.}$$

$$e' = 1 - \cos r = 1 - \cos 0.474 \text{ rads} = 0.11.$$

$$U_h = 2 \times 2,566.4 \times 15.2 \times 1.11 \times 0.474 = 41,049 \text{ in.lbs}$$

Total = 349,833 in.lbs

Two 67.5 Degree Fins - Direct Crushing

No effective crushing.

Two 67.5 Degree Fins - Plastic Hinges

Mode 1 Action

Height of fin action = 9.2 inches  
 Crush distance = 3.8 inches (Fig. 9.2)

$$e' = 3.8/9.2 = 0.41$$

$$\cos r = 1 - 0.41 = 0.59$$

$$r = 54.1 \text{ degrees} = 0.944 \text{ radians}$$

$$U_h = 2 \times 2,566.4 \times 6.81 \times 1.41 \times 4 \times 0.944 = 186,103 \text{ in.lbs}$$

#### Mode 2 Action

Not considered to be significant	=	<u>0 in.lbs</u>
Total	=	186,103 in.lbs

### 9.3 TOTAL ENERGY ABSORBED BY THE IMPACT LIMITER

One zero degree fin - direct crushing	=	185,076 in.lbs
One zero degree fin - plastic hinges	=	503,364 in.lbs
Two 22.5 degree fins - direct crushing	=	75,824 in.lbs
Two 22.5 degree fins - plastic hinges	=	917,430 in.lbs
Two 45 degree fins - direct crushing	=	0 in.lbs
Two 45 degree fins - plastic hinges	=	349,833 in.lbs
Two 67.5 degree fins - direct crushing	=	0 in.lbs
Two 67.5 degree fins - plastic hinges	=	186,103 in.lbs
Total	=	<u>2,217,630 in.lbs</u>

### 9.4 ESTIMATION OF THE CRUSHING LOADS

#### The Load to Produce Fin Buckling

At the initial buckling stage, three fins participate in resisting the crushing load. The largest load occurs when Fin No. 1 (Fig. 2.2) has already buckled and Fins No. 2 are at their buckling load. Assume that the load on Fin No. 1 has been reduced to 60% of its buckling value when Fins No. 2 buckle. Then the total force =  $2.6 \times 68,600 = 178,360 \text{ lbs} = 178,360/8,500 = 21 \text{ g's}$ .

#### The Average Load to Absorb the Drop Energy

Estimate the total crush distance to be half the crush distance of Mode 1 plus the total crush distance of Mode 2 =  $9.9/2 + 5.0 = 10.0 \text{ inches}$ .

The average force =  $2,217,630/10.0 = 221,763 \text{ lbs} = 221,763/8,500 = 26 \text{ g's}$ .

#### The Average Force to Crush the Combined Outer Plates and Fins

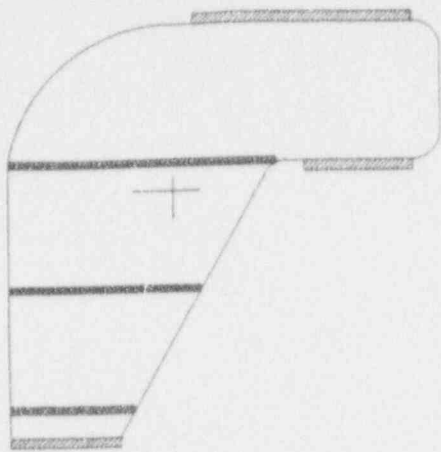
Because of the slope relative to the load of the outer plates undergoing crushing, assume a direct crushing stress for these plates of 35,000 psi. The crush area from three junctions between fins and outside plates =  $3 \times 0.375 \times (8.375 + 1.5)$  (Fig. 10.3) = 11.1 sq.in.

Crushing force =  $35,000 \times 11.1 = 388,500 \text{ lbs}$ .

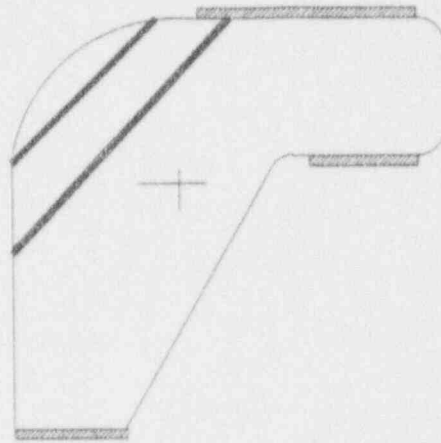
When this force is being developed, the fins will have already buckled to a substantial degree and the load resisted by the fins will have been substantially reduced.

Using Mode 2 plastic hinge energies, assume a force from the fin plastic hinge action of  $0.4 \times (283,804/5.0 + 493,679/4.1 + 41,049/1.67) = 80,700 \text{ lbs}$ .

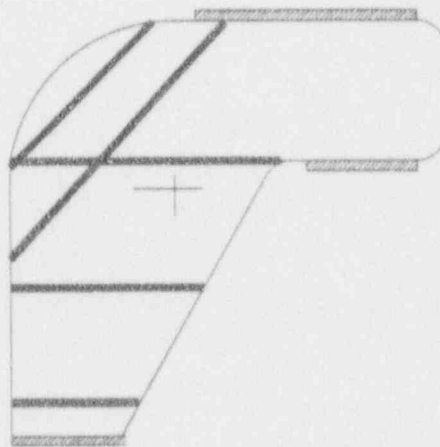
The total force =  $388,500 + 80,700 = 469,200 \text{ lbs} = 469,200/8,500 = 55 \text{ g's}$ .



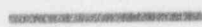
(a) Mode 1



(b) Mode 2



(c) Mode 3 (Mode 1 + Mode 2)

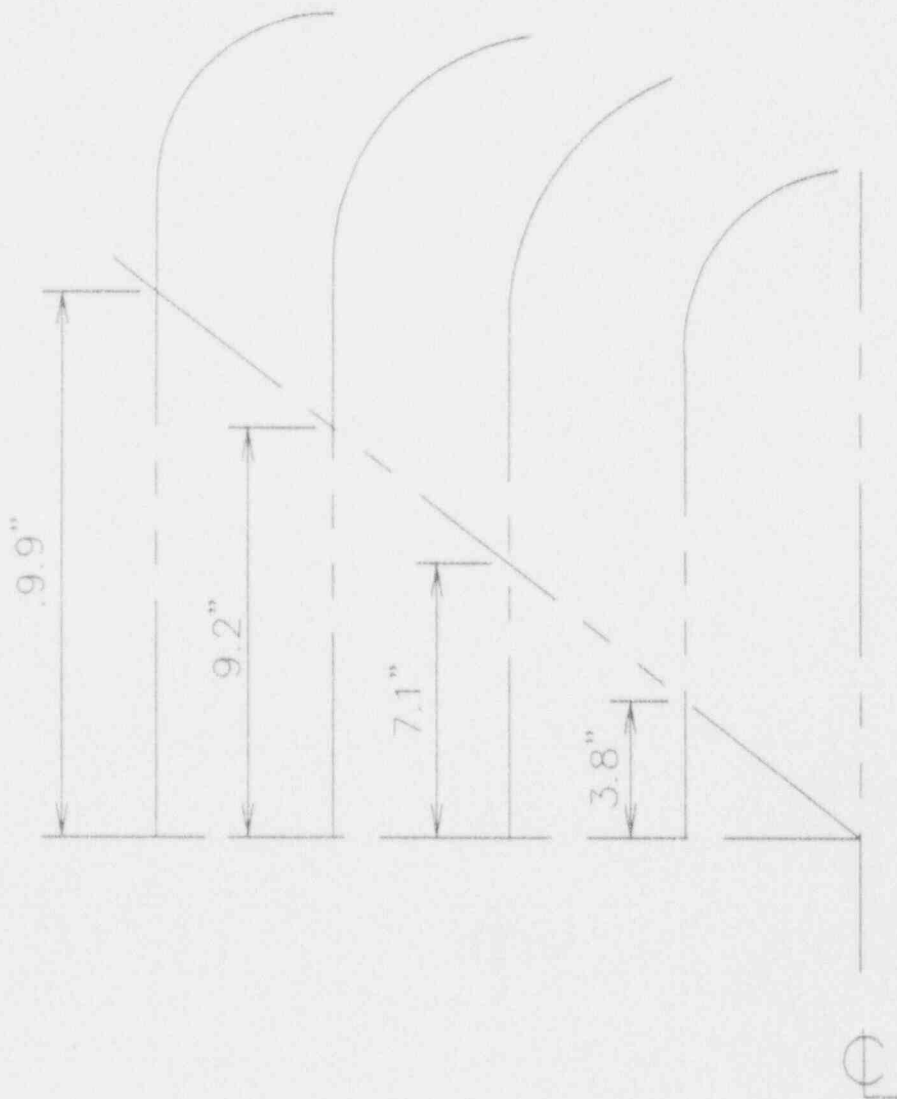


Single Plastic Hinge



Double Plastic Hinge

Figure 9.1 Possible Modes of Plastic Hinge Action  
with Drop 42 Degrees from Central Axis



Distances shown are action distances of fins.

Figure 9.2 Estimated Shortening of Individual Fins in Mode 1 Buckling with Drop Angle 42 Degrees from Vertical

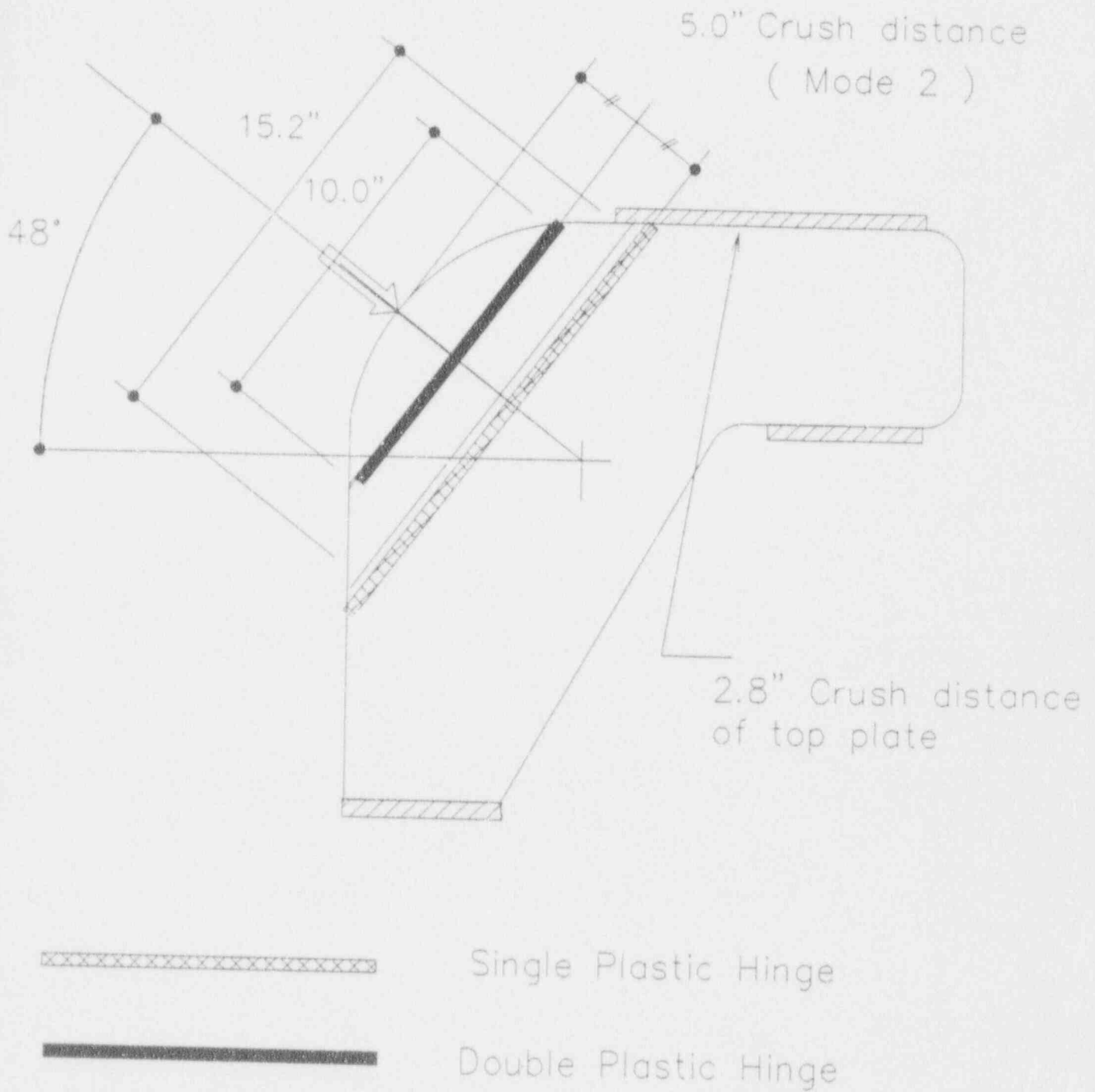
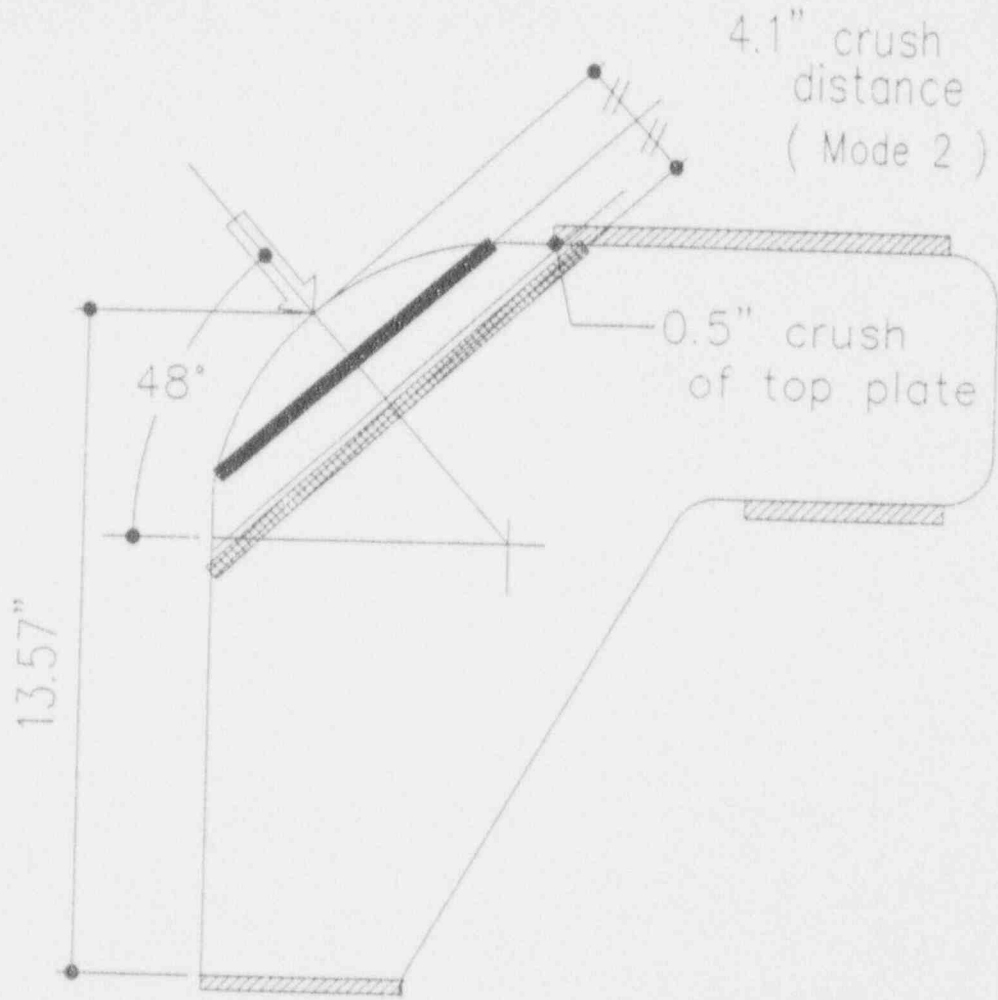


Figure 9.3 Crush Distance and Location of Plastic Hinges for Drop  
42 Degrees from Vertical in Fin at Zero Degree Angle





 Single Plastic Hinge


 Double Plastic Hinge

Figure 9.4 Crush Distance and Location of Plastic Hinges for Drop 42 Degrees from Vertical in Fin at 22.5 Degree Angle (View from Zero Degree Angle)

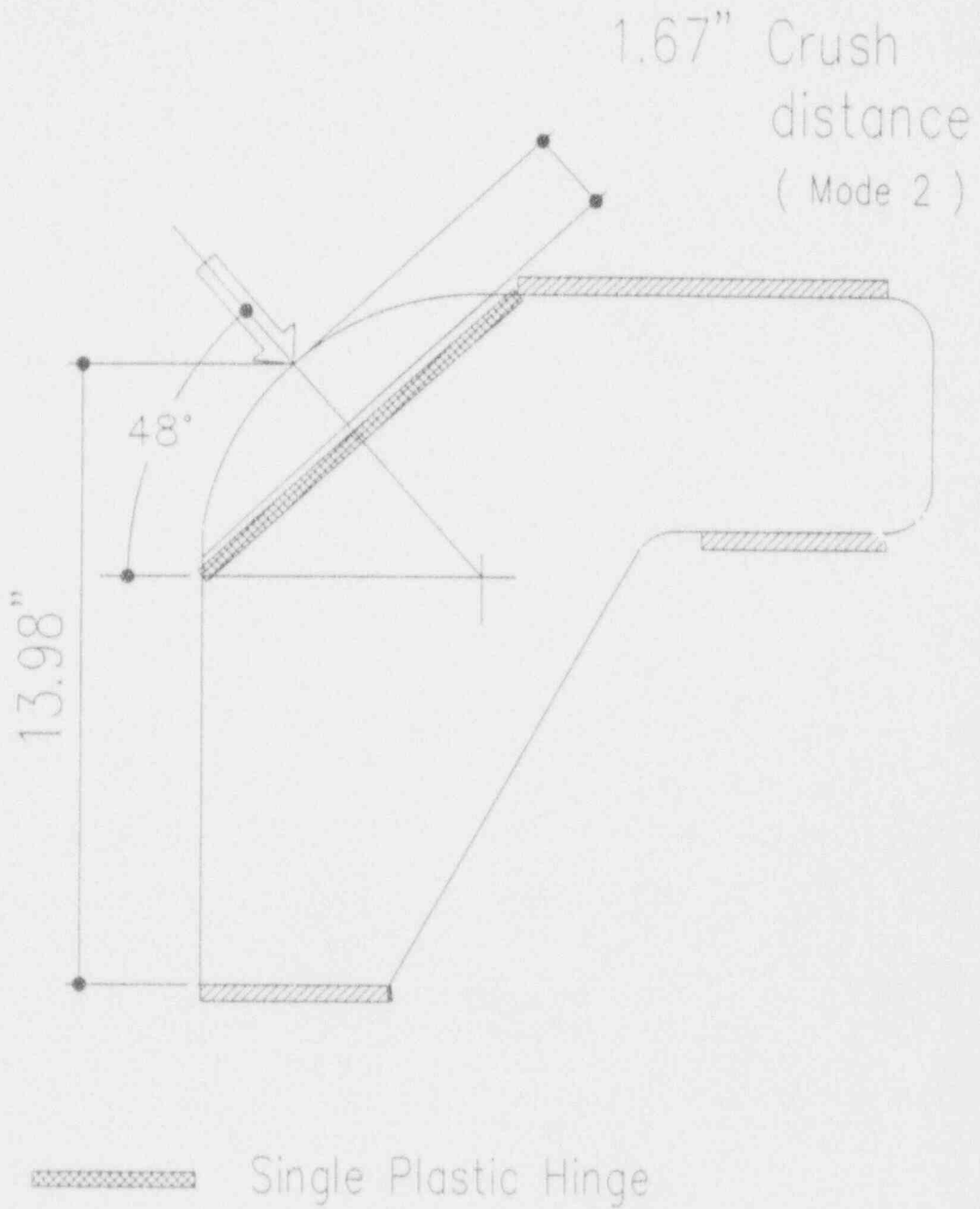


Figure 9.5 Crush Distance and Location of Plastic Hinges for Drop 42 Degrees from Vertical in Fin at 45 Degree Angle (View from Zero Degree Angle)

SECTION 10 - IMPACT LIMITER WITH LOADING 74.5 DEGREES FROM CENTRAL AXIS  
(15.5 DEGREES FROM HORIZONTAL)

10.1 INTRODUCTION

The condition with one fin vertical and the two adjacent fins at 22.5 degrees from that fin can be shown to be more critical than with the crush load applied equally on two nearest-to-vertical fins both equally close to vertical.

10.2 ENERGY ABSORBED BY THE FINS IN DIRECT CRUSHING AND PLASTIC HINGE ACTION

One Zero Degree Slope Fin - Direct Crushing

Crushing of One Fin

Ref. Section 3.5

$$U_b = 1.6 \times 8,100 = 12,960 \text{ in.lbs}$$

Crushing of Outside Plate

Crush distance = 3.0 inches

See Figs. 10.1 and 10.3.

$$U_b = 73,000 \times 0.375 \times (3.375 + 1.5) \times 3.0 = 400,359 \text{ in.lbs}$$

$$\text{Total} = 413,319 \text{ in.lbs}$$

One Zero Degree Slope Fin - Plastic Hinges

Height of fin action = 5.5 inches.

Crush distance = 5.5 inches.

The position of the plastic hinges will be as shown in Fig. 10.1.

The length of the central hinge = 10.0 inches.

The length of the right hand hinge = 16.0 inches.

$$e' = 1.0$$

With complete crushing of the central fin, energy absorbed is:

$$U_h = 2,566.4 (10.0 \times \pi + 16.0) \times (\pi/2) \times 2.00 \\ = 2,566.4 \times 18.0 \pi \times 2.00 = 290,254 \text{ in.lbs}$$

Two 22.5 Degree Slope Fins - Direct Crushing

Crushing of Outside Plate

Crush distance = 1.5 inches

$$U_b = 2 \times 73,000 \times 0.375 \times (3.375 + 1.5) \times 1.5 = 400,359 \text{ in.lbs}$$

### Direct Crushing of Two Fins

$$2 \times 1.6 \times 3,700 = 14,800 \text{ in.lbs}$$
$$\text{Total} = 415,159 \text{ in.lbs}$$

### Two 22.5 Degree Slope Fins - Plastic Hinges

See Fig. 10.2

The angle between the load and the plane of the fin  
 $= 22.5 \cos (90^\circ - 74.5^\circ) = 21.7^\circ$   
 $= 0.378 \text{ rads.}$   
The crush distance = 4.1 inches.  
Assume one double plastic hinge plus one single hinge.  
Height of fin action = 5.2 inches.  
 $e_b$  is negligible.

Referring to Subsection 4.4 and Fig. 4.5:  
 $h' = h_f \cos a = 5.2 \cos 21.7^\circ = 4.83 \text{ inches.}$   
 $g = h_f \sin a = 5.2 \sin 21.7^\circ = 1.92 \text{ inches.}$   
 $h'' = h' - d = 4.83 - 4.1 = 0.73 \text{ inches.}$   
 $\tan a'' = g/h'' = 1.92/0.73 = 2.63$   
 $a'' = 69.2^\circ = 1.21 \text{ rads.}$   
 $m = h'' \sec a'' = 0.73 \times 2.82 = 2.06 \text{ inches.}$   
 $e' = 1 - m/h_f = 1 - 2.06/5.2 = 0.60.$   
 $\cos r = 1 - e' = 1 - 0.60 = 0.40.$   
 $r = 66.4^\circ = 1.16 \text{ rads.}$   
 $r' = (r + a'') - a$   
 $= 1.16 + 1.21 - 0.38 = 1.99 \text{ rads.}$

$$U_b = 2 \times 2,566.4 \times (10.0 \times 2 \times 1.16 + 15.2 \times 1.99) \times 1.60 = 438,941 \text{ in.lbs.}$$

### 10.3 TOTAL ENERGY ABSORBED BY THE IMPACT LIMITER

One zero degree fin - direct crushing	=	413,319 in.lbs
One zero degree fin - plastic hinges	=	290,254 in.lbs
Two 22.5 degree fins - direct crushing	=	415,159 in.lbs
Two 22.5 degree fins - plastic hinges	=	438,941 in.lbs
		<hr/>
Total	=	1,542,342 in.lbs

### 10.4 ESTIMATION OF THE CRUSHING LOADS

#### The Load to Produce Fin Buckling

At the initial buckling stage, three fins participate in resisting the crushing load. The largest buckling load occurs when Fin No. 1 has already buckled and Fins No. 2 are at their buckling load. Assume that the load on Fin No. 1 has been reduced to 60% of its buckling value when Fins No. 2 buckle. Then the total force =  $2.6 \times 42,900 = 111,540 \text{ lbs} = 111,540/8,500 = 13 \text{ g's.}$

**The Average Force to Absorb the Drop Energy**

The crush distance = 5.5 inches.

The average force =  $1,542,342/5.5 = 280,426 \text{ lbs} = 280,426/8,500 = 33 \text{ g's}$ .

**The Average Force to Crush the Combined Outer Plates and Fins**

Toward the end of the crushing, the outside plates will undergo direct crushing. Assume a direct crushing yield stress of 73,000 psi.

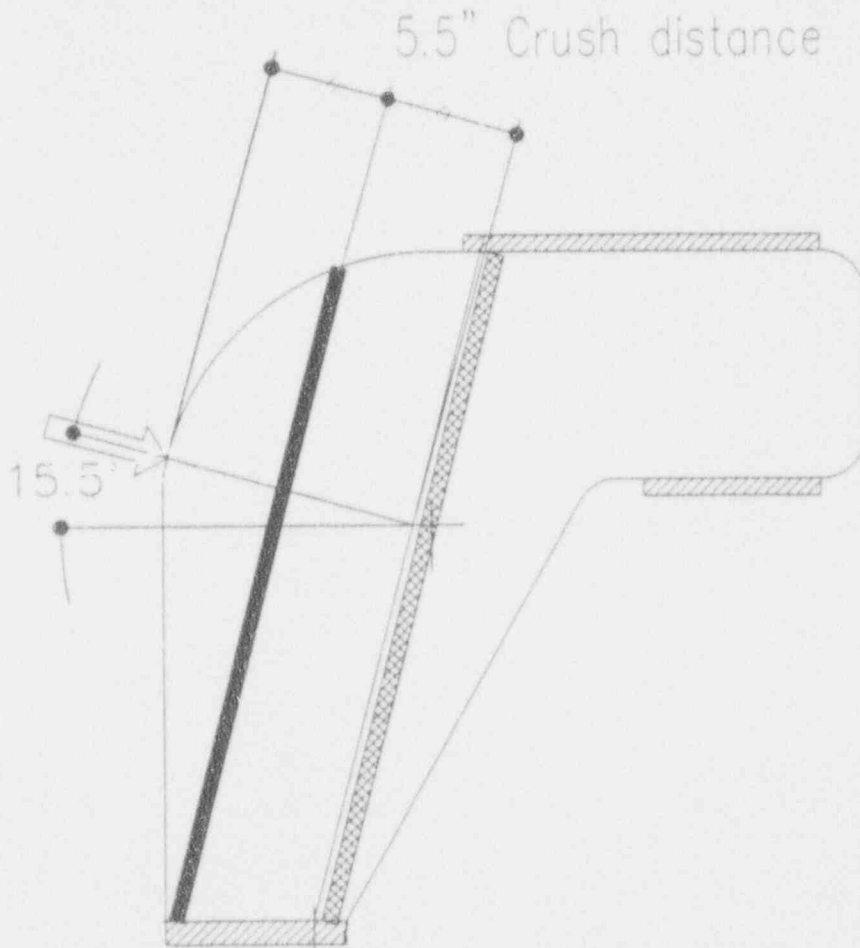
The crush area of the junctions of three fins and the outside plate =  $3 \times 0.375 \times (3.375 + 1.5) = 5.5 \text{ sq.in.}$

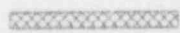

The crushing force =  $73,000 \times 5.5 = 401,500 \text{ lbs}$ .

When this force is being developed, the fins will have already buckled to a substantial degree and the load resisted by the fins will be substantially reduced.

Assume a force of  $0.5 \times (290,254/5.5 + 438,941/4.1) = 79,916 \text{ lbs}$ .

Total force =  $401,500 + 79,916 = 481,416 \text{ lbs} = 481,416/8,500 = 57 \text{ g's}$ .



-  Single Plastic Hinge
-  Double plastic Hinge

Assume full collapse of fin.

Figure 10.1 Crush Distance and Location of Plastic Hinges for Drop 74.5 Degrees from Vertical at Zero Degree Angle (View from Zero Degree Angle)

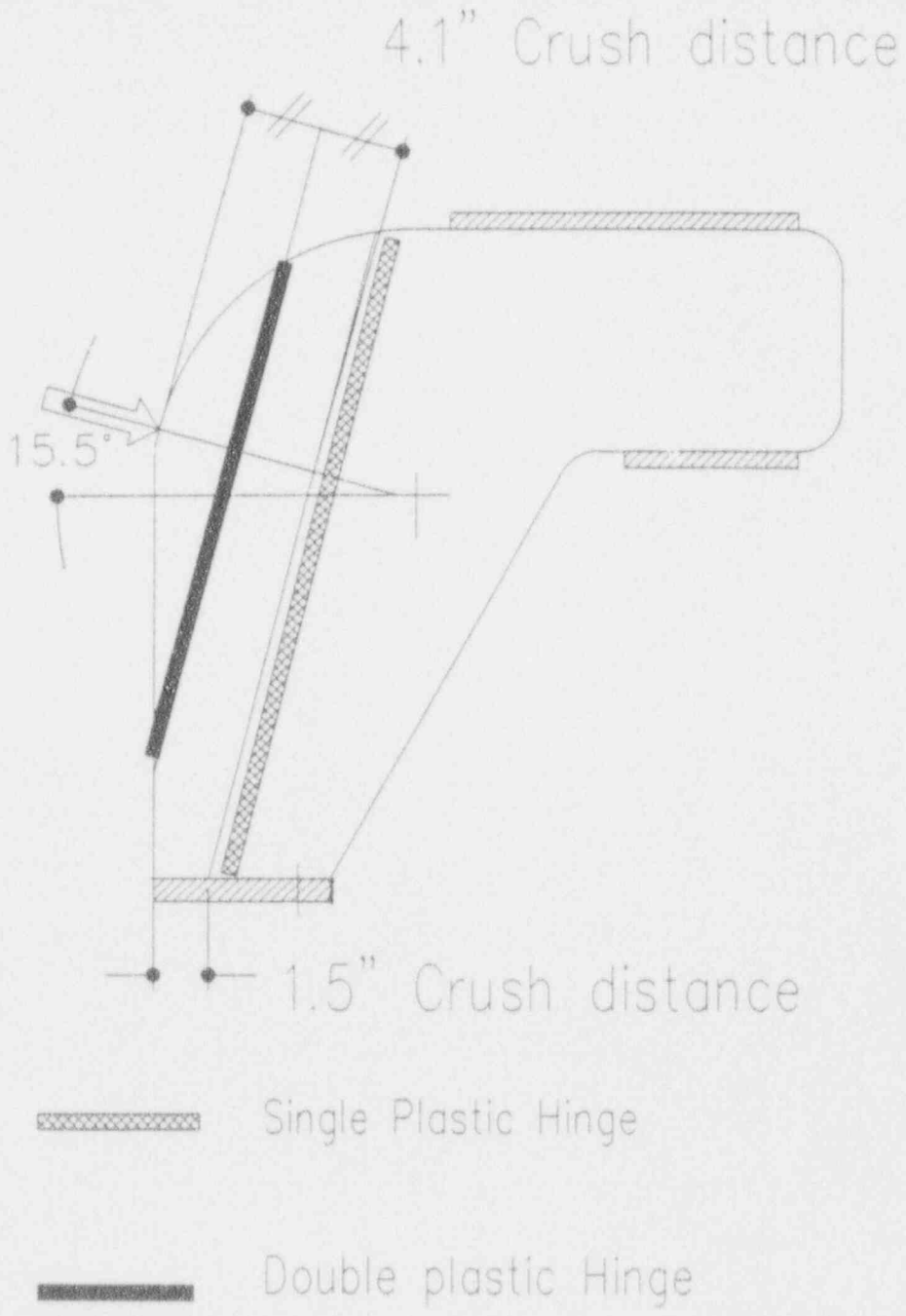
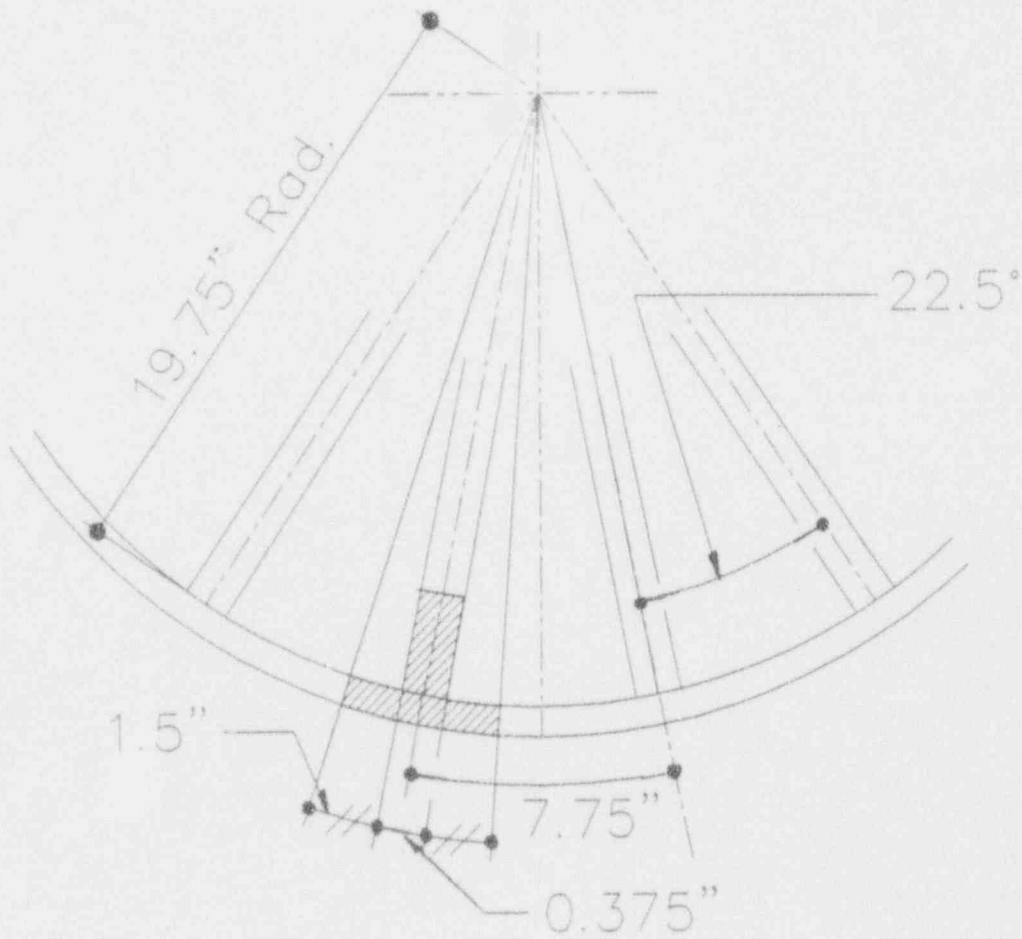


Figure 10.2 Crush Distance and Location of Plastic Hinges for Drop 74.5 Degrees from Vertical at 22.5 Degree Angle (View from Zero Degree Angle)



The hatched area is assumed to undergo direct crushing.

Figure 10.3 Direct Crushing of Outside Plate and Attached Portion of Fin



## SECTION 11 - SUMMARY OF DESIGN RULES

This summary deals with proposed rules for the analysis of the drop test behaviour of transfer units of radioactive material covered by IAEA Safety Standards, Safety series No. 10 Code of Federal Regulations, Nuclear Regulatory Commission, Part 71, Packaging and Transportation of Radioactive Material.

The symbols used in this report are defined in Section 12.

- (1) When the affected materials, low-carbon steel, stainless steel and lead, are subjected to high plastic strain rates, the material strength is increased very considerably. This report deals only with low carbon steel and stainless steel.
- (2) The best source of information about the effect of high strain rate upon the behaviour of low carbon steel and stainless steel is the ORNL report by Evans, "Experimental Study of the Stress-Strain Properties of Cask Materials Under Specified Impact Conditions".

Based upon the data contained in this report, we propose, for the purpose of analysis, that the following formulas be used, where  $F_{eds}$  = the material strength under high strain rate and  $e$  = the material strain:

Hot-rolled low-carbon steel:

$$F_{eds} = 73,000 + 345,000 e \text{ psi, with an upper limit of } 107,500 \text{ psi.}$$

Hot-rolled and annealed 304L stainless steel:

$$F_{eds} = 50,300 + 642,000 e \text{ psi, with an upper limit of } 114,500 \text{ psi.}$$

- (3) The behaviour of the fins is a function of the following:
  - (a) The effective slenderness ratio  $K h/t$ , where  $K$  = end restraint factor,  $h$  = height,  $t$  = fin thickness
  - (b) The slope angle of the fins.

For compact fins (low  $K h/t$ ) with small slope angle, there is an initial interval where the fin undergoes direct plastic shortening before it buckles sideways. For other fins, the lateral buckling occurs without this initial interval of direct shortening.

The initial interval of direct shortening, when it exists, is important in that it is capable of absorbing substantial energy.

When the lateral buckling occurs, energy is absorbed by the action of plastic hinges. The detailed behaviour of these plastic hinges is complex. However their energy absorption capabilities can be reasonably approximated as a straight-line function of the fin shortening - after any direct shortening of the fin has taken place. For certain fin proportions, a transition curve should be used between the region of direct shortening and the region of full plastic hinge action.

- (4) The behaviour of the fins, as described above, could conceivably be derived in detail from a knowledge of the material behaviour. However, to our knowledge, this exercise has not been carried out. Instead, the behaviour of whole fins has been examined in the following report:
  - (a) ORNL Irvine et al (1971)
  - (a) ORNL Davis (1971)

We have derived our proposed analysis rules from the Davis and the Evans reports.

- (5) Maximum direct stress and strain for vertical fins:

K h/t	Buckling Stress (psi)	Buckling Strain
0 - 4.5	100,000	0.400
5.0	100,000	0.350
5.5	95,200	0.308
6.0	91,067	0.272
6.5	87,446	0.240
7.0	84,229	0.212
7.5	81,333	0.187
8.0	78,700	0.164
8.5	76,282	0.142
9.0	74,044	0.123
9.5	71,958	0.105
10.0	70,000	0.087
10.5	68,152	0.075
11.0	66,400	0.065
11.5	64,730	0.055
12.0	63,133	0.045
12.5	61,600	0.035
13.0	60,123	0.025
13.5	58,696	0.015
14.0	57,314	0.005

The energy absorbed by direct shortening of the fin per unit fin volume is:

$$U_b = 50,000 e_b + 70,000 e_b^2 \text{ in.lbs/in}^3$$

- (6) Effect of slope of fins on extent of direct strain: The direct strain of a sloping fin, before lateral buckling, is approximated by the following rule:

The direct strain of a sloping fin equals the direct strain of a vertical fin multiplied by the cosine of 3 times the slope angle. Thus, for a 30 degree slope, no fin would have an interval of direct strain before lateral buckling.

- (7) Estimation of end restraint K factor for lateral buckling: For non-rectangular fin shapes, a procedure is available for estimating the end restraint K factor for lateral buckling. The details are given in Section 4, under "Proposed Procedure for Energy Absorbed by Direct Shortening for ASTM A36 Steel", "Evaluating the End Restraint Factor K for Fins of Complex Shapes".

- (8) Number of plastic hinges and extent of plastic hinge rotation: For dynamic reasons, a vertical plastic hinge is in effect provided with full lateral support at its loaded edge. This forces the fin to form two plastic hinges, giving a hinge rotation at full collapse of  $1.5 \pi$  radians. With increasing hinge slope, the effectiveness of lateral support decreases on a probabilistic basis.

For steeply sloping fins, the maximum plastic rotation angle is  $\pi/2$ . We would suggest the following practical probabilistic formula for the effect of fin slope on the onset of lateral buckling:

Fin Slope A - Degrees	Maximum Plastic Hinge Rotation Angle - Radians
0 - 30	$1.5 \pi \cos(2.3 a)$
30 - 90	$0.5 \pi$

- (9) Energy expended by a vertical fin due to plastic hinge rotation: The energy expended in the plastic hinge rotation is the product of the plastic moment in a hinge and the sum of the rotation angles of all the hinges. To compute the energy absorbed by the plastic hinges:

- (a) Subtract the fin direct shortening, if any, from the fin height.  
 (b) Compute  $e'$ , the ratio of the additional fin shortening to the remaining fin length.

$$e' = (e_o - e_b)/(1 - e_b).$$

- (c) For fin slopes between 0 and 30 degrees, multiply the quantity obtained in Step (b) by  $\cos(2.3 a)$ , where  $a$  = fin slope angle. For larger values of  $a$ , multiply the quantity from Step (b) by 1/3.  
 (d) Multiply the quantity obtained in Step (c) by the appropriate factor related to  $e'$ , which we will call  $U$ .  
 (e) The  $U$  factor, obtained from the Davis curves, is as follows:

$$U_h \text{ per single hinge} = 18,250 b t^2 (1 + e') r$$

where  $r$  is the rotation of a "single" hinge.

$$\cos r = 1 - e'$$

A rectangular fin with a slope of 20 degrees or less is assumed to contain effectively three single hinges, one double hinge at mid-height plus one single hinge at the base. A fin with a slope greater than 20 degrees is assumed to have only a single hinge at the base.

- (f) Sloping Fins:

Detailed procedures for the analysis of sloping fins are given in Subsections 4.4 and 5.2 of this report.

SECTION 12 - SYMBOLS AND CONVENTIONS

- a = fin slope angle, measured from the vertical.
- b = fin width (inches).
- d = fin shortening due to the plastic hinge bending (inches).
- E = modulus of elasticity, psi.
- e = plastic strain.
- $e_b$  = plastic strain at onset of lateral buckling of fin.
- $e'$  = ratio of plastic hinge shortening due to lateral buckling to the height of plastic hinge after direct plastic yielding has taken place.  
 $= (e_o - e_b) h/h' = (e_o - e_b)/(1 - e_b)$
- $e_o$  = ratio of plastic shortening to initial fin height.
- F = stress or strength (psi).
- $F_y$  = yield strength of steel (psi).
- h =  $h_f$  for a vertical fin; initial vertical height of a sloping fin (inches).
- $h_f$  = total height of a vertical uncrushed fin (inches).
- $h'$  =  $h_f (1 - e_b)$  for a vertical fin;  $h_f (1 - e_b) \cos a'$  for a sloping fin (Fig. 4.5).
- $h''$  = vertical height of a crushed fin (initially vertical or sloping)
- K = lateral stability end restraint factor.
- L = plastic hinge length.
- $M_p$  = plastic hinge moment (in.lbs).
- P = axial load (lbs).
- r = plastic hinge rotation (see Figs. 4.2, 4.5 and 5.1) (radians or degrees); radius of gyration of fin about weak axis (in.).
- t = fin thickness (inches) time (seconds).
- U = total absorbed energy. For a crushed fin, in the most general case,  
 $U = U_b + U_h$ .
- $U'$  = U, but corrected for fin slope angle.

### Subscripts

- a = formula value of a stress, used for analysis or investigation of impact behaviour.
- b = buckling condition, where the interval of direct plastic shortening has substantially come to an end.
- c = stress in direct compression.
- d = dynamic (high strain rate).
- e = (1) as applied to stress, value of stress after appreciable plastic strain has taken place; (2) as applied to load, the direct Euler buckling load.
- h = condition of a fully developed plastic hinge (full  $M_{pe}$ ).
- o = initial assumed value for static stress.
- p = plastic moment.
- r = reduced value of some property, e.g.  $E_r$  = reduced modulus of elasticity.
- s = static (low strain rate).
- t = result obtained from test, or from a formula used to represent test results.
- y = yield, as contrasted to the condition when appreciable plastic strain has already taken place.

### Abbreviations

- in. = inches.
- kip = thousands of pounds.
- psi = pounds per square inch.

APPENDIX A

INPUT DATA FOR FINITE ELEMENT STUDIES OF FINS

FINITE ELEMENT RUN NO. 5

Elements with Moduli of Elasticity Different from 29,000,000 psi.

The numbers given refer to elements.

Load Case No. 1 Minimum load = 109,400 lbs.

E = 2,587,500 psi.

7	16	19	22	23	28	29	32	35	36
41	42	43	44	45	54	58	61	63	66
73	78	81	85	86	87	94	95	97	101
102	104	109	110	112	119	125	126	127	134
139	140	141	142	148	149	156	161	163	169
170	177								

E = 1,207,500 psi.

6	15	50	57	65	67	69	70	71	74
79	88	89	118	133	135	147	155	162	

E = 931,500 psi.

14	68	72							
----	----	----	--	--	--	--	--	--	--

E = 813,215 psi.

8	75	80	82						
---	----	----	----	--	--	--	--	--	--

E = 747,500 psi.

5									
---	--	--	--	--	--	--	--	--	--

Load Case No. 2 Minimum load = 78,050 lbs.

E = 2,587,500 psi.

3	4	5	13	20	21	22	79	95	101
109	110	130	138	145	153				

E = 1,207500 psi.

12	96	102	103	104					
----	----	-----	-----	-----	--	--	--	--	--

Load Case No. 3 Minimum load = 60,410 lbs.

E = 257,500 psi.

3	4	11	12	104	109	128			
---	---	----	----	-----	-----	-----	--	--	--

E = 931,500 psi.

112	118	120							
-----	-----	-----	--	--	--	--	--	--	--

E = 813,215 psi.

119									
-----	--	--	--	--	--	--	--	--	--

Load Case No. 4 Minimum load = 64,330 lbs.

E = 257,500 psi.

5	6	7	13	14	23	30	38	45	51
52	53	60	67	68	75	76	84	92	99
100	101	108	109	114	121	125	126	127	136
138	139	144	146	147	148	150	151	154	160
161									

E = 1,207,500 psi.  
8 16 29 36 37 44 59 117 133 134  
135 140 141 153

E = 931,500 psi.  
22

FINITE ELEMENT RUN NO. 6

Elements with Moduli of Elasticity Different from 29,000,000 psi.

The numbers given refer to elements.

Load Case No. 1 Minimum load = 76,580 lbs.

E = 1,725,000 psi.  
2 3 11 20 21 30 46 55 62 71  
79 86 88 92 103 107 108 115 123 136  
138 146 153

E = 805,000 psi.  
72 76 78 87 90 91 99 100 105 106  
114 122 130 145

E = 621,000 psi.  
1 80 83 84 93 98 113

E = 542,143 psi.  
77

E = 498,333 psi.  
121

E = 470,455 psi.  
129

E = 437,000 psi.  
137

Load Case No. 2 Minimum load = 54,635 lbs.

E = 1,725,000 psi.  
2 9 10 11 19 78 87 93 94 95  
104 111 121

E = 805,000 psi.  
96 129 137

E = 621,000 psi.  
1

Load Case No. 3 Minimum load = 42,287 lbs.

E = 1,725,000 psi.  
10 110

E = 805,000 psi.  
1 112

E = 621,000 psi.  
11



Load Case No. 4 Minimum load = 50,582 lbs.

E = 1,725,000 psi.

19	27	35	66	74	89	97	105	106	107
113	122	123	124	129	131	132	142	143	149
152	158	159							

E = 805,000 psi.

1	2	3	9	10	11	12	18	25	26
33	34	41	42	49	50	57	58	65	73
81	82	90	98	115	130	137			

E = 621,000 psi.

4 17

FINITE ELEMENT RUN NO. 7

Elements with Moduli of Elasticity Different from 29,000,000 psi.

The numbers given refer to elements.

Load Case No. 1

E = 1,725,000 psi.

6	7	12	14	31	41	49	54	57	63
65	68	69	71	72	74	75	79	85	89
110	116	117	125	131	132	133	139	140	141
148	154	155	161	169					

E = 805,000 psi.

5	8	13	22	80	82	88	94	95	101
102	109	124	147						

E = 621,000 psi.

4 70

Load Case No. 2

E = 1,725,000 psi.

3	4	13	20	21	96	101	104	110	122
130	138	145							

E = 805,000 psi.

12

E = 621,000 psi.

102

E = 542,143 psi.

103

Load Case No. 3

E = 1,725,000 psi.

2	3	4	5	6	7	8	13	14	15
18	21	22	23	25	26	27	28	29	30
33	34	35	36	37	38	41	42	43	44
45	50	51	52	53	59	60	61	67	68
69	75	76	77	83	84	85	92	93	94
95	100	101	103	104	116	121	122	123	124
127	130	131	132	133	134	135	138	145	

E = 805,000 psi.  
12 17 19 20 108 125 129

E = 621,000 psi.  
1 9 11 117 126 137

E = 542,000 psi.  
109 112 136

E = 437,000 psi.  
128

E = 400,000 psi.  
118 119 120

Load Case No. 4

E = 1,725,000 psi.  
31 38 46 53 60 61 68 76 84 91  
92 93 99 101 109 110 117 118 119 128  
154 155 157 160 161 162

E = 805,000 psi.  
5 16 20 22 23 29 30 37 43 44  
45 51 52 59 67 75 83 100 108 116  
125 126 127 138 146 147 148 153

E = 621,000 psi.  
6 14 15 21 28 135 139 141 145 150  
151

E = 542,143 psi.  
7 13 36 133 134 136 140

E = 498,333 psi.  
144

E = 470,455 psi.  
8

## APPENDIX B - THE EVANS REPORT

### B.1 INTRODUCTION

The Evans report deals only with material strength at high strain rates. It does not deal with whole fins. However, the Evans report is very useful in that it is generally consistent and it directly addresses important questions. Specifically, the Evans report addresses the question of the effect of high strain upon low carbon steel and stainless steel in direct compression.

Symbols are defined in section 8 of this report.

### B.2 THE EXPERIMENTAL DATA FROM THE EVANS REPORT

The experimental high-strain-rate curve for low-carbon steel is shown in Fig. B.1 of this report (Fig. 5 of the Evans Report). The experimental high-strain-rate curve for 304L Hot Rolled and Annealed Stainless Steel is shown in Fig. B.2 of this report (Fig. 6 of the Evans Report).

### B.3 WORKING FORMULAS

Based upon his experimental data, Evans proposes the following formulas to represent the tests for the grades of low carbon steel and stainless steel considered.

Low carbon steel:

$$F_{edt} = 73,000 + 345,000 \epsilon \text{ psi.} \quad [B.1]$$

Stainless steel:

$$F_{edt} = 50,300 + 642,000 \epsilon \text{ psi.} \quad [B.1a]$$

Because the Evans tests were done in direct compression and the stresses were apparently computed on the basis of the original cross-section, we would recommend an upper limit of 0.10 to the strain used in formulas B.1 and B.1a. This gives an upper limit to the stresses to be used, as follows:

Low carbon steel: 107,500 psi

Stainless steel: 114,500 psi

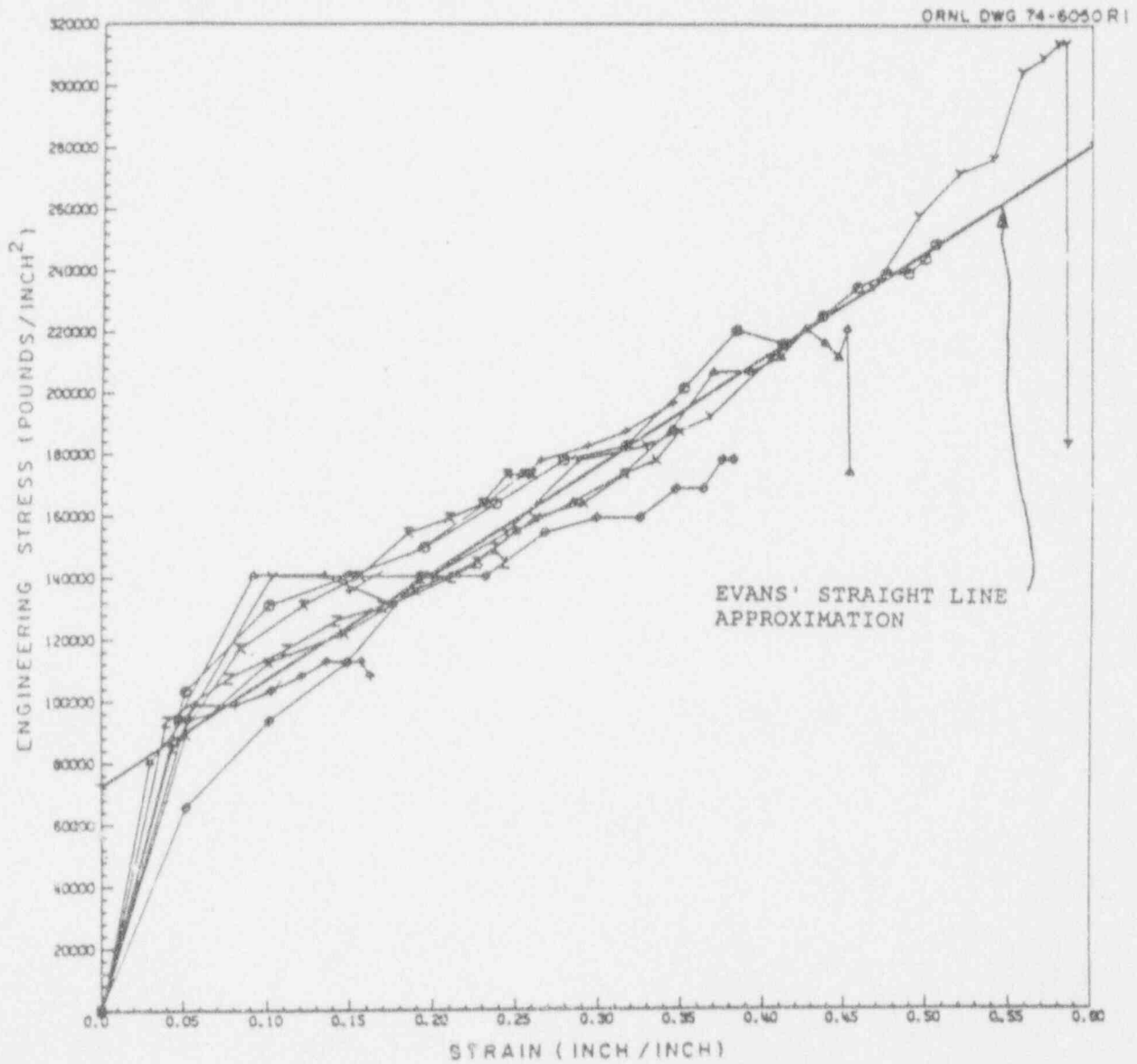


Figure B.1 Dynamic Compressive Stress-Strain Data  
 For AISC 1020 Hot Rolled Steel  
 (Fig. 5 in Evans Report.)

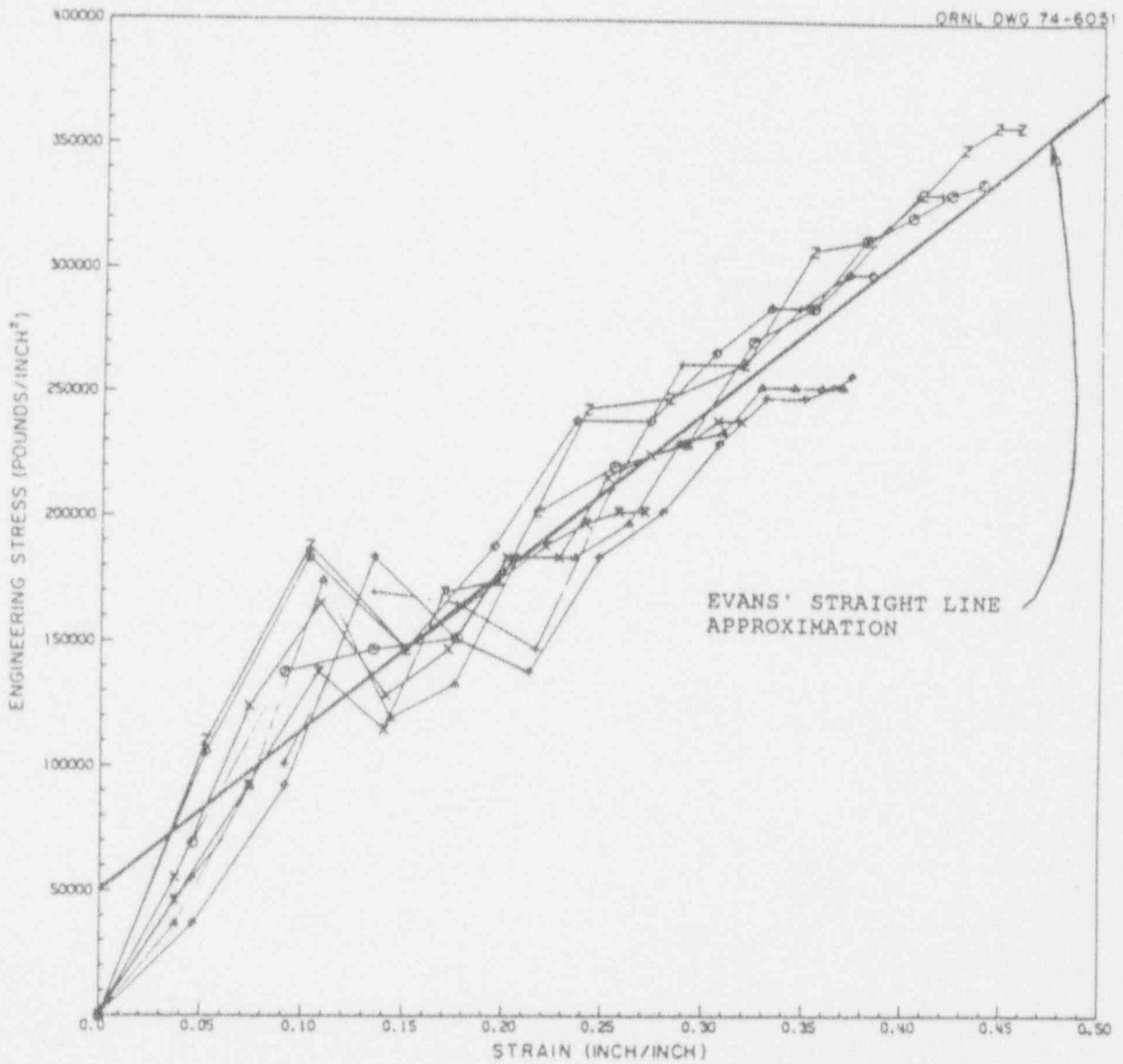


Figure B.2 Dynamic Compressive Stress-Strain Data  
for 304L Hot Rolled and Annealed Stainless Steel  
(Fig. 6 in Evans Report.)

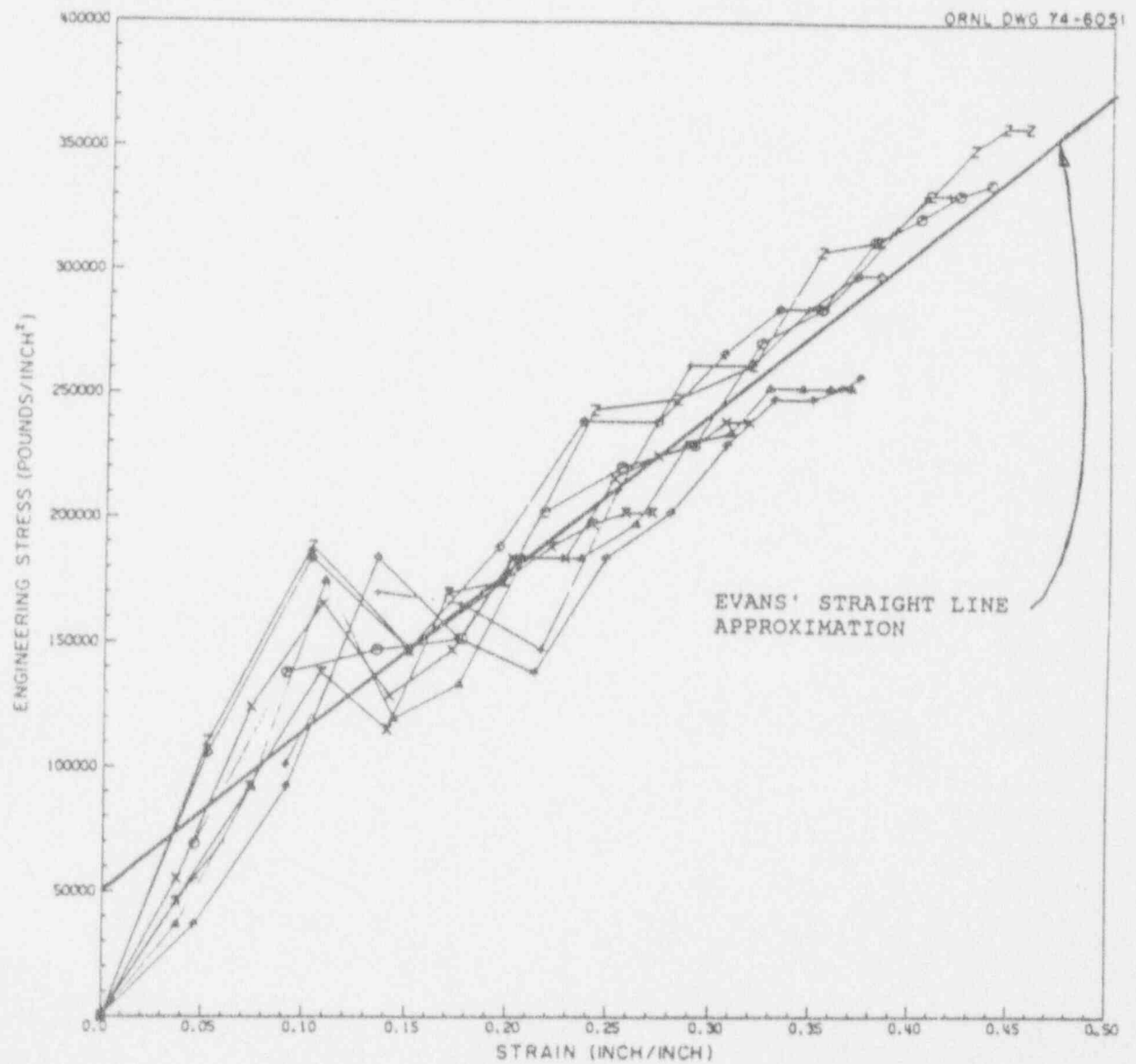


Figure B.2 Dynamic Compressive Stress-Strain Data for 304L Hot Rolled and Annealed Stainless Steel (Fig. 6 in Evans Report.)

APPENDIX 3.6-E SENSITIVITY ANALYSIS OF THE FEM MODEL

## APPENDIX 3.6-E

### 3.6-E.1 INTRODUCTION

This appendix demonstrates that the analysis presented in section 3.6.4 yields conservative results. In particular, the sensitivity of the results is evaluated with respect to:

- a) The assumption of zero equivalent air gap between the lead and the external steel elements.
- b) The amount of removed kaowool.

### 3.6-E.2 CHANGES TO THE MODEL FOR ACCIDENT CONDITIONS OF TRANSPORT

The FEM model described in this appendix is identical to the one described in Appendix 3.6-C, with the following exceptions:

- 1) A 0.020 inch equivalent air gap is added as shown in Figure 3.6-E-F1. Elements 400 through 425 are inserted between the lead elements and steel elements along the outside boundary. Heat transfer across these elements is by conduction alone.

In order to accommodate this air gap, lead nodes are shifted by 0.020 inches. The new lead nodes are given a new node number 500 higher than the old lead node number. For example, node 109 of the previous thermal model is now node number 609.

Most of the added elements are four noded. In some cases, maintaining element connectivity required three noded elements to be used. (Elements 400, 401, 424 and 425 are all three noded.) For the inner head plug, it was not possible to insert an air gap without altering the model geometry. In each of these areas, the analysis overpredicts the lead temperature.

Use of the 0.020 inch air gap is justified by the results of studies described in section 3.6-E.5.

- 2) Additional kaowool was removed from the outer radius of the unit, as shown in Figure 3.6-E-F2. In addition, a special case was run assuming that all of the kaowool insulation has been removed.
- 3) For all added lead nodes, the initial temperature was assumed to be equal to the initial temperature of its companion node from case BC. For example, node 609 was assigned an initial temperature equal to the former initial temperature of node 109.

The input files used in the parametric studies are described in Table 3.6-E-T1. Input files are listed in section 3.6-E.6.



Table 3.6-E-T1. List of Parametric Studies

CASE	DESCRIPTION	ADDITIONAL INPUT FILE(S)
BC	Basic Case, as described in Section 3.6.4	Not applicable
G20	Basic Case with additional air gap	GAP20.INP
G20K1	Basic case with additional air gap and additional kaowool removed as shown in Figure 3.6-E-F2.	GAP20.INP DELKO1.INP
G20NK	Basic case with additional air gap and all kaowool removed.	GAP20.INP DELKO.INP

### 3.6-E.3 RESULTS

Table 3.6-E-T2 gives the results of these parametric studies.

### 3.6-E.4 DISCUSSION

The thermal model of Appendix 3.5-C showed a maximum lead melt of about 0.77 inches. Even with this amount of lead melt, the surface field was estimated to be well within regulatory limits. In fact, the removal of about 5 inches of lead is required to cause a radiation field of 1 R/hr 1 metre from the package. As such the existing model provides a large margin of safety. However, as it is difficult to analytically justify the amount of removed kaowool at the start of the fire test, it is important to perform some sensitivity studies to assess the performance of the unit during the regulatory fire.

The two most important assumptions of Appendix 3.6-C are:

- 1) An equivalent area of 756 in<sup>2</sup> of kaowool is removed from the unit as compared to the expected 195 in<sup>2</sup>. This assumption was used as the arguments for the degree of kaowool removal are somewhat qualitative. A factor of safety of about 4 was judged to adequately offset the uncertainty in the amount of removed kaowool.
- 2) There is no thermal contact resistance between the lead and the outer stainless steel shell. Section 3.6-E.5 shows that a 0.020 in (0.5 mm) equivalent air gap to exist between lead and a surrounding steel shell even if ultrasonic tests show perfect bonding. A more realistic analysis of the performance of the GC220 should incorporate an air gap.

Table 3.6-E-T2. Results of Parametric Studies  
(Temperatures in °F)

NODE	CASE	t = 0 (min)	t = 5 (min)	t = 10 (min)	t = 20 (min)	t = 30 (min)	t = 40 (min)
234	BC	208.40	460.80	545.63	647.35	693.14	457.61
	G20	208.40	900.11	1090.89	1170.38	1194.79	478.18
	G20K1	208.40	956.60	1181.69	1253.73	1274.19	538.73
	G20NK	208.40	947.42	1191.27	1270.20	1297.48	588.84
609*	BC	208.00	437.51	522.89	625.51	671.32	459.02
	G20	208.00	272.56	326.93	396.05	447.63	394.92
	G20K1	208.00	284.11	360.86	460.96	533.80	479.14
	G20NK	208.00	283.65	372.93	507.35	616.71	587.53
106	BC	208.60	389.59	473.48	576.81	620.52	460.58
	G20	208.60	256.83	306.76	375.10	427.31	392.08
	G20K1	208.60	267.01	338.67	438.96	513.16	476.83
	G20NK	208.60	266.80	350.73	486.08	597.66	586.87
100	BC	209.40	289.02	360.89	461.55	526.39	459.18
	G20	209.40	227.32	261.67	323.45	375.89	379.61
	G20K1	209.40	232.79	284.52	379.16	455.68	464.00
	G20NK	209.40	233.05	295.37	426.64	543.61	578.69
94	BC	211.90	225.60	265.26	350.38	424.04	441.76
	G20	211.90	213.47	226.53	270.97	319.89	353.57
	G20K1	211.90	214.60	235.97	308.51	383.44	432.03
	G20NK	211.90	214.93	243.13	351.93	472.21	552.22

\*Node 609 was node 109 in case BC.

The results were found to be extremely sensitive to the zero air gap assumption and somewhat less sensitive to the amount of removed kaowool.

Introducing a 0.020 inch (0.5 mm) air gap between the lead and the steel dramatically changes the results. Comparing cases BC and G20 shows the air gap results in lower lead temperatures. Most lead temperatures dropped by 100-200 °F. (This temperature drop is consistent with the results quoted in section 3.6-E.5.) In case G20, the maximum lead temperature was found to be 448 °F, 30 minutes into the fire. This represents a large margin of safety with respect to the melting point of lead (621 °F). It also means that no significant change in the radiation fields from the package is expected to result from the regulatory fire test.

The effect of introducing the air gap is significant enough to allow for the total loss of kaowool after the drop tests. Case G20NK represents the combination of the equivalent air gap and a total loss of kaowool insulation. The results show temperatures approaching the melting point of lead. Case G20K1 is included to show the effect of removing an arbitrary intermediate amount of kaowool. Neither case shows any lead melt.

While case G20NK does not represent the expected performance of the package, it does show that the model of Appendix 3.6-C is conservative, and that the assumptions regarding equivalent air gap and amount of removed kaowool tend to offset each other. It is submitted that the results of these parametric studies combined with the analysis of Appendix 3.6-C demonstrate that the GC-220 meets the requirements of 10 CFR Part 71.

#### 3.6-E.5 REFERENCES

The following pages 170 and 171 are extracted from: Transnucleaire SA, Report on the Implications of the Test Requirements for Type B Packagings and a Study of Practical Solutions, Euratom Contract No. 024-65-ECIC,

a) No bond -

When fabrication is made without trying to obtain bonding between lead and outer shell, shrinkage occurs during cooling after casting due to the difference of dilatation coefficients of lead and steel.

The importance of shrinkage depends on casting methods and outer shell dimensions and materials.

With a stainless steel outer shell and adequate casting method, shrinkage is on the order of  $4^{\circ}/100$ , i.e. for instance 2 mm at the radius for a packaging of 1 m diameter.

With a mild steel outer shell, whose dilatation coefficient is lower than for stainless steel, shrinkage may be greater.

b) Lead bonded -

Bonding can be obtained by various processes, which we will not explain here.

Let us say only that bonding can be easily achieved on an open steel wall : it is much more difficult inside a steel vessel practically closed. It is also more difficult with stainless steel than with mild steel.

If bonding is perfect, which can be checked by ultra-sonic inspection, thermal bond should also be perfect.

This is actually obtained for instance with a plane steel wall and a certain thickness of lead bonded, the outer surface of the lead being bare.

On the other hand, our experience shows us that in the case of packagings and in spite of a perfect bonding to the outer shell, ultra-sonic checked, there is always some discrepancy between thermal test and calculations for the heat transmission through the inner shell/lead/outer shell assembly.

Compared with calculations based on a perfect thermal bonding, tests show that in fact there is a certain extra resistance to the passage of heat.

Thus, on a series of six identical cylindrical 20 ton packagings (constructed by the Société Lyonnaise de Plomberie Industrielle), an extra resistance to the passage of heat compared with calculations is found equivalent to an air gap of 0.5mm varying slightly around this value according to the packaging. Ultrasonic inspection, however, showed perfect outer shell/lead bonding.

There are a number of possible explanations :

- The calculation cannot be very accurate particularly when there is a great difference between the outer shell surface area and the inner cavity surface area. This was the case for the six packagings mentioned above.

If the heat flux introduced in the calculation is the flux on the inner cavity, there is then good agreement between tests and calculation.

- Bonding to the outer shell has a tendency to work against hooping on the inner shell.
- Lack of homogeneity in the lead mass which is being drawn both towards the outer shell and towards the inner shell.
- Traces of oxide over a varying surface area at the outside shell/lead interface (which does not show up with ultra-sonic controls).

We have no knowledge of the results obtained by other constructors.

c) Behavior in the thermal test -

In the case of not bonded lead, an air gap of say, 2 mm, corresponds to a temperature drop of several hundred degrees, for the initial heat fluxes involved in the thermal test.

### 3.6-E.6 INPUT FILES

The following input files were used as indicated in Table 3.6-E-T1. They were appended to the thermal model described in Appendix 3.6-E.6.1 File GAP20.INP

This file creates the air gap elements shown in Figure 3.6-E-F1.

```

EGROUP,1,PLANE2D,0,1,1,0,0,0,0,
EDEL,300,311,1,
ACTSET,MP,3,
EL,312,SF,0,4,132,164,188,188,0,0,0,0,0,0,
EL,210,SF,0,4,36,223,226,49,0,0,0,0,0,0,
EL,426,SF,0,4,226,225,223,223,0,0,0,0,0,0,
ACTSET,EG,1,
ACTSET,MP,1,
ACTSET,RC,1,
ACTSET,ECS,-1,
C* Add internal lead nodes
ND,531,0,29.855,0,0,0,0,0,0,0,
ND,674,7.31434,30.282,0,0,0,0,0,0,0,
ND,675,7.80178,30.282,0,0,0,0,0,0,0,
ND,676,8.14645,30.282,0,0,0,0,0,0,0,
ND,677,8.39017,30.282,0,0,0,0,0,0,0,
ND,678,8.55400,30.282,0,0,0,0,0,0,0,
ND,649,9.47800,29.331,0,0,0,0,0,0,0,
ND,643,12.1700,26.561,0,0,0,0,0,0,0,
ND,637,14.8550,23.798,0,0,0,0,0,0,0,
ND,661,14.855,21.4541,0,0,0,0,0,0,0,
ND,655,14.855,20.0961,0,0,0,0,0,0,0,
ND,629,14.855,19.312,0,0,0,0,0,0,0,
ND,630,14.855,18.4255,0,0,0,0,0,0,0,
ND,631,14.855,17.1718,0,0,0,0,0,0,0,
ND,609,14.855,15.3988,0,0,0,0,0,0,0,
ND,610,14.855,13.5809,0,0,0,0,0,0,0,
ND,611,14.855,12.2955,0,0,0,0,0,0,0,
ND,588,14.855,11.3865,0,0,0,0,0,0,0,
ND,589,14.855,10.4776,0,0,0,0,0,0,0,
ND,590,14.855,9.19212,0,0,0,0,0,0,0,
ND,557,14.855,7.38100,0,0,0,0,0,0,0,
ND,556,12.0180,4.4820,0,0,0,0,0,0,0,
ND,549,9.18000,1.5820,0,0,0,0,0,0,0,
ND,536,6.5,1.582,0,0,0,0,0,0,0,
ND,501,0.,0.645,0,0,0,0,0,0,0,
C* Reconnect lead elements to the new nodes
ACTSET EG 1
ACTSET MP 1
ACTSET RC 1
ACTSET ECS -1
EL, 1,SF, 1,4,501, 2, 4, 3, 6 120 119 8 1 0
EL, 14,SF,17,4, 29, 30, 32, 531, 180 177 9 179 17 0
EL, 17,SF, 7,4, 35, 536, 38, 37, 131 132 0 10 7 0
EL, 23,SF, 8,4,536, 549, 50, 38, 133 134 0 132 8 0
EL, 29,SF, 9,4,549, 556, 58, 50, 81 0 0 134 9 0
EL, 30,SF, 9,4,556, 557, 59, 58, 81 135 0 0 9 0
EL, 56,SF,19,4, 85, 86, 589, 588, 0 0 204 205 19 0
EL, 57,SF,19,4, 86, 87, 590, 589, 0 0 204 0 19 0
EL, 58,SF,19,4, 87, 59, 557, 590, 0 206 204 0 19 0
EL, 74,SF,20,4,106, 107, 610, 609, 0 0 207 208 20 0

```



EL, 75,SF,20,4,107,	108,	611,	610,	0	0	207	0	20	0
EL, 76,SF,20,4,108,	85,	588,	611,	0	205	207	0	20	0
EL, 92,SF,21,4,126,	127,	630,	629,	0	0	209	210	21	0
EL, 93,SF,21,4,127,	128,	631,	630,	0	0	209	0	21	0
EL, 94,SF,21,4,128,	106,	609,	631,	0	208	209	0	21	0
EL, 99,SF,22,4,136,	637,	643,	142,	130	212	0	0	22	0
EL,104,SF,22,4,142,	643,	649,	148,	0	212	166	0	22	0
EL,114,SF,11,4,154,	655,	661,	160,	0	128	0	0	11	0
EL,119,SF,11,4,160,	661,	637,	136,	0	128	130	0	11	0
EL,120,SF,11,4,154,	126,	629,	655,	0	210	128	0	11	0
EL,131,SF,26,4,173,	144,	145,	674,	83	166	0	86	26	0
EL,132,SF,26,4,674,	145,	146,	675,	0	166	0	86	26	0
EL,133,SF,26,4,675,	146,	147,	676,	0	166	0	86	26	0
EL,134,SF,26,4,676,	147,	148,	677,	0	166	0	86	26	0
EL,135,SF,26,4,677,	148,	649,	678,	0,	166,	90,	86,	26,	0

C\* Initialize temperatures based on steady state run.

INITIAL,TEMP,1,1,1,208.89999,  
INITIAL,TEMP,2,2,1,208.60001,  
INITIAL,TEMP,3,3,1,209.2,  
INITIAL,TEMP,4,4,1,208.89999,  
INITIAL,TEMP,5,5,1,209.39999,  
INITIAL,TEMP,6,6,1,209.2,  
INITIAL,TEMP,7,7,1,209.8,  
INITIAL,TEMP,8,8,1,209.5,  
INITIAL,TEMP,9,9,1,210.39999,  
INITIAL,TEMP,10,10,1,210,  
INITIAL,TEMP,11,11,1,211.5,  
INITIAL,TEMP,12,12,1,210.89999,  
INITIAL,TEMP,13,13,1,213.8,  
INITIAL,TEMP,14,14,1,212.60001,  
INITIAL,TEMP,15,15,1,219.7,  
INITIAL,TEMP,16,16,1,217.3,  
INITIAL,TEMP,17,17,1,222.89999,  
INITIAL,TEMP,18,18,1,221.8,  
INITIAL,TEMP,19,19,1,227,  
INITIAL,TEMP,20,20,1,230.89999,  
INITIAL,TEMP,21,21,1,229.5,  
INITIAL,TEMP,22,22,1,233.8,  
INITIAL,TEMP,23,23,1,222.39999,  
INITIAL,TEMP,24,24,1,224.10001,  
INITIAL,TEMP,25,25,1,221.89999,  
INITIAL,TEMP,26,26,1,220,  
INITIAL,TEMP,27,27,1,221.5,  
INITIAL,TEMP,28,28,1,218.7,  
INITIAL,TEMP,29,29,1,208.3,  
INITIAL,TEMP,30,30,1,207.89999,  
INITIAL,TEMP,31,31,1,208.3,  
INITIAL,TEMP,32,32,1,207.39999,  
INITIAL,TEMP,33,33,1,211.39999,  
INITIAL,TEMP,34,34,1,210.7,  
INITIAL,TEMP,35,35,1,208.89999,  
INITIAL,TEMP,36,36,1,208.39999,  
INITIAL,TEMP,37,37,1,209,  
INITIAL,TEMP,38,38,1,208.60001,  
INITIAL,TEMP,39,39,1,209.3,  
INITIAL,TEMP,40,40,1,208.89999,  
INITIAL,TEMP,41,41,1,209.8,  
INITIAL,TEMP,42,42,1,209.39999,  
INITIAL,TEMP,43,43,1,210.60001,  
INITIAL,TEMP,44,44,1,210.10001,  
INITIAL,TEMP,45,45,1,212.10001,  
INITIAL,TEMP,46,46,1,211.3,

INITIAL,TEMP,47,47,1,215.2,  
INITIAL,TEMP,48,48,1,213.89999,  
INITIAL,TEMP,49,49,1,208,  
INITIAL,TEMP,50,50,1,208.2,  
INITIAL,TEMP,51,51,1,208.5,  
INITIAL,TEMP,52,52,1,208.89999,  
INITIAL,TEMP,53,53,1,209.60001,  
INITIAL,TEMP,54,54,1,210.8,  
INITIAL,TEMP,55,55,1,213.39999,  
INITIAL,TEMP,56,56,1,208.2,  
INITIAL,TEMP,57,57,1,207.89999,  
INITIAL,TEMP,58,58,1,208.3,  
INITIAL,TEMP,59,59,1,208.10001,  
INITIAL,TEMP,60,60,1,208.60001,  
INITIAL,TEMP,61,61,1,208.39999,  
INITIAL,TEMP,62,62,1,209,  
INITIAL,TEMP,63,63,1,208.8,  
INITIAL,TEMP,64,64,1,209.7,  
INITIAL,TEMP,65,65,1,209.60001,  
INITIAL,TEMP,66,66,1,211.10001,  
INITIAL,TEMP,67,67,1,210.89999,  
INITIAL,TEMP,68,68,1,213.8,  
INITIAL,TEMP,69,69,1,214.2,  
INITIAL,TEMP,70,70,1,215.39999,  
INITIAL,TEMP,71,71,1,215.2,  
INITIAL,TEMP,72,72,1,214.8,  
INITIAL,TEMP,73,73,1,211.60001,  
INITIAL,TEMP,74,74,1,211.5,  
INITIAL,TEMP,75,75,1,211.3,  
INITIAL,TEMP,76,76,1,210.10001,  
INITIAL,TEMP,77,77,1,210,  
INITIAL,TEMP,78,78,1,209.8,  
INITIAL,TEMP,79,79,1,209.3,  
INITIAL,TEMP,80,80,1,209.2,  
INITIAL,TEMP,81,81,1,209.10001,  
INITIAL,TEMP,82,82,1,208.8,  
INITIAL,TEMP,83,83,1,208.8,  
INITIAL,TEMP,84,84,1,208.60001,  
INITIAL,TEMP,85,85,1,208.5,  
INITIAL,TEMP,86,86,1,208.5,  
INITIAL,TEMP,87,87,1,208.3,  
INITIAL,TEMP,88,88,1,208.3,  
INITIAL,TEMP,89,89,1,208.3,  
INITIAL,TEMP,90,90,1,208.10001,  
INITIAL,TEMP,91,91,1,215.8,  
INITIAL,TEMP,92,92,1,215.7,  
INITIAL,TEMP,93,93,1,215.60001,  
INITIAL,TEMP,94,94,1,211.89999,  
INITIAL,TEMP,95,95,1,211.8,  
INITIAL,TEMP,96,96,1,211.7,  
INITIAL,TEMP,97,97,1,210.3,  
INITIAL,TEMP,98,98,1,210.2,  
INITIAL,TEMP,99,99,1,210.2,  
INITIAL,TEMP,100,100,1,209.39999,  
INITIAL,TEMP,101,101,1,209.39999,  
INITIAL,TEMP,102,102,1,209.3,  
INITIAL,TEMP,103,103,1,208.89999,  
INITIAL,TEMP,104,104,1,208.89999,  
INITIAL,TEMP,105,105,1,208.89999,  
INITIAL,TEMP,106,106,1,208.60001,  
INITIAL,TEMP,107,107,1,208.60001,  
INITIAL,TEMP,108,108,1,208.60001,



INITIAL,TEMP,109,109,1,208.5,  
INITIAL,TEMP,110,110,1,208.5,  
INITIAL,TEMP,111,111,1,208.399999,  
INITIAL,TEMP,112,112,1,215.399999,  
INITIAL,TEMP,113,113,1,215.399999,  
INITIAL,TEMP,114,114,1,215.60001,  
INITIAL,TEMP,115,115,1,211.5,  
INITIAL,TEMP,116,116,1,211.8,  
INITIAL,TEMP,117,117,1,209.7,  
INITIAL,TEMP,118,118,1,210,  
INITIAL,TEMP,119,119,1,210.10001,  
INITIAL,TEMP,120,120,1,209,  
INITIAL,TEMP,121,121,1,209.2,  
INITIAL,TEMP,122,122,1,209.3,  
INITIAL,TEMP,123,123,1,208.60001,  
INITIAL,TEMP,124,124,1,208.7,  
INITIAL,TEMP,125,125,1,208.8,  
INITIAL,TEMP,126,126,1,208.3,  
INITIAL,TEMP,127,127,1,208.399999,  
INITIAL,TEMP,128,128,1,208.60001,  
INITIAL,TEMP,129,129,1,208.10001,  
INITIAL,TEMP,130,130,1,208.2,  
INITIAL,TEMP,131,131,1,208.399999,  
INITIAL,TEMP,132,132,1,211.60001,  
INITIAL,TEMP,133,133,1,209.399999,  
INITIAL,TEMP,134,134,1,208.5,  
INITIAL,TEMP,135,135,1,208,  
INITIAL,TEMP,136,136,1,207.60001,  
INITIAL,TEMP,137,137,1,207.5,  
INITIAL,TEMP,138,138,1,209.399999,  
INITIAL,TEMP,139,139,1,208.5,  
INITIAL,TEMP,140,140,1,208,  
INITIAL,TEMP,141,141,1,207.7,  
INITIAL,TEMP,142,142,1,207.60001,  
INITIAL,TEMP,143,143,1,207.399999,  
INITIAL,TEMP,144,144,1,207.2,  
INITIAL,TEMP,145,145,1,207,  
INITIAL,TEMP,146,146,1,206.899999,  
INITIAL,TEMP,147,147,1,206.8,  
INITIAL,TEMP,148,148,1,206.8,  
INITIAL,TEMP,149,149,1,206.8,  
INITIAL,TEMP,150,150,1,212.10001,  
INITIAL,TEMP,151,151,1,210,  
INITIAL,TEMP,152,152,1,209,  
INITIAL,TEMP,153,153,1,208.5,  
INITIAL,TEMP,154,154,1,208.2,  
INITIAL,TEMP,155,155,1,208,  
INITIAL,TEMP,156,156,1,211.899999,  
INITIAL,TEMP,157,157,1,209.8,  
INITIAL,TEMP,158,158,1,208.8,  
INITIAL,TEMP,159,159,1,208.3,  
INITIAL,TEMP,160,160,1,208,  
INITIAL,TEMP,161,161,1,207.8,  
INITIAL,TEMP,162,162,1,212.2,  
INITIAL,TEMP,163,163,1,216.899999,  
INITIAL,TEMP,164,164,1,212.5,  
INITIAL,TEMP,165,165,1,210.60001,  
INITIAL,TEMP,166,166,1,209.899999,  
INITIAL,TEMP,167,167,1,207.7,  
INITIAL,TEMP,168,168,1,207.3,  
INITIAL,TEMP,169,169,1,207.2,  
INITIAL,TEMP,170,170,1,206.8,

INITIAL,TEMP,171,171,1,206.7,  
INITIAL,TEMP,172,172,1,206.3,  
INITIAL,TEMP,173,173,1,206.399999,  
INITIAL,TEMP,174,174,1,206.399999,  
INITIAL,TEMP,175,175,1,206.3,  
INITIAL,TEMP,176,176,1,206.2,  
INITIAL,TEMP,177,177,1,206.10001,  
INITIAL,TEMP,178,178,1,206.10001,  
INITIAL,TEMP,179,179,1,232.2,  
INITIAL,TEMP,180,180,1,216.899999,  
INITIAL,TEMP,181,181,1,221.3,  
INITIAL,TEMP,182,182,1,215.3,  
INITIAL,TEMP,183,183,1,234.60001,  
INITIAL,TEMP,184,184,1,217.3,  
INITIAL,TEMP,185,185,1,225.2,  
INITIAL,TEMP,186,186,1,216.60001,  
INITIAL,TEMP,187,187,1,218.3,  
INITIAL,TEMP,188,188,1,215.5,  
INITIAL,TEMP,189,189,1,205.60001,  
INITIAL,TEMP,190,190,1,208.5,  
INITIAL,TEMP,191,191,1,206,  
INITIAL,TEMP,192,192,1,207.10001,  
INITIAL,TEMP,193,193,1,205.60001,  
INITIAL,TEMP,194,194,1,205.899999,  
INITIAL,TEMP,195,195,1,205.60001,  
INITIAL,TEMP,196,196,1,205.7,  
INITIAL,TEMP,197,197,1,206.10001,  
INITIAL,TEMP,198,198,1,205.899999,  
INITIAL,TEMP,199,199,1,205.7,  
INITIAL,TEMP,200,200,1,205.399999,  
INITIAL,TEMP,201,201,1,205.60001,  
INITIAL,TEMP,202,202,1,205.899999,  
INITIAL,TEMP,203,203,1,205.2,  
INITIAL,TEMP,204,204,1,205.399999,  
INITIAL,TEMP,205,205,1,205.7,  
INITIAL,TEMP,206,206,1,205,  
INITIAL,TEMP,207,207,1,205.2,  
INITIAL,TEMP,208,208,1,205.399999,  
INITIAL,TEMP,209,209,1,204.7,  
INITIAL,TEMP,210,210,1,204.899999,  
INITIAL,TEMP,211,211,1,205.10001,  
INITIAL,TEMP,212,212,1,204.8,  
INITIAL,TEMP,213,213,1,204.60001,  
INITIAL,TEMP,214,214,1,204.8,  
INITIAL,TEMP,215,215,1,204.7,  
INITIAL,TEMP,216,216,1,204.7,  
INITIAL,TEMP,217,217,1,204.60001,  
INITIAL,TEMP,218,218,1,205.60001,  
INITIAL,TEMP,219,219,1,208.60001,  
INITIAL,TEMP,220,220,1,208.3,  
INITIAL,TEMP,221,221,1,208.2,  
INITIAL,TEMP,222,222,1,208.399999,  
INITIAL,TEMP,223,223,1,208.10001,  
INITIAL,TEMP,224,224,1,207.399999,  
INITIAL,TEMP,225,225,1,207.5,  
INITIAL,TEMP,226,226,1,208,  
INITIAL,TEMP,227,227,1,208.10001,  
INITIAL,TEMP,228,228,1,207.899999,  
INITIAL,TEMP,229,229,1,208.10001,  
INITIAL,TEMP,230,230,1,208.2,  
INITIAL,TEMP,231,231,1,208.3,  
INITIAL,TEMP,232,232,1,208.3,

INITIAL,TEMP,233,233,1,208.39999,  
INITIAL,TEMP,234,234,1,208.39999,  
INITIAL,TEMP,235,235,1,208.3,  
INITIAL,TEMP,236,236,1,208.2,  
INITIAL,TEMP,237,237,1,208.10001,  
INITIAL,TEMP,238,238,1,208,  
INITIAL,TEMP,239,239,1,207.8,  
INITIAL,TEMP,240,240,1,207.39999,  
INITIAL,TEMP,241,241,1,207.39999,  
INITIAL,TEMP,242,242,1,206.8,  
INITIAL,TEMP,243,243,1,204.8,  
INITIAL,TEMP,244,244,1,203.89999,  
INITIAL,TEMP,245,245,1,164.8,  
INITIAL,TEMP,246,246,1,124.1,  
INITIAL,TEMP,247,247,1,164.89999,  
INITIAL,TEMP,248,248,1,124.1,  
INITIAL,TEMP,249,249,1,164.8,  
INITIAL,TEMP,250,250,1,124.1,  
INITIAL,TEMP,251,251,1,164.8,  
INITIAL,TEMP,252,252,1,124,  
INITIAL,TEMP,253,253,1,164.2,  
INITIAL,TEMP,254,254,1,124,  
INITIAL,TEMP,255,255,1,166,  
INITIAL,TEMP,256,256,1,123.7,  
INITIAL,TEMP,257,257,1,155.7,  
INITIAL,TEMP,258,258,1,122.3,  
INITIAL,TEMP,259,259,1,170.2,  
INITIAL,TEMP,260,260,1,129.89999,  
INITIAL,TEMP,261,261,1,153.89999,  
INITIAL,TEMP,262,262,1,121.7,  
INITIAL,TEMP,263,263,1,163.89999,  
INITIAL,TEMP,264,264,1,122.9,  
INITIAL,TEMP,265,265,1,163.2,  
INITIAL,TEMP,266,266,1,120.9,  
INITIAL,TEMP,267,267,1,127.8,  
INITIAL,TEMP,268,268,1,111.6,  
INITIAL,TEMP,269,269,1,166.5,  
INITIAL,TEMP,270,270,1,123.6,  
INITIAL,TEMP,271,271,1,162.7,  
INITIAL,TEMP,272,272,1,122.9,  
INITIAL,TEMP,273,273,1,165.8,  
INITIAL,TEMP,274,274,1,124.2,  
INITIAL,TEMP,275,275,1,165.89999,  
INITIAL,TEMP,276,276,1,124.3,  
INITIAL,TEMP,277,277,1,165.60001,  
INITIAL,TEMP,278,278,1,124.3,  
INITIAL,TEMP,279,279,1,166.39999,  
INITIAL,TEMP,280,280,1,124.3,  
INITIAL,TEMP,291,291,1,166,  
INITIAL,TEMP,292,292,1,124.3,  
INITIAL,TEMP,293,293,1,165.8,  
INITIAL,TEMP,294,294,1,124.3,  
INITIAL,TEMP,295,295,1,166.5,  
INITIAL,TEMP,296,296,1,124.3,  
INITIAL,TEMP,297,297,1,162.89999,  
INITIAL,TEMP,298,298,1,122.9,  
INITIAL,TEMP,299,299,1,166.10001,  
INITIAL,TEMP,300,300,1,124.3,  
INITIAL,TEMP,301,301,1,168.60001,  
INITIAL,TEMP,302,302,1,125.2,  
INITIAL,TEMP,303,303,1,182.2,  
INITIAL,TEMP,304,304,1,128.10001,

```
INITIAL,TEMP,305,305,1,148.39999,
INITIAL,TEMP,306,306,1,117.6,
INITIAL,TEMP,307,307,1,152.10001,
INITIAL,TEMP,308,308,1,118.6,
INITIAL,TEMP,309,309,1,167.2,
INITIAL,TEMP,310,310,1,124.7,
INITIAL,TEMP,311,311,1,165.89999,
INITIAL,TEMP,312,312,1,124.8,
INITIAL,TEMP,313,313,1,171.8,
INITIAL,TEMP,314,314,1,124.7,
C* Set initial temperature to temperature of "matching node"
C* from steady state run.
INITIAL,TEMP,531,531,1,208
INITIAL,TEMP,574,574,1,211
INITIAL,TEMP,575,575,1,211
INITIAL,TEMP,576,576,1,210
INITIAL,TEMP,577,577,1,210
INITIAL,TEMP,578,578,1,210
INITIAL,TEMP,649,649,1,207
INITIAL,TEMP,643,643,1,207
INITIAL,TEMP,637,637,1,207
INITIAL,TEMP,661,661,1,208,
INITIAL,TEMP,655,655,1,208,
INITIAL,TEMP,629,629,1,208,
INITIAL,TEMP,630,630,1,208,
INITIAL,TEMP,631,631,1,208,
INITIAL,TEMP,609,609,1,208,
INITIAL,TEMP,610,610,1,208,
INITIAL,TEMP,611,611,1,208,
INITIAL,TEMP,588,588,1,208,
INITIAL,TEMP,589,589,1,208,
INITIAL,TEMP,590,590,1,208,
INITIAL,TEMP,557,557,1,208,
INITIAL,TEMP,556,556,1,208,
INITIAL,TEMP,549,549,1,208,
INITIAL,TEMP,536,536,1,208,
INITIAL,TEMP,535,535,1,208,
INITIAL,TEMP,501,501,1,208,
TIMES,0,1,0.0013888889,
TOFFSET,460,
TREF,0,
VIEW,0,0,1,0,
SCALE,0,
C* Add air gap elements
ACTSET,EG,1,
ACTSET,MP,5,
EL,400,SF,0,4,31,531,32,32,0,0,0,0,0,0,
EL,401,SF,0,4,174,674,173,173,0,0,0,0,0,0,
EL,402,SF,0,4,174,175,675,674,0,0,0,0,0,0,
EL,403,SF,0,4,175,176,676,675,0,0,0,0,0,0,
EL,404,SF,0,4,176,177,677,676,0,0,0,0,0,0,
EL,405,SF,0,4,177,178,678,677,0,0,0,0,0,0,
EL,406,SF,0,4,178,149,649,678,0,0,0,0,0,0,
EL,407,SF,0,4,149,143,643,649,0,0,0,0,0,0,
EL,408,SF,0,4,143,137,637,643,0,0,0,0,0,0,
EL,409,SF,0,4,137,161,661,637,0,0,0,0,0,0,
EL,410,SF,0,4,161,155,655,661,0,0,0,0,0,0,
EL,411,SF,0,4,155,129,629,655,0,0,0,0,0,0,
EL,412,SF,0,4,129,130,630,629,0,0,0,0,0,0,
EL,413,SF,0,4,130,131,631,630,0,0,0,0,0,0,
EL,414,SF,0,4,131,109,609,631,0,0,0,0,0,0,
EL,415,SF,0,4,109,110,610,609,0,0,0,0,0,0,
```

EL,416,SF,0,4,110,111,611,610,0,0,0,0,0,0,  
EL,417,SF,0,4,111,88,588,611,0,0,0,0,0,0,  
EL,418,SF,0,4,88,89,589,588,0,0,0,0,0,0,  
EL,415,SF,0,4,89,90,590,589,0,0,0,0,0,0,  
EL,420,SF,0,4,90,57,557,590,0,0,0,0,0,0,  
EL,421,SF,0,4,57,56,556,557,0,0,0,0,0,0,  
EL,422,SF,0,4,56,49,549,556,0,0,0,0,0,0,  
EL,423,SF,0,4,49,36,536,549,0,0,0,0,0,0,  
EL,424,SF,0,4,536,36,35,35,0,0,0,0,0,0,  
EL,425,SF,0,4,1,501,2,2,0,0,0,0,0,0,

### 3.6-E.6.2 File DELKO1.INP

This file deletes the kaowool elements as shown in Figure 3.6-E-F2 and reassigns surface heat transfer properties to the exposed stainless steel elements.

```
ACTSET,TP,0,  
EDEL,259,263,2,  
EDEL,258,262,2,  
EDEL,277,281,2,  
EDEL,276,280,2,  
CEL,222,6.94E-3,1,2,224,1,1,  
CEL,213,6.94E-3,1,2,215,1,1,  
REPAINT,  
REL,213,.8,1,1,2,215,1,1,  
REL,222,.8,1,1,2,224,1,1,
```

### 3.6-E.6.3 File DELKO.INP

This file deletes all kaowool elements and reassigns surface heat transfer properties to the exposed stainless steel elements.

```
ESELPROP,MP,4,4,1,  
EDEL,1,999,1,  
RESET,  
SCALE,0,  
VIEW,0,0,1,0,  
ACTSET,TP,0,  
CEL,211,6.94E-3,1,2,227,1,1,  
CEL,228,6.94E-3,1,1,229,1,1,  
CEL,142,6.94E-3,1,3,144,2,1,  
CEL,145,6.94E-3,1,4,151,2,1,  
CEL,154,6.94E-3,1,2,156,2,1,  
CEL,155,6.94E-3,1,3,156,1,1,  
CEL,426,6.94E-3,1,1,426,1,1,  
CEL,426,6.94E-3,1,2,426,1,1,  
CEL,205,6.94E-3,1,2,205,1,1,  
CEL,206,6.94E-3,1,1,206,1,1,  
CEL,208,6.94E-3,1,2,208,1,1,  
CEL,208,6.94E-3,1,3,208,1,1,  
REL,211,.8,1,1,2,227,1,1,  
REL,228,.8,1,1,1,229,1,1,  
REL,142,.8,1,1,3,144,2,1,  
REL,145,.8,1,1,4,151,2,1,  
REL,154,.8,1,1,2,156,2,1,  
REL,155,.8,1,1,3,156,1,1,  
REL,426,.8,1,1,1,426,1,1,  
REL,426,.8,1,1,2,426,1,1,  
REL,205,.8,1,1,2,205,1,1,  
REL,206,.8,1,1,1,206,1,1,  
REL,208,.8,1,1,2,208,1,1,  
REL,208,.8,1,1,3,208,1,1,
```

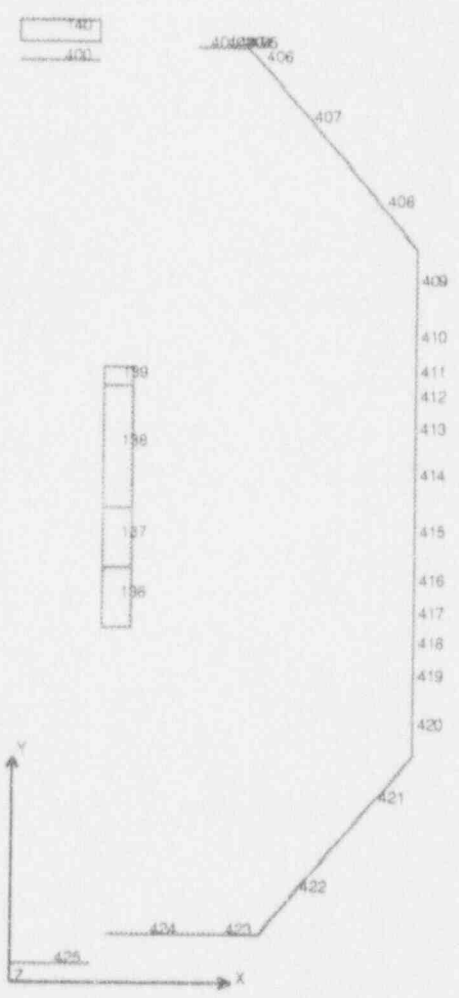


Figure 3.6-E-F1. Air Gap Elements

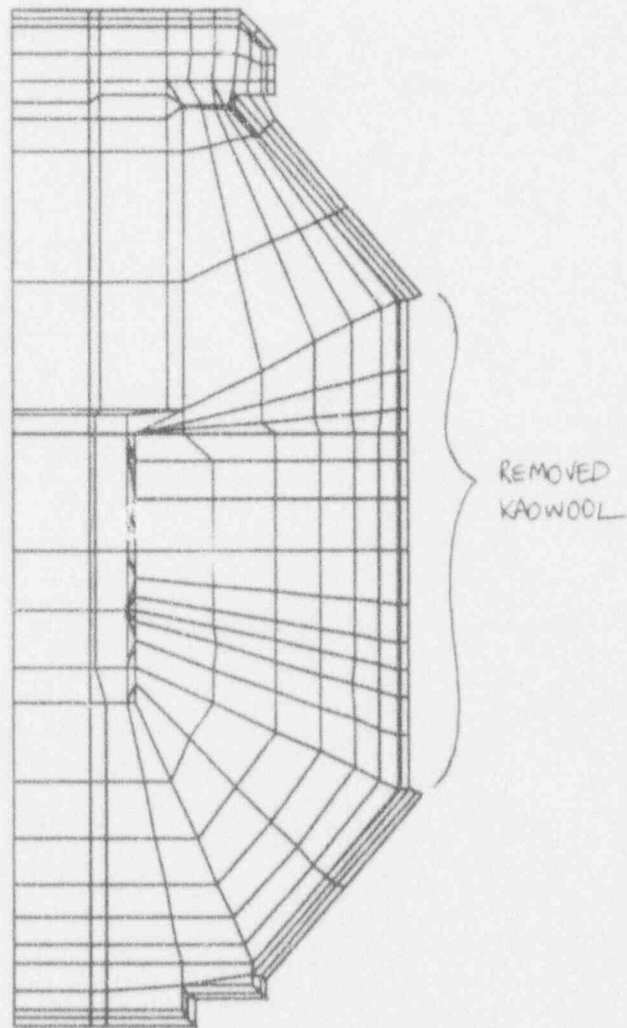


Figure 3.6-E-F2. Case G2051 (Additional Kaowool Removed)